Mechanism of Versatile DNA Damage Recognition by Xeroderma Pigmentosum Group C (XPC) Protein

Graduate School for Cellular and Biomedical Sciences

University of Bern

PhD Thesis

Submitted by

Flurina Christina Clement Frey

from Tschiertschen-Praden and Tamins (GR)

Thesis advisor

Prof. Dr. Hanspeter Naegeli
Institute of Veterinary Pharmacology and Toxicology
Vetsuisse Faculty of the University of Zürich

Accepted by the Faculty of Medicine, the Faculty of Science and the Vetsuisse Faculty of the University of Bern at the request of the Graduate School for Cellular and Biomedical Sciences

Bern, Dean of the Faculty of Medicine

Bern, Dean of the Faculty of Science

Bern, Dean of the Vetsuisse Faculty Bern

SUMMARY

Global genome repair (GGR), a subpathway of the mammalian nucleotide excision repair (NER), deals with the removal of UV light-induced DNA damages which is essential for the maintenance of genome stability. GGR is triggered by xeroderma pigmentosum group C (XPC) protein, a key general sensor of a wide array of different DNA lesions such as bulky adducts, inter- and intrastrand DNA crosslinks and oxidative base lesions arising from environmental mutagens, sunlight and endogenous reactive metabolites. Against the classical "lock-and-key" scheme, XPC protein operates by detecting the single-stranded character of non-hydrogen-bonded bases opposing damaged sites without touching the damaged nucleotides, a fact that is supported by the crystal structure analysis of the yeast Rad4 homolog. This crystal structure revealed several evolutionary highly conserved residues closely contacting extrahelical nucleotides of the intact complementary DNA strand. Using truncated or mutated protein fusion constructs, the minimal domain necessary for DNA damage detection was investigated. I identified four critical amino acids within this short DNA-binding motif interacting with flipped-out nucleotides opposite to the lesion site that play an important role in DNA damage detection (N754, F756, F797) and are crucial for the damage transfer to the next following GGR factors (F797, F799). Residue F799 plays an important role in stabilizing XPC protein at the repair site. Furthermore, N754 together with E755, a non-conserved negatively charged residue located in the β-turn motif, accounts for protein mobility and therefore possibly enables facilitated diffusion, a fast and effective search for damaged sites within the genome.

TABLE OF CONTENTS

Chapter 1

Introduction and Aim of the Thesis

1.1. DNA damage and ultra-violet (UV) light

Our genome's integrity is constantly challenged by endogenous and exogenous agents deriving from oxidative stress, metabolism, food, drugs, chemicals in textiles and cosmetics, exhaust emissions and particulate matters. All these carcinogens cause DNA adducts, oxidative base lesions or inter- and intrastrand crosslinks, which can lead to mutations and eventually to cancer in the absence of appropriate repair mechanisms. Another important source of intrastrand DNA crosslinks is the short-wave UV spectrum of sunlight since it causes cyclobutane-pyrimidine dimers (CPDs) and (6-4) pyrimidine-pyrimidone photoproducts (6-4PPs) (Fig 1). A CPD lesion is formed by the covalent linkage of C=C double bonds between two neighboring pyrimidines (thymines or cytosines). Crosslinking of a pyrimidine's C6 atom with a C5 atom of an adjacent pyrimidine generates a highly DNA-distorting 6-4PP. UVC induces CPDs and to a lesser extent also 6-4PPs, but since UVC light is fully absorbed by ozone (O_3) particles in the stratosphere it does not reach our skin. However, in research, a UVC lamp is a helpful tool to induce photolesions in cellular systems. In our daily exposure to sunlight, UVB light is of most importance since on the one hand it is responsible for sunburn by activation of inflammation processes, and on the other hand, it causes CPDs and 6-4PPs. UVA light, the longest-wave UV radiation, provokes skin aging and erythema. So far, the general opinion was that UVA did not contribute to the carcinogenic effect of sunlight because photosensitizers such as chlorophyll, non-iron porphyrins or flavins were necessary to induce CPDs. A new study however proposes that UVA light-induced CPDs are formed via a direct photochemical mechanism, without mediation of a cellular photosensitizer (*Mouret et al*. 2010). Therefore, UVA light gains more and more significance in the prevention of skin cancer. UV light-induced DNA damages are exclusively removed via the nucleotide excision repair (NER) pathway initiated by the DNA damage sensor XPC. Although CPDs are about four times more abundant than 6-4PPs, their repair poses a special challenge for mammalian cells (see sections 1.2. and 1.4.).

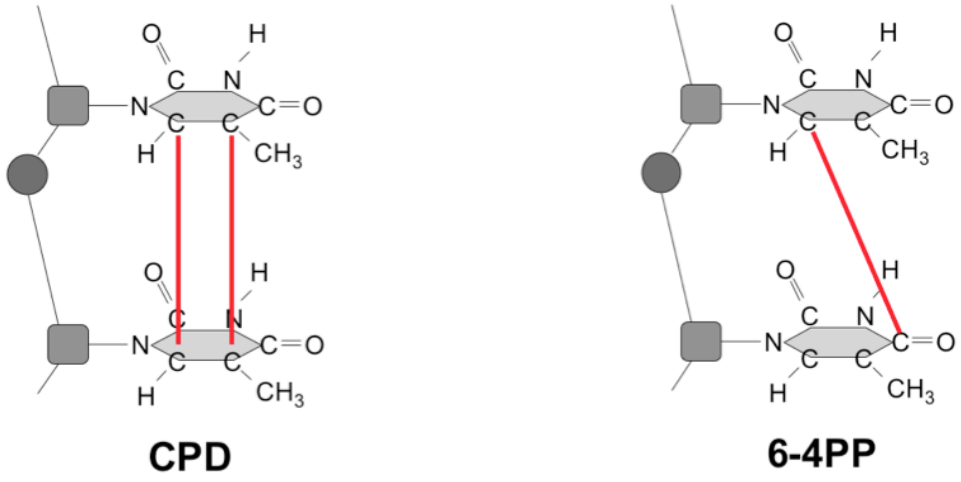

Fig. 1 *Left: Scheme of a CPD lesion. The coupling of two C5=C6 double bonds of two neighboring pyrimidines (here: thymines) leads to the formation of a four-membered ring. Right: Scheme of a 6-4PP lesion. Two thymine bases are dimerized by a covalent bond between C6 and C4. This lesion results in substantial helical distortion of the DNA. Red lines, intrastrand crosslinks of two adjacent pyrimidines. The DNA backbone is drafted with circles (phosphates) and squares (riboses).*

1.2. Nucleotide excision repair (NER) pathway

The mammalian skin is equipped with a sophisticated repair mechanism recognizing conformational changes in the DNA structure caused by 6-4PPs and CPDs, DNA adducts generated by electrophilic chemicals as well as intrastrand DNA crosslinks, DNA-protein crosslinks and a subset of oxidative lesions (*Huang et al.* 1994, *Kuraoka et al.* 2000, *Reardon* and *Sancar* 2006). This 'cut-patch-cut-patch' mechanism is called nucleotide excision repair (NER) pathway (Fig. 2) and can be subdivided into two branches: Transcription-coupled repair (TCR) and global genome repair (GGR). Many of the NER key players are able to bind DNA at the lesion site, but which one of these key players acts first depends on the transcriptional activity of the damaged gene. TCR is triggered by stalled RNA polymerase II in transcriptionally active parts of the genome (*Hanawalt and Spivak* 2008). Upon arrest of this polymerase, Cockayne syndrome A and B (CSA and CSB) proteins are located to the damage. In contrast, GGR takes place in the vast amount of non-active genes and silent chromatin regions independently of transcription (*Sugasawa et al.* 1998, *Friedberg* 2001, *Nishi et al.* 2005). In GGR, the initial DNA damage sensor is XPC protein, accompanied by the ubiquitin-binding protein Rad23B (a homolog of the yeast Rad23 protein) and centrin-2 (a protein required for centriole duplication in mammalian cells; *Salisbury et al.* 2002) exerting

stabilizing functions (*Araki et al.* 2001). XPC protein displays a general preference for DNA substrates that contain helix-destabilizing lesions including 6-4PPs (*Batty et al.* 2000, *Sugasawa et al.* 2001). It avoids direct contacts with the damaged bases and uses a single-stranded DNA-binding motif to recognize the local single-stranded character of the intact complementary strand opposite to the lesion site (*Maillard et al.* 2007). The special case of CPD recognition depends on an additional protein discovered on the basis of its characteristic UV-damaged DNA-binding (UV-DDB) activity (*Nichols et al.* 2000, *Fitch et al.* 2003). Since CPDs distort the DNA double helix only to a minor extent and therefore are poorly recognized by XPC, this part is taken over by the DDB2 subunit of UV-DDB complex exhibiting an affinity for UV-damaged substrates (*Scrima et al.* 2008). Both CSA/CSB and XPC-Rad23B-centrin-2 serve as molecular platforms to initiate a common NER pathway by sequential attraction of the subsequent repair proteins transcription factor IIH (TFIIH), Xeroderma pigmentosum protein group A-replication protein A (XPA-RPA), Xeroderma pigmentosum protein group F (XPF), and Xeroderma pigmentosum protein group G (XPG) (*Yokoi et al.* 2000, *Uchida et al.* 2002). TFIIH unwinds the double helix to create space for the next following repair factors and locates the chemically damaged base (*Naegeli et al.* 1995, *Fan et al.* 2006). XPA verifies the damage and, together with RPA, masks the naked native DNA strand (*Li et al.* 1995, *Camenisch et al.* 2006). XPF performs the first incision at the 5' side of the lesion and a DNA polymerase immediately starts synthesizing the new strand (*Staresincic et al.* 2009). Then, XPG cleaves the damaged strand 3' of the lesion thereby releasing an oligonucleotide of 25-32 bases containing the damage. When the repair synthesis is completed, the nick in the backbone is sealed by a DNA ligase (*Evans et al.* 1997, *Staresincic et al.* 2009). Mutations in genes specific for repair of damages in transcribed genes (TCR) result in developmental and neurogenerative disorders such as Cockayne syndrome (CS) and trichothiodystrophy (TTD) but not in tumors, while defects in genes specific for GGR, a repair pathway that deals with lesions in inactive parts of the DNA, lead to predominant cancer development and only rarely to neurological symptoms (*Cleaver* 2005).

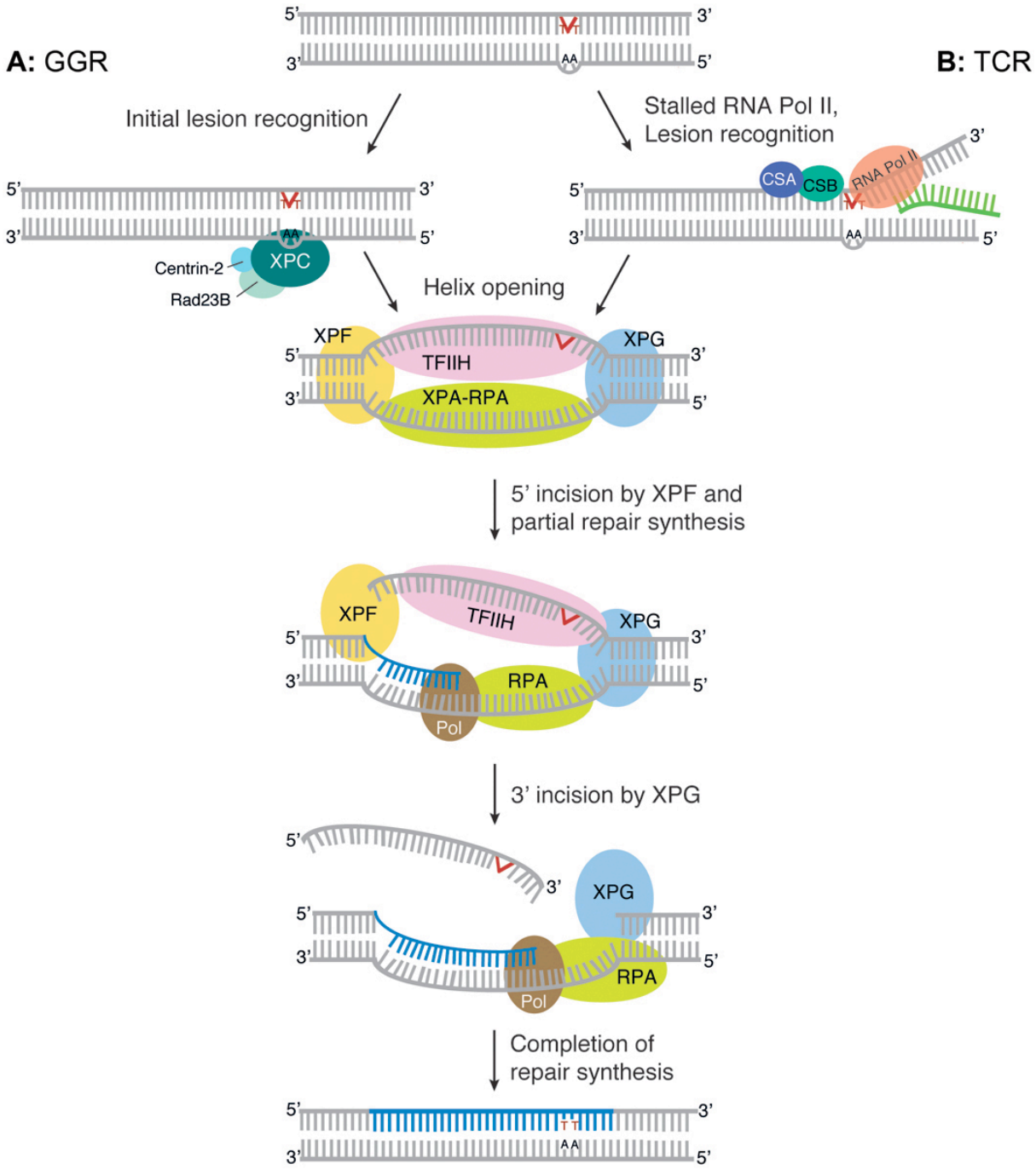

Fig. 2 *Nucleotide excision repair pathway. TVT, 6-4 photoproduct; GGR, global genome repair; TCR, transcription-coupled repair; XPC, xeroderma pigmentosum group C protein; CSA, Cockayne syndrome protein A; CSB, Cockayne syndrome protein B; RNA Pol II, RNA polymerase II; XPF, xeroderma pigmentosum group F protein; XPG, xeroderma pigmentosum group G protein; TFIIH, transcription factor IIH; XPA-RPA, xeroderma pigmentosum group A protein-replication protein A; Pol, DNA polymerase. NER consists of four main steps: Lesion recognition, damage verification and helix opening, dual incision, repair synthesis. See text for further information.*

1.3. Xeroderma pigmentosum

Xeroderma pigmentosum (XP, meaning 'dry and pigmented skin') is an inherited autosomal recessive disease. XP patients exhibit a NER deficiency due to mutated *XP* genes resulting in truncated or mutated XP proteins. There are eight complementation groups known (XP-A to XP-G and a XP-variant) each leading to the phenotype of XP (*Cleaver et al.* 1999, *Lehmann* 2003). XP-variant (XP-V) refers to a defect in translesion synthesis by polymerase η with a clinical phenotype indistinguishable from other XP patients but exhibiting a normal NER capacity (*Cleaver* 1972, *Masutani et al.* 1999). XP is characterized by skin hyperpigmentation, extreme photosensitivity and a 2000-fold increase in skin cancer development (basal cell carcinomas, squamous cell carcinomas, and malignant melanomas) in sun-exposed areas (*Cleaver* 2005, *Andressoo et al.* 2006, *Friedberg et al.* 2006). Typically, the patients are diagnosed at the young age of two years young when they are presented at medical institutions with severe sunburns and skin abnormalities. The mean onset of skin cancer is at the age of eight years. Since there is no treatment for XP, the only possibility for these patients to prevent cancer is to shield themselves completely from UV radiation derived from sunlight or light bulbs. The average life expectancy of patients taking the necessary precautions is reduced by 30 years compared to healthy individuals, non-protected patients die within the first decade of their life. The frequency of XP ranges from 1:40'000 (Japan) to 1:250'000 (USA, EU). In Germany, there are 90 cases estimated at the moment (www.onmeda.de/krankheiten/xeroderma_pigmentosum.html).

The most severe phenotypes are caused by a defect in XPG, showing both GGR- and TCR-related diseases (*Clarkson* 2003), and XPC because it acts as the initial damage sensor. XPE patients are only mildly affected due to XPC's ability to detect DNA damages by itself (*Tang and Chu* 2002). XP symptoms are not only restricted to skin abnormalities. Rarely, patients also develop neurological symptoms and internal tumors (*Cleaver* 2005, *Andressoo et al.* 2006), a fact that photolesions are not accountable for because UV radiation does not penetrate the dermis. A possible explanation arises from the finding that XPC exerts an unexpected role in cell protection from oxidative damage. Usually, oxidative damage is excised via base excision repair (BER) pathway. But a study shows that XP-C cells (cells lacking functional XPC protein due to a H780Stop mutation in the *XPC* gene) fail to efficiently remove 8-OH-Gua, a typical oxidative lesion eliminated by BER (*D'Errico et al.* 2006). 8-OH-Gua lesions lead to G→T transversions, a mutation that can cause cancer in all kinds of tissues.

1.4. XPC protein

XPC protein comprises 940 amino acids and is 125 kDa in size. Several domains have been mapped to its sequence (Fig. 3), such as interaction domains with other repair factors and a minimal DNA damage sensor domain (*Masutani et al.* 1994, *Batty et al.* 2000, *Nishi et al.* 2005, *Min* and *Pavletich* 2007). According to the crystal structure of Rad4, the yeast homolog of human XPC, this protein consists of four significant structural domains, a transglutaminase-homology domain (TGD) and three structurally related β-hairpin domains (BHD1-3) that are characterized by two opposing β-sheets linked by a short hairpin (*Min* and *Pavletich* 2007). BHD2 and BHD3 are connected via a β-turn sequence (Fig. 3). XPC binds to the damaged DNA in two parts. With its TGD and BHD1 domains, it attaches to the double stranded part next to the lesion. BHD2 and BHD3 form a clamp-like structure that encloses the native strand opposite the damaged site. Furthermore, BHD3 inserts its β-hairpin into the lesion thereby flipping out two unpaired bases (*Min* and *Pavletich* 2007).

As mentioned above, XPC protein is *the* initial DNA damage sensor in GGR exerting an incredible substrate versatility. The ability to identify such a vast spectrum of different DNA lesions arises from the efficient recognition of helical distortions and strand oscillations without contacting the damaged site (*Buterin et al.* 2005, *Maillard et al.* 2007). Due to the fact that 6-4PPs lead to a substantial change in DNA conformation, they are recognized more efficiently by XPC protein and eliminated at least 5-fold faster than CPDs, which have a half-life of 24 hours (*reviewed in Balajee* and *Bohr 2000*). Therefore, the effective detection of CPD lesions needs the help of an additional factor. UV damage-DNA binding protein (UV-DDB), a heterodimeric protein consisting of DDB1 and DDB2 (the latter encoded by the *XPE* gene), identifies CPDs and hands them over to XPC, which in turn triggers GGR.

In XP-C patients, the *XPC* gene is mutated in a way that leads to early protein termination resulting in non-functional protein. There is only one single patient known featuring a tryptophane-to-serine substitution at position 690 and showing a strong XP phenotype (*Chavanne et al.* 2000).

Since it is still unknown by which exact mechanism XPC recognizes the damaged bases in the vast excess of native DNA, we focused on the DDB-independent repair of 6-4PPs exclusively detected by XPC. We mainly used Chinese hamster ovary (CHO) cells in our experiments, a cell line failing to express the DDB2 subunit of UV-DDB protein due to promoter methylation and hence allowing us to study XPC protein autonomously (*Fitch et al.* 2003).

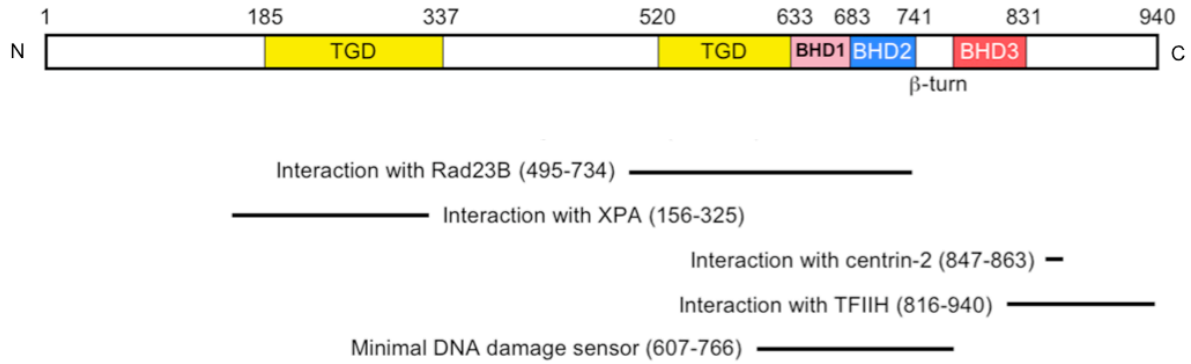

Fig. 3 *Scheme of XPC protein domains. TGD, transglutaminase-homology domain; BHD1, β-hairpin domain 1; BHD2, β-hairpin domain 2; BHD3, β-hairpin domain 3; N, N-terminus; C, C-terminus; numbers depict amino acids.*

1.5. Aim of the thesis

During my thesis work, I aimed at elucidating the DNA damage recognition mechanism by XPC protein. Based on crystallographic and biochemical knowledge, I created mutated or truncated XPC proteins fused to specific tags using site-directed mutagenesis and molecular cloning procedures. I identified critical amino acids within a minimal DNA-binding motif that play an important role in DNA damage detection by closely contacting flipped-out nucleotides opposite to the lesion site (residues N754, F756, F797). Residues N754 and E755 located in the β-turn motif account for protein mobility and therefore enable a fast and effective search for damaged sites within the genome. Furthermore, I found that residues F797 and F799 are crucial for the damage transfer to the next following GGR factors and that F799 plays an important role in stabilizing XPC protein at the repair site.

1.6. Introductory Review:

Dynamic two-stage mechanism of versatile DNA damage recognition by xeroderma pigmentosum group C protein

1.6.1. Aims of the review

The emphasis of this review is on how XPC protein interrogates the native DNA double helix in its search for base lesions within the vast excess of intact genome. We elucidate the state of the art regarding the mechanism of DNA damage recognition of XPC protein. This work gives an overview on the global genome repair pathway and describes the interaction of the XPC complex with DNA at damaged sites. Also, it deals with the challenging case of CPD recognition and provides a dynamic model for lesion identification based on novel results from our laboratory.

1.6.2. Main conclusions

XPC protein binds to damaged DNA in an effective double-check process. In step one, the BHD1/BHD2 domains perform an energetically beneficient search for non-hydrogen-bonded bases in conjunction with the β-turn motif exerting a dynamic role in the interplay with normal duplex DNA. In a second step, the single-stranded DNA binding activity of BHD3 is responsible for the installation of a stable recognition complex.

1.6.3. Contribution to this review

I was substantially involved in writing this review and in literature search on NER topics. All three figures were designed by myself.

1.6.4. Reference

Clement FC, Camenisch U, Fei J, Kaczmarek N, Mathieu N, and Naegeli H (2010) Dynamic two-stage mechanism of versatile DNA damage recognition by xeroderma pigmentosum group C protein. *Mutation Research* 685: 21-28.

1.6.5. Review

Mutation Research 685 (2010) 21–28

Contents lists available at ScienceDirect

Mutation Research/Fundamental and Molecular Mechanisms of Mutagenesis

journal homepage: www.elsevier.com/locate/molmut
Community address: www.elsevier.com/locate/mutres

Review

Dynamic two-stage mechanism of versatile DNA damage recognition by xeroderma pigmentosum group C protein

Flurina C. Clement, Ulrike Camenisch, Jia Fei, Nina Kaczmarek, Nadine Mathieu, Hanspeter Naegeli*

Institute of Pharmacology and Toxicology, University of Zürich-Vetsuisse, Winterthurerstrasse 260, CH-8057 Zürich, Switzerland

ARTICLE INFO

Article history:
Received 3 August 2009
Accepted 7 August 2009
Available online 15 August 2009

Keywords:
Aging
Carcinogenesis
DNA damage
Mutagenesis
Xeroderma pigmentosum

ABSTRACT

The recognition and subsequent repair of DNA damage are essential reactions for the maintenance of genome stability. A key general sensor of DNA lesions is xeroderma pigmentosum group C (XPC) protein, which recognizes a wide variety of helix-distorting DNA adducts arising from ultraviolet (UV) radiation, genotoxic chemicals and reactive metabolic byproducts. By detecting damaged DNA sites, this unique molecular sensor initiates the global genome repair (GGR) pathway, which allows for the removal of all the aforementioned lesions by a limited repertoire of excision factors. A faulty GGR activity causes the accumulation of DNA adducts leading to mutagenesis, carcinogenesis, neurological degeneration and other traits of premature aging. Recent findings indicate that XPC protein achieves its extraordinary substrate versatility by an entirely indirect readout strategy implemented in two clearly discernible stages. First, the XPC subunit uses a dynamic sensor interface to monitor the double helix for the presence of non-hydrogen-bonded bases. This initial screening generates a transient nucleoprotein intermediate that subsequently matures into the ultimate recognition complex by trapping undamaged nucleotides in the abnormally oscillating native strand, in a way that no direct contacts are made between XPC protein and the offending lesion itself. It remains to be elucidated how accessory factors like Rad23B, centrin-2 or the UV-damaged DNA-binding complex contribute to this dynamic two-stage quality control process.

Contents

Abbreviations: 6-4PPs, (6-4) photoproducts; B[*a*]P, benzo[*a*]pyrene; BHD, β-hairpin domain; CPDs, cyclobutane pyrimidine dimers; ERCC1, excision repair cross complementing-1; GGR, global genome repair; NER, nucleotide excision repair; PCNA, proliferating cell nuclear antigen; RFC, replication factor C; RPA, replication protein A; TGD, transglutaminase homology domain; TFIIH, transcription factor IIH; UV, ultraviolet; UV-DDB, UV-damaged DNA-binding; XP, xeroderma pigmentosum.

* Corresponding author. Tel.: +41 44 635 87 63; fax: +41 44 635 89 10.
E-mail address: naegelih@vetpharm.uzh.ch (H. Naegeli).

0027-5107/$ – see front matter © 2009 Elsevier B.V. All rights reserved.
doi:10.1016/j.mrfmmm.2009.08.005

1. Introduction

Nucleotide excision repair (NER) is a central component of the DNA damage response network that protects the genetic integrity against permanent attacks from both environmental mutagens and endogenous reactive metabolites. In humans, NER is the only system that promotes the error-free removal of UV-induced crosslinks between adjacent bases, mainly (6-4) pyrimidine–pyrimidone photoproducts (6-4PPs) and cyclobutane pyrimidine dimers (CPDs) [1–4]. The same excision system eliminates other intrastrand crosslinks, produced for example by the antitumor drug cisplatin, and a wide diversity of bulky carcinogen–DNA adducts. In addition, this versatile reaction eliminates a subset of oxidative base lesions like 8,5′-cyclopurine nucleosides, which are not amenable to excision by DNA glycosylases [5,6], as well as DNA adducts formed from lipid peroxidation products such as malondialdehyde [7]. A common feature of these different lesions channeled into the same repair pathway is their ability to cause helical distortions, leading to abnormal oscillations of non-hydrogen-bonded nucleotides primarily in the undamaged strand [8].

The NER process operates in two distinct subpathways that differ only in the initial mechanism of DNA damage recognition. One subpathway, known as transcription-coupled repair, takes place when the transcriptional activity is obstructed by DNA lesions in the transcribed strand (reviewed by Hanawalt and Spivak [9]). In contrast, the global genome repair (GGR) subpathway is triggered by the recognition of damaged sites anywhere in the genome, including non-transcribed strands and silent chromatin regions (reviewed by Friedberg [10]). Many core factors participating in the GGR reaction are encoded by genes that, when mutated, give rise to xeroderma pigmentosum (XP), an autosomal recessive disorder characterized by photosensitivity, skin atrophy, hyperpigmentation and sunlight-induced skin cancer [1,2]. XP patients also have an increased risk of developing internal tumors and the disease is often associated with neurological manifestations attributable to oxidative damage [5–7]. Indeed, various clinical and pathological features of XP patients are similar to those seen in elderly people and, hence, reflect premature aging triggered by the accumulation of unrepaired DNA lesions [11].

Over 30 gene products are employed in the GGR pathway, which is thought to proceed by the stepwise assembly of a multiprotein excision machinery, followed by the recruitment of dedicated DNA synthesis and DNA ligation factors [1,4,10]. In higher eukaryotes, this sequential reaction is initiated by a versatile DNA damage sensor composed of XPC, Rad23B and centrin-2 [12,13]. XPC is the actual sensor subunit of this initiator complex, whereas Rad23B and centrin-2 exert accessory functions (see Section 3). The present review addresses the central question of how XPC protein examines the Watson–Crick double helix to search for base lesions and how this factor faces the task of actually finding rare sites of DNA damage among the vast excess of native DNA in a typical mammalian genome.

2. Overview of the GGR pathway

Individual steps of the GGR reaction, *i.e.*, DNA damage sensing, local DNA melting, dual DNA incision, damage excision, repair patch synthesis and DNA ligation are illustrated in Fig. 1. Upon recognition of lesion sites, the XPC complex acts as a landing platform for the recruitment of TFIIH, which among its 10 subunits comprises the two DNA helicases XPB and XPD responsible for strand separation. Further GGR players that are sequentially recruited to target sites include XPA, RPA, XPG and, finally, XPF-ERCC1 [14,15]. The DNA unwinding activity of TFIIH generates a central nucleoprotein intermediate, in which the duplex undergoes partial melting by

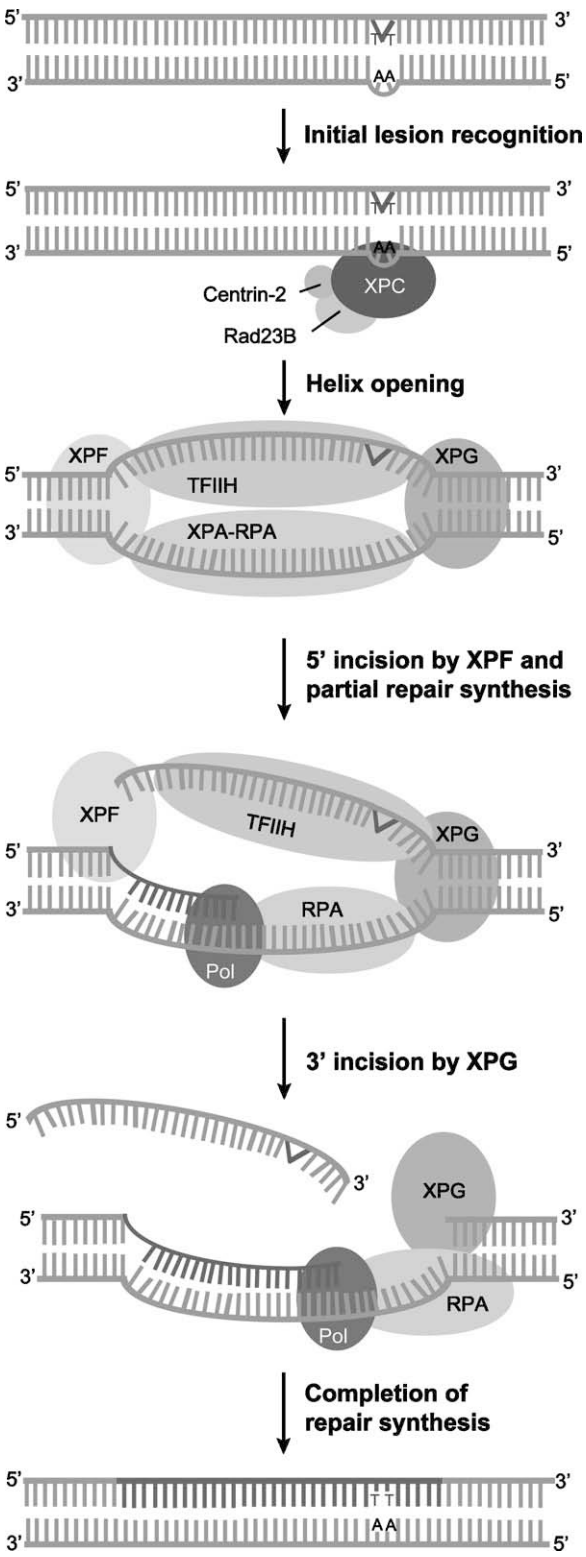

Fig. 1. Mammalian GGR pathway. Target DNA sites containing an offending lesion, for example a UV-induced 6-4PP, are detected by the XPC-Rad23B-centrin-2 complex. Subsequently, this XPC complex triggers a sequential reaction involving local DNA unwinding by TFIIH, stabilization of the open intermediate by XPA-RPA and dual DNA incision by XPF-ERCC1 and XPG. Excision and DNA repair patch synthesis occur in a coordinated manner. After completion of this cut-and-patch process, the duplex integrity is restored by DNA ligation.

about 25 nucleotides [16–18]. This open intermediate is framed by "Y-shaped" double- to single-stranded junctions, which constitute a preferred substrate for the structure-specific DNA endonucleases XPF and XPG [19,20]. The 5′ incision by XPF-ERCC1 precedes the 3′ incision by XPG [21]. Through double cleavage of the damaged strand, the combined action of these two endonucleases leads to excision of the offending lesion in the form of an oligonucleotide segment of 24–32 residues [22,23]. Duplex integrity is reestablished by the action of DNA polymerases δ, ε and κ [24,25], in conjunction with RFC and PCNA. This DNA repair synthesis is carried out in line with the initial 5′ incision, thus avoiding that excision of an oligonucleotide fragment causes the transient exposure of single-stranded DNA, which is at risk to be converted to a double-stranded break by inadvertent nuclease activity [21]. Finally, the newly synthesized repair patch is joined to the pre-existing strand by DNA ligase I and DNA ligase III [26,27].

3. Initiation of GGR activity by the XPC complex

In the cellular context, the XPC polypeptide (125 kDa) is found in association with Rad23B, a 58-kDa homolog of the yeast Rad23 protein [28], and centrin-2, a 18-kDa centrosomal factor [29]. XPC protein itself possesses DNA-binding activity, whereas the ubiquitin-binding Rad23B and the calcium-binding centrin-2 protect the initiator complex from degradation and stimulate its activity in DNA repair [28,30]. In double-mutant mouse cells lacking Rad23B as well as the functionally redundant Rad23A ortholog, XPC protein is completely degraded by proteasomal activity [31].

The XPC subunit alone or in combination with Rad23B binds preferentially to damaged DNA substrates containing, for example, 6-4PPs, B[*a*]P diol epoxide adducts, acetylaminofluorene adducts or cisplatin crosslinks [32–34]. More detailed biochemical analyses with defined nucleic acid substrates revealed that XPC protein displays a general affinity for DNA sites that deviate from the canonical Watson–Crick geometry, including single-stranded loops, mismatched bubbles or single-stranded overhangs [35,36]. According to scanning force microscopy studies, the binding of XPC protein to DNA induces a kink of 39–49° in the nucleic acid backbone regardless of whether the substrate is damaged or not [37]. Permanganate footprinting studies demonstrate that the observed sharp bending is accompanied by partial melting of the duplex extending over 4–7 base pairs [34,38].

These conformational changes in the DNA helix have been further examined at atomic resolution by crystallization of parts of Rad4 protein, a yeast ortholog that shares ∼40% similarity and ∼25% identity with the human XPC sequence. In co-crystals with heteroduplex DNA carrying a single CPD, Rad4 protein binds to the substrate in a bimodal manner [39]. One portion of Rad4 protein, consisting of its large transglutaminase homology domain (TGD) in conjunction with a short β-hairpin domain (BHD1), forms a C-clamp-like structure that interacts with 11 base pairs of native double-stranded DNA located on the 3′ side of the lesion (Fig. 2A). The TGD region, which provides one tip of the C-clamp, displays an intriguing similarity to the transglutaminase fold of peptide-*N*-glycanases that remove glycan modifications from proteins. Unlike other members of this enzyme family, however, Rad4 lacks the predicted catalytic triad (Cys-His-Asp) [40]. As illustrated in the scheme of Fig. 2B, the homologous TGD segment of human XPC protein is separated into two individual parts by a disordered ∼180 residue insertion [41].

Another portion of Rad4 protein, composed of the β-hairpin domains BHD2 and BHD3, folds into a hand-like structure that associates with a 4-nucleotide DNA segment at the lesion site. As will be discussed in Section 4, most of these interactions made by BHD2/BHD3 are van der Waals contacts with the undamaged strand of the substrate. We previously found that there is ∼75% amino acid similarity and ∼30% identity between this central DNA-binding region of XPC protein (Fig. 2B) and the oligonucleotide/oligosaccharide-binding fold (OB-fold) of RPA-B, one of the single-stranded DNA-binding motifs of human RPA [42]. Such an intriguing sequence similarity extends to two OB-folds of breast cancer protein-2, another factor with selectivity for single-stranded conformations, thus suggesting that the damage sensor core of XPC protein may have emerged during evolution from an ancient single-stranded DNA-binding protein.

In proximity to the CPD lesion, the Rad4 protein-DNA structure is characterized by two characteristic features (Fig. 2A). First, a long β-hairpin protruding from BHD3 is inserted into the double helix, thus inducing a kink of 42° in the DNA backbone. Second, this β-hairpin invasion causes extrahelical displacements involving not only the crosslinked pyrimidines, making up the CPD, but also the opposing native bases in the undamaged strand (Fig. 2A). Each one of these flipped-out normal residues is sandwiched between aromatic side chains provided by the BHD2/BHD3 motifs. Finally, the crystallized Rad4 complex also includes a polypeptide fragment representing Rad23 protein and, therefore, has been able to solve the previous ambiguity [43,44] over the precise amino acids mediating the Rad4–Rad23 association. In fact, the incorporated Rad23 polypeptide interacts with several residues mapping to the beginning and the end of the TGD region, in the N-terminal region of Rad4. These particular Rad4–Rad23 interaction sites are consistent with an earlier report demonstrating that an XPC fragment extending from residues 607 to 940, not containing the TGD region, fails to form complexes with the human Rad23 homolog [44]. The N-terminal region of human XPC is responsible for an association with XPA [41]. On the other hand, the carboxy-terminal tail of XPC protein harbors domains that interact with centrin-2 (residues 847–863) and TFIIH (residues 816–940) [30,44].

4. The molecular basis for substrate versatility

A long unanswered question has been the mechanism by which Rad4/XPC protein achieves its ability to detect a wide spectrum of damaged substrates. There is no common chemical feature of the different DNA adducts that would permit a classic "lock and key" recognition scheme. Instead, the observed substrate versatility of the GGR pathway implies that its promiscuous initiator, XPC protein, acts by recognizing damage-induced distortions of the DNA helix rather than specific base modifications. In support of this hypothesis, it has been observed that the GGR system exhibits a general preference for base adducts that lower the melting temperature of double-stranded DNA [45], suggesting that XPC protein may detect the single-stranded character of damaged sites carrying bulky lesions. However, not in all cases the degree of duplex destabilization correlates with excision efficiency. For example, the more helix-destabilizing (+)- or (−)-*trans*-B[*a*]P-dG adducts are excised at lower rates in reconstituted GGR systems compared to their (+)- or (−)-*cis*-B[*a*]P-dG isomers, where the pyrenyl ring moiety exerts helix-stabilizing effects by intercalating between neighboring base pairs [34,46].

A straightforward approach to address the mechanism of bulky lesion recognition has been to identify a critical structural determinant of damaged DNA that provides the initial binding site for the assembly of GGR complexes. Towards that goal, Hess et al. [47] constructed a series of synthetic DNA duplexes to show that a non-distorting adduct is only amenable to excision in a reconstituted GGR system when the substrate also contains a DNA bulge generated by the insertion of 1–3 base pair mismatches. Subsequently, Buterin et al. [48] elaborated on this molecular strategy to generate substrates where a non-distorting adduct is accompanied by

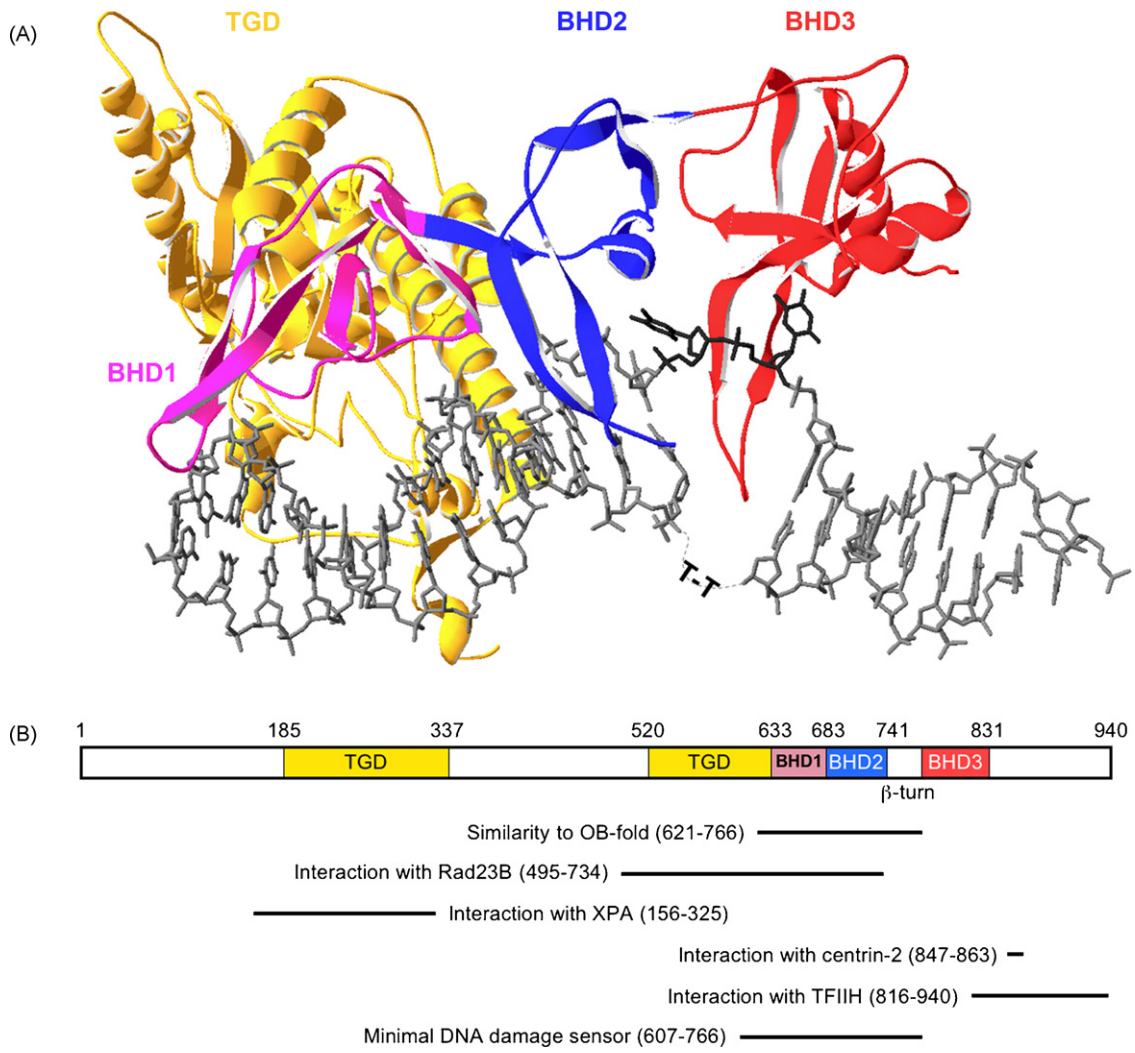

Fig. 2. Structure of XPC protein inferred from the yeast (*Saccaromyces cerevisiae*) Rad4 homolog. (A) Ribbon diagram of the crystal structure of a Rad4 protein fragment (residues 123–632) in complex with heteroduplex DNA carrying a CPD lesion [39]. Multiple Rad4 domains interact with the DNA substrate: TGD (gold), BHD1 (magenta), BHD2 (blue) and BHD3 (red). T-T denotes the CPD, which is totally expelled from the duplex. The figure was made with the Swiss-PdbViewer using the coordinates PDB 2QSG. (B) Scheme of the homologous domains in the human XPC sequence. Also shown are the region of sequence similarity with OB-folds [42], the domains involved in interactions with Rad23B [44], XPA [41], centrin-2 [30] and TFIIH [44], as well as the newly identified minimal DNA damage sensor interface [54].

local duplex deformations in opposite directions relative to the long axis of DNA. They discovered that the target adduct becomes refractory to GGR activity when, by deletion of 3 nucleotides in the undamaged strand, only the adduct-carrying sequence is bulged out of the double helix. In contrast, the same non-distorting adduct is efficiently excised when, by insertion of 3 nucleotides in the undamaged strand, the opposing native strand is bulged out of the double helix. These findings obtained with artificial constructs were confirmed by the observation that at least one destabilized nucleotide in the undamaged strand is necessary to attract the GGR system to B[*a*]P or acetylaminofluorene carcinogen–DNA adducts. Also, excision activity was suppressed by various backbone or base modifications introduced in the undamaged strand across lesion sites indicating that adduct removal involves intimate contacts with the distorted but chemically intact complementary strand [48].

Collectively, these findings converge on the conclusion that XPC protein initiates the GGR reaction by detecting non-hydrogen-bonded bases on the undamaged side of the double helix. In agreement with the identification of an amino acid sequence related to single-stranded DNA-binding motifs (see Section 3), we found that purified XPC protein indeed displays a strong preference for single-stranded oligonucleotides over duplexes of the same length. Surprisingly, XPC exhibits an unfavorable binding to damaged single-stranded oligonucleotides compared to the more efficient interaction with native counterparts [33,42]. This exquisite affinity for single-stranded conformations, in combination with its aversion to interact with damaged single strands, confirms that XPC protein binds primarily to non-hybridizing nucleotides in the undamaged strand, where it makes close interactions with backbone moieties and bases of the normal complementary sequence, in order to load downstream GGR subunits onto damaged substrates. This mechanism has been defined as "indirect conformational readout" because XPC protein detects an abnormal conformational feature in the undamaged strand rather than recognizing specifically modified groups in the damaged sequence [42]. Further support for this unprecedented mode of DNA lesion recognition has been provided by the Rad4 crystal structure, where the BHD2/BHD3 region interacting with the target site makes contacts exclusively with the native complementary strand (Fig. 2A). Conversely, absolutely no interactions occur between Rad4 protein and the modified bases, which are expelled from the recognition complex [39]. This inverted mode of DNA quality control presents the obvious advantage that the

initial sensor does not need to recognize the adducts themselves and, as outlined before, actually avoids close contacts with damaged residues. The general affinity for destabilized DNA sites may facilitate other repair processes, as XPC has been shown to interact with 3-methyladenine DNA glycosylase [49], thymine DNA glycosylase [50] and 8-oxoguanine DNA glycosylase [6]. It is relevant to note that even a subtle 8-oxoguanine lesion perturbs the thermodynamic stability of the duplex [51]. Accordingly, the XPC complex may provide a molecular platform not only for the loading of GGR players onto damaged DNA, but also for the recruitment of a battery of enzymes involved in base excision or other repair pathways.

5. Dynamic search for DNA lesions in the physiologic chromatin context

In cultured mammalian cells, the nuclear distribution of XPC protein correlates with the degree of DNA condensation yielding a typical chromatin-like pattern. Photobleaching experiments indicate that this non-homogenous distribution reflects a tight association with native DNA. In fact, unlike other GGR subunits, XPC protein is not freely mobile in the nuclear compartment, presumably due to constitutive interactions with the normal DNA helix [52,53].

The apparently tight association of XPC protein with undamaged DNA raises the question of how this recognition factor scrutinizes the genome to detect rare aberrant sites among a vast background of the native nucleic acid. In order to address this fundamental issue, we took advantage of fluorescence-based imaging techniques to visualize the mobility of XPC molecules at work in the chromatin context. Real-time kinetics (based on laser-induced high-resolution tracks of UV lesions) and protein dynamics studies (based on fluorescence recovery after photobleaching) were combined to bidirectional truncation analyses, thus revealing that a surprisingly short recognition hotspot, comprising ~15% of human XPC, is necessary and sufficient to detect UV lesions in living cells [54]. This minimal sensor interface of human XPC includes BHD1 and BHD2, together with a short adjacent motif that folds into a β-turn structure (Fig. 2B), but not BHD3, which was thought to represent the primary lesion recognition module on the basis of the Rad4 crystal structure [39]. On its own, a purified polypeptide fragment consisting only of BHD1 and BHD2 displays a preference for heteroduplex over homoduplex and single-stranded oligonucleotides, confirming that the newly identified minimal sensor interface recognizes damaged sites using its inherent affinity for non-hydrogen-bonded bases. However, in living cells, the efficacy of this minimal recognition hotspot depends on the DNA-repulsive action exerted by an additional motif that coincides with the adjacent β-turn structure [54].

In brief, the evidence for a dynamic DNA-repulsive role of the β-turn motif (residues 742–766) in enhancing the efficiency of DNA damage recognition is as follows. First, C-terminal XPC truncates containing this motif display a residual GGR activity, determined by host-cell reactivation assays, that is missing with shorter truncates lacking the β-turn sequence. Second, the partial GGR proficiency observed in the presence of the β-turn structure correlates with a more efficient relocation to tracks of UV lesions. Third, protein dynamics assays performed by photobleaching demonstrate that the β-turn motif confers an increased nuclear mobility in living cells. Fourth, again in photobleaching experiments, only the nuclear mobility of C-terminal XPC truncates containing the β-turn motif is retarded upon UV irradiation, confirming that this critical subdomain increases the rate of DNA damage recognition. Fifth, as outlined before, a polypeptide fragment comprising BHD1 and BHD2 acts as a minimal sensor of DNA damage in living cells only in conjunction with the accompanying β-turn structure. Sixth, biochemical experiments indicate that the nuclear mobility mediated by this β-turn structure is the consequence of a repulsion from native double-stranded DNA. Finally, in the context of full-length XPC protein, the dynamic role of this β-turn structure is supported by a site-directed glutamic acid to lysine substitution. This charge inversion was introduced on the assumption that it may mitigate repulsive electrostatic forces between the negatively charged protein side chain and phosphate moieties in the DNA backbone. As expected, the tested charge inversion increases the affinity for native DNA, thus generating mutant XPC molecules that display a reduced nuclear mobility and diminished GGR activity [54]. In conclusion, these novel findings converge on a key role of the β-turn structure in regulating the dynamic interplay with normal duplex DNA. By virtue of its DNA-repellent activity, this subdomain facilitates damage recognition by providing sufficient mobility to XPC molecules searching for lesions in the genome.

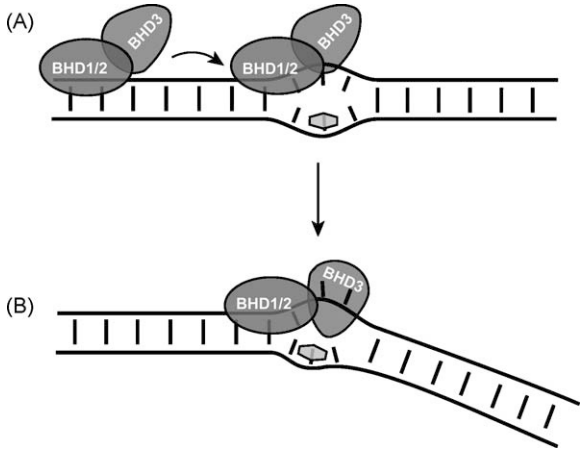

Fig. 3. Two-stage detection of DNA lesions by XPC protein. (A) The minimal sensor interface, consisting of BHD1, BHD2 and the β-turn structure, scrutinizes base pair integrity and forms a labile nucleoprotein intermediate in the proximity to non-hydrogen-bonded bases. (B) The single-stranded DNA-binding activity of BHD3 promotes the subsequent transition to a stable recognition complex by capturing extrahelically oscillating nucleotides in the undamaged strand.

6. Two-stage discrimination process

Although the BHD3 segment of XPC protein and its long protruding β-hairpin are not required for the initial damage sensing process (Section 5), photobleaching experiments in living cells demonstrate that this additional domain is responsible for the formation of stable nucleoprotein complexes, thus generating an immobile fraction of XPC protein in response to UV irradiation [54]. The biochemical analysis of purified fragments shows that, in contrast to the BHD1/BHD2/β-turn minimal sensor, which displays a preference for non-hydrogen-bonded bases in duplex DNA, BHD3 confers an exquisite selectivity for single-stranded DNA conformations. In fact, like full-length XPC protein [42], a polypeptide fragment covering BHD1–BHD3 binds preferentially to single-stranded oligonucleotides. From these findings, it appears that BHD3 does not participate in the early and transient recognition intermediate but, instead, facilitates the subsequent stabilization of a repair-initiating nucleoprotein complex using its single-stranded DNA-binding activity to encircle the strand across lesion sites.

Taken together, our recent studies of XPC kinetics and dynamics point to a two-stage discrimination mechanism by which XPC protein carries out its versatile recognition function (Fig. 3). This two-stage process obviates the difficulty of probing every genomic base pair for its susceptibility to undergo β-hairpin insertion, which is one of the principal features of the reported Rad4 crystal structure

[39]. Instead, the rapid and energetically less demanding search conducted by the dynamic BHD1/BHD2/β-turn interface is likely to precede the more extensive conformational adjustments required for the β-hairpin intrusion. As illustrated in Fig. 3, this initial search leads to the detection of non-hydrogen-bonded bases that are more prone than native residues to be displaced from the double helix by engagement of the β-hairpin. A critical step of this two-stage quality control process is the transition from an initially labile sensor intermediate to the more stable ultimate recognition complex. It is likely that the energetic cost of this nucleoprotein transition is lowered by damage-induced strand oscillations appearing primarily on the undamaged side of the double helix [8], thus displacing the unstable nucleotides into an extrahelical position where they are easily captured by the single-stranded DNA-binding motif of XPC protein. However, it is also possible that Rad23B or centrin-2 may promote the two-stage discrimination process of XPC protein by accelerating the nucleoprotein rearrangements required for engagement of the β-hairpin with damaged sites.

7. The special case of CPD recognition

Another interaction partner of XPC is the UV-damaged DNA-binding (UV-DDB) protein. This factor has been isolated from tissue extracts in view of its characteristic binding to UV-irradiated DNA [55] and, indeed, UV-DDB displays the highest reported affinity for substrates containing 6-4PPs and CPDs [56–58]. UV-DDB consists of p127 (DDB1) and p48 (DDB2), with the small subunit being encoded by the *XPE* gene [59–61]. A recent crystallographic analysis demonstrated that the binding of UV-DDB to UV lesions is entirely mediated by the DDB2 subunit, which accommodates the crosslinked pyrimidines into a specialized binding pocket and inserts a three-amino acid hairpin into the DNA minor groove [62]. DDB1, on the other hand, is an adaptor that connects the Cul4A-RBX1 ubiquitin ligase to WD40-repeat target proteins [63,64], including DDB2 itself [65,66]. Other known substrates of the Cul4A-RBX1-DDB1 ubiquitin ligase include XPC [67] as well as the core histones H2A, H3 and H4 [68,69].

Although CPDs represent the most frequent lesions generated by sunlight, this particular type of DNA injury escapes direct detection by the XPC complex because it causes only a low degree of structural perturbation. The problem of CPD recognition is exemplified by XP-E cells, which are heavily compromised in the repair of CPDs due to their defective UV-DDB activity, but nevertheless retain the ability to excise 6-4PPs [70,71]. Similarly, rodent cells that fail to express DDB2 protein, as a consequence of promoter methylation, are inefficient in CPD repair [72]. The DDB2 subunit rapidly accumulates at sites of UV-induced DNA lesions and the recruitment of XPC protein to DNA repair foci containing exclusively CPDs is dependent on the UV-DDB complex [73,74]. Two major hypotheses have been forwarded for the mechanism by which UV-DDB contributes to the recognition of UV lesions. The handover hypothesis has been proposed on the basis of *in vitro* assays indicating that ubiquitin modulates the DNA-binding affinity of DDB2 and XPC [67]. In this scenario, UV-DDB recognizes UV lesions and recruits XPC protein through direct protein–protein interactions. Subsequently, polyubiquitylation of DDB2 reduces its affinity for DNA and results in degradation, whereas polyubiquitylation of XPC preserves its affinity for the DNA substrate [67]. The chromatin remodeling hypothesis is prompted by the observation that DDB2 is not absolutely required for the excision of CPDs by reconstituted GGR systems using naked DNA as the substrate [74]. This finding may be taken as evidence in favor of a function of UV-DDB in mediating a local relaxation of chromatin, which in turn facilitates XPC binding to damaged sites [68,69]. Additionally, the recently discovered two-stage discrimination process of XPC protein (Fig. 3) raises the possibility that UV-DDB may act in an analogous two-step manner. First, UV-DDB may bypass the initial sensing process, which is ineffective for CPDs, through direct XPC recruitment as postulated in the handover hypothesis. Subsequently, UV-DDB may coordinate the correct positioning of the BHD1–BHD3 motifs onto the undamaged strand and trigger the β-hairpin insertion at CPD sites.

8. Conclusion

The earlier hypothesis that XPC protein simply detects the single-stranded character of lesion sites [42] has been revisited in light of recent findings that this versatile sensor adopts a two-stage mechanism of substrate discrimination [54]. As illustrated in Fig. 3, XPC protein deploys a dynamic interface to screen for non-hydrogen-bonded bases in duplex DNA before undergoing tight interactions mediated by its intrinsic single-stranded DNA-binding activity. Both stages of this substrate discrimination process are directed to the native complementary strand across lesion sites, such that this early recognition step becomes independent of the variable chemistry of damaged sites, thereby broadening the spectrum of DNA lesions that can be channeled into the versatile GGR system. It is important to point out that XPC protein detects non-hydrogen-bonded bases even in the absence of DNA lesions, implying the existence of "proofreading" or "damage verification" factors in the GGR pathway. Candidate mechanisms for this downstream function are the enzymatic scanning by DNA helicases [75] or the sensing of DNA bendability by XPA protein [76,77]. The participation of a scanning mechanism, involving active translocation along the DNA molecule, is supported by our observation that an effective double check process, leading to excision, still takes place on composite substrates where the site of XPC binding is physically dislocated from the target adduct [78].

Acknowledgments

Work in the authors' laboratory is supported by the Swiss National Science Foundation (grant 31003A-127499) and by Oncosuisse (grant KLS-01827-02-2006).

References

[1] E.C. Friedberg, G.C. Walker, W. Siede, R.D. Wood, R.A. Schultz, T. Ellenberger, DNA Repair and Mutagenesis, ASM Press, Washington, D.C., 2006.
[2] J.H. Hoeijmakers, Genome maintenance mechanisms for preventing cancer, Nature 411 (2001) 366–374.
[3] A. Sancar, DNA excision repair, Annu. Rev. Biochem. 65 (1996) 43–81.
[4] R.D. Wood, Nucleotide excision repair in mammalian cells, J. Biol. Chem. 272 (1997) 23465–23468.
[5] I. Kuraoka, C. Bender, A. Romieu, J. Cadet, R.D. Wood, T. Lindahl, Removal of oxygen free-radical-induced 5′,8-purine cyclodeoxynucleosides from DNA by the nucleotide excision-repair pathway in human cells, Proc. Natl. Acad. Sci. U.S.A. 97 (2000) 3832–3837.
[6] M. D'Errico, E. Parlanti, M. Teson, B.M. de Jesus, P. Degan, A. Calcagnile, P. Jaruga, M. Bjoras, M. Crescenzi, A.M. Pedrini, J.M. Egly, G. Zambruno, M. Stefanini, M. Dizdaroglu, E. Dogliotti, New functions of XPC in the protection of human skin cells from oxidative damage, EMBO J. 25 (2006) 4305–4315.
[7] K.A. Johnson, S.P. Fink, L.J. Marnett, Repair of propanodeoxyguanosine by nucleotide excision repair *in vivo* and *in vitro*, J. Biol. Chem. 272 (1997) 11434–11438.
[8] O. Maillard, U. Camenisch, F.C. Clement, K.B. Blagoev, H. Naegeli, DNA repair triggered by sensors of helical dynamics, Trends Biochem. Sci. 32 (2007) 494–499.
[9] P.C. Hanawalt, G. Spivak, Transcription-coupled DNA repair: two decades of progress and surprises, Nat. Rev. Mol. Cell Biol. 9 (2008) 958–970.
[10] E.C. Friedberg, How nucleotide excision repair protects against cancer, Nat. Rev. Cancer 1 (2001) 22–33.
[11] L.J. Niedernhofer, Tissue-specific accelerated aging in nucleotide excision repair deficiency, Mech. Ageing Dev. 129 (2008) 408–415.
[12] K. Sugasawa, J.M. Ng, C. Masutani, S. Iwai, P.J. van der Spek, A.P. Eker, F. Hanaoka, D. Bootsma, J.H. Hoeijmakers, Xeroderma pigmentosum group C protein complex is the initiator of global genome nucleotide excision repair, Mol. Cell 2 (1998) 223–232.

[13] M. Volker, M.J. Mone, P. Karmakar, A. van Hoffen, W. Schul, W. Vermeulen, J.H. Hoeijmakers, R. van Driel, A.A. van Zeeland, L.H. Mullenders, Sequential assembly of the nucleotide excision repair factors in vivo, Mol. Cell 8 (2001) 213–224.
[14] D. Mu, D.S. Hsu, A. Sancar, Reaction mechanism of human DNA repair excision nuclease, J. Biol. Chem. 271 (1996) 8285–8294.
[15] S.J. Araujo, F. Tirode, F. Coin, H. Pospiech, J.E. Syväoja, M. Stucki, U. Hübscher, J.-M. Egly, R.D. Wood, Nucleotide excision repair of DNA with recombinant human proteins: definition of the minimal set of factors, active forms of TFIIH, and modulation by CAK, Genes Dev. 14 (2000) 349–359.
[16] E. Evans, J. Fellows, A. Coffer, R.D. Wood, Open complex formation around a lesion during nucleotide excision repair provides a structure for cleavage by human XPG protein, EMBO J. 16 (1997) 625–638.
[17] M. Wakasugi, A. Sancar, Assembly, subunit composition, and footprint of human DNA repair excision nuclease, Proc. Natl. Acad. Sci. U.S.A. 95 (1998) 6669–6674.
[18] F. Tirode, D. Busso, F. Coin, J.M. Egly, Reconstitution of the transcription factor TFIIH: assignment of functions for the three enzymatic subunits, XPB, XPD, and cdk7, Mol. Cell 3 (1999) 87–95.
[19] A.M. Sijbers, W.L. de Laat, R.R. Ariza, M. Biggerstaff, Y.F. Wei, J.C. Moggs, K.C. Carter, B.K. Shell, E. Evans, M.C. de Jong, S. Rademakers, J. de Rooij, N.G. Jaspers, J.H. Hoeijmakers, R.D. Wood, Xeroderma pigmentosum group F caused by a defect in a structure-specific DNA repair endonuclease, Cell 86 (1996) 811–822.
[20] A. O'Donovan, A.A. Davies, J.C. Moggs, S.C. West, R.D. Wood, XPG endonuclease makes the 3′ incision in human DNA nucleotide excision repair, Nature 371 (1994) 432–435.
[21] L. Staresincic, A.F. Fagbemi, J.H. Enzlin, A.M. Gourdin, N. Wijgers, I. Dunand-Sauthier, G. Giglia-Mari, S.G. Clarkson, W. Vermeulen, O.D. Schärer, Coordination of dual incision and repair synthesis in human nucleotide excision repair, EMBO J. 28 (2009) 1111–1120.
[22] J.C. Huang, D.L. Svoboda, J.T. Reardon, A. Sancar, Human nucleotide excision nuclease removes thymine dimers from DNA by incising the 22nd phosphodiester bond 5′ and the 6th phosphodiester bond 3′ to the photodimer, Proc. Natl. Acad. Sci. U.S.A. 89 (1992) 3664–3668.
[23] J.G. Moggs, K.J. Yarema, J.M. Essigmann, R.D. Wood, Analysis of incision sites produced by human cell extracts and purified proteins during nucleotide excision repair of a 1,3-intrastrand d(GpTpG)-cisplatin adduct, J. Biol. Chem. 271 (1996) 7177–7186.
[24] M.K. Shivji, V.N. Podust, U. Hübscher, R.D. Wood, Nucleotide excision repair DNA synthesis by DNA polymerase epsilon in the presence of PCNA, RCF, and RPA, Biochemistry 34 (1995) 5011–5017.
[25] T. Ogi, A.R. Lehmann, The Y-family DNA polymerase kappa (pol kappa) functions in mammalian nucleotide-excision repair, Nat. Cell Biol. 8 (2006) 640–642.
[26] A. Aboussekhra, M. Biggerstaff, M.K. Shivji, J.A. Vilpo, V. Moncollin, V.N. Podust, M. Protic, U. Hübscher, J.M. Egly, R.D. Wood, Mammalian DNA nucleotide excision repair reconstituted with purified protein components, Cell 80 (1995) 859–868.
[27] J. Moser, H. Kool, I. Giakzidis, K. Caldecott, L.H. Mullenders, M.I. Fousteri, Sealing of chromosomal DNA nicks during nucleotide excision repair requires XRCC1 and DNA ligase III alpha in a cell-cycle-specific manner, Mol. Cell 27 (2007) 311–323.
[28] C. Masutani, K. Sugasawa, J. Yanagisawa, T. Sonoyama, M. Ui, T. Enomoto, K. Takio, K. Tanaka, P.J. van der Spek, D. Bootsma, J.H. Hoeijmakers, F. Hanaoka, Purification and cloning of a nucleotide excision repair complex involving the xeroderma pigmentosum group C protein and a human homologue of yeast RAD23, EMBO J. 13 (1994) 1831–1843.
[29] M. Araki, C. Masutani, M. Takemura, A. Uchida, K. Sugasawa, J. Kondoh, Y. Ohkuma, F. Hanaoka, Centrosome protein centrin 2/caltractin 1 is part of the xeroderma pigmentosum group C complex that initiates global genome nucleotide excision repair, J. Biol. Chem. 276 (2001) 18665–18672.
[30] R. Nishi, Y. Okuda, E. Watanabe, T. Mori, S. Iwai, C. Masutani, K. Sugasawa, F. Hanaoka, Centrin 2 stimulates nucleotide excision repair by interacting with xeroderma pigmentosum group C protein, Mol. Cell. Biol. 25 (2005) 5664–5674.
[31] J.M. Ng, W. Vermeulen, G.T. van der Horst, S. Bergink, K. Sugasawa, H. Vrieling, J.H. Hoeijmakers, A novel regulation mechanism of DNA repair by damage-induced and RAD23-dependent stabilization of xeroderma pigmentosum group C protein, Genes Dev. 17 (2003) 1630–1645.
[32] D. Batty, V. Rapic'-Otrin, A.S. Levine, R.D. Wood, Stable binding of human XPC complex to irradiated DNA confers strong discrimination for damaged sites, J. Mol. Biol. 300 (2000) 275–290.
[33] K.S. Trego, J.J. Turchi, Pre-steady-state binding of damaged DNA by XPC-hHR23B reveals a kinetic mechanism for damage discrimination, Biochemistry 45 (2006) 1961–1969.
[34] V. Mocquet, K. Kropachev, M. Kolbanovskiy, A. Kolbanovskiy, A. Tapias, Y. Cai, S. Broyde, N.E. Geacintov, J.M. Egly, The human DNA repair factor XPC-HR23B distinguishes stereoisomeric benzo[*a*]pyrenyl-DNA lesions, EMBO J. 26 (2007) 2923–2932.
[35] K. Sugasawa, T. Okamoto, Y. Shimizu, C. Masutani, S. Iwai, F. Hanaoka, A multistep damage recognition mechanism for global genomic nucleotide excision repair, Genes Dev. 15 (2001) 507–521.
[36] K. Sugasawa, Y. Shimizu, S. Iwai, F. Hanaoka, A molecular mechanism for DNA damage recognition by the xeroderma pigmentosum group C protein complex, DNA Repair 1 (2002) 95–107.
[37] A. Janicijevic, K. Sugasawa, Y. Shimizu, F. Hanaoka, N. Wijgers, M. Djurica, J.H. Hoeijmakers, C. Wyman, DNA bending by the human damage recognition complex XPC-HR23B, DNA Repair (Amst) 2 (2003) 325–336.
[38] E. Evans, J.G. Moggs, J.R. Hwang, J.M. Egly, R.D. Wood, Mechanism of open complex and dual incision formation by human nucleotide excision repair factors, EMBO J. 16 (1997) 6559–6573.
[39] J.-H. Min, N.P. Pavletich, Recognition of DNA damage by the Rad4 nucleotide excision repair protein, Nature 449 (2007) 570–575.
[40] V. Anantharaman, E.V. Koonin, L. Aravind, Peptide-N-glycanases and DNA repair proteins, Xp-C/Rad4, are, respectively, active and inactivated enzymes sharing a common transglutaminase fold, Hum. Mol. Genet. 10 (2001) 1627–1630.
[41] C.G. Bunick, M.R. Miller, B.E. Fuller, E. Fanning, W.J. Chazin, Biochemical and structural domain analysis of xeroderma pigmentosum complementation group C protein, Biochemistry 45 (2006) 14965–14979.
[42] O. Maillard, S. Solyom, H. Naegeli, An aromatic sensor with aversion to damaged strands confers versatility to DNA repair, PLoS Biol. 5 (2007) e79.
[43] L. Li, X. Lu, C. Peterson, R. Legerski, XPC interacts with both HHR23B and HHR23A in vivo, Mutat. Res. 383 (1997) 197–203.
[44] A. Uchida, K. Sugasawa, C. Masutani, N. Dohmae, M. Araki, M. Yokoi, Y. Ohkuma, F. Hanaoka, The carboxy-terminal domain of the XPC protein plays a crucial role in nucleotide excision repair through interactions with transcription factor IIH, DNA Repair 1 (2002) 449–461.
[45] D. Gunz, M.T. Hess, H. Naegeli, Recognition of DNA adducts by human nucleotide excision repair. Evidence for a thermodynamic probing mechanism, J. Biol. Chem. 271 (1996) 25089–25098.
[46] M.T. Hess, D. Gunz, N. Luneva, N.E. Geacintov, H. Naegeli, Base pair conformation-dependent excision of benzo[a]pyrene diol epoxide-guanine adducts by human nucleotide excision repair enzymes, Mol. Cell. Biol. 17 (1997) 7069–7076.
[47] M.T. Hess, U. Schwitter, M. Petretta, B. Giese, H. Naegeli, Bipartite substrate discrimination by human nucleotide excision repair, Proc. Natl. Acad. Sci. U.S.A. 94 (1997) 6664–6669.
[48] T. Buterin, C. Meyer, B. Giese, H. Naegeli, DNA quality control by conformational readout on the undamaged strand of the double helix, Chem. Biol. 12 (2005) 913–922.
[49] F. Miao, M. Bouziane, R. Dammann, C. Masutani, F. Hanaoka, G. Pfeifer, T.R. O'Connor, 3-Methyladenine-DNA glycosylase (MPG protein) interacts with human RAD23 proteins, J. Biol. Chem. 275 (2000) 28433–28438.
[50] Y. Shimizu, S. Iwai, F. Hanaoka, K. Sugasawa, Xeroderma pigmentosum group C protein interacts physically and functionally with thymine DNA glycosylase, EMBO J. 22 (2003) 164–173.
[51] G.E. Plum, A.P. Grollman, F. Johnson, K.J. Breslauer, Influence of the oxidatively damaged adduct 8-oxodeoxyguanosine on the conformation, energetics, and thermodynamic stability of a DNA duplex, Biochemistry 34 (1995) 16148–16160.
[52] D. Hoogstraten, S. Bergink, V.H.M. Verbiest, M.S. Luijsterburg, B. Geverts, A. Raams, C. Dinant, J.H.J. Hoeijmakers, W. Vermeulen, A.B. Houtsmuller, Versatile DNA damage detection by the global genome nucleotide excision repair protein XPC, J. Cell Sci. 121 (2008) 2850–2859.
[53] L. Solimando, M.S. Luijsterburg, L. Vecchio, W. Vermeulen, R. van Driel, S. Fakan, Spatial organization of nucleotide excision repair proteins after UV-induced DNA damage in the human cell nucleus, J. Cell Sci. 122 (2009) 83–91.
[54] U. Camenisch, D. Träutlein, F. Clement, J. Fei, A. Leitenstorfer, E. Ferrando-May, H. Naegeli, Two-stage dynamic DNA quality check by xeroderma pigmentosum group C protein, EMBO J. 28 (2009) 2387–2399.
[55] R.S. Feldberg, L. Grossman, A DNA binding protein from human placenta specific for ultraviolet damaged DNA, Biochemistry 15 (1976) 2402–2408.
[56] B.J. Hwang, G. Chu, Purification and characterization of a human protein that binds to damaged DNA, Biochemistry 32 (1993) 1657–1666.
[57] J.T. Reardon, A.F. Nichols, S. Keeney, C.A. Smith, J.S. Taylor, S. Linn, A. Sancar, Comparative analysis of binding of human damaged DNA-binding protein (XPE) and *Escherichia coli* damage recognition protein (UvrA) to the major ultraviolet photoproducts: T[c,s]T, T[t,s]T, T[6-4]T, and T[Dewar]T, J. Biol. Chem. 268 (1993) 21301–21308.
[58] B.O. Wittschieben, S. Iwai, R.D. Wood, DDB1–DDB2 (xeroderma pigmentosum group E) protein complex recognizes a cyclobutane pyrimidine dimer, mismatches, apurinic/apyrimidinic sites, and compound lesions in DNA, J. Biol. Chem. 280 (2005) 39982–39989.
[59] R. Dualan, T. Brody, S. Keeney, A.F. Nichols, A. Admon, S. Linn, Chromosomal localization and cDNA cloning of the genes (*DDB1* and *DDB2*) for the p127 and p48 subunits of a human damage-specific DNA binding protein, Genomics 29 (1995) 62–69.
[60] A.F. Nichols, P. Ong, S. Linn, Mutations specific to the xeroderma pigmentosum group E $DDB^{(-)}$ phenotype, J. Biol. Chem. 271 (1996) 24317–24320.
[61] V. Rapic-Otrin, V. Navazza, T. Nardo, E. Botta, M. McLenigan, D.C. Bisi, A.S. Levine, M. Stefanini, True XP group E patients have a defective UV-damaged DNA binding protein complex and mutations in *DDB2* which reveal the functional domains of its p48 product, Hum. Mol. Genet. 12 (2003) 1507–1522.
[62] A. Scrima, R. Konickova, B.K. Czyzewski, Y. Kawasaki, P.D. Jeffrey, R. Groisman, Y. Nakatani, S. Iwai, N.P. Pavletich, N.H. Thomä, Structural basis of UV DNA-damage recognition by the DDB1– DDB2 complex, Cell 135 (2008) 1213–1223.
[63] P. Shiyanov, A. Nag, P. Raychaudhuri, Cullin 4A associates with the UV-damaged DNA-binding protein DDB, J. Biol. Chem. 274 (1999) 35309–35312.
[64] R. Groisman, J. Polanowska, I. Kuraoka, J. Sawada, M. Saijo, R. Drapkin, A.F. Kisselev, K. Tanaka, Y. Nakatani, The ubiquitin ligase activity in the DDB2 and CSA

complexes is differentially regulated by the COP9 signalosome in response to DNA damage, Cell 113 (2003) 357–367.
[65] X. Chen, Y. Zhang, L. Douglas, P. Zhou, UV-damaged DNA-binding proteins are targets of CUL-4A-mediated ubiquitination and degradation, J. Biol. Chem. 276 (2001) 48175–48182.
[66] A. Nag, T. Bondar, S. Shiv, P. Raychaudhuri, The xeroderma pigmentosum group E gene product *DDB2* is a specific target of cullin 4A in mammalian cells, Mol. Cell. Biol. 21 (2001) 6738–6747.
[67] K. Sugasawa, Y. Okuda, M. Saijo, R. Nishi, N. Matsuda, G. Chu, T. Mori, S. Iwai, K. Tanaka, K. Tanaka, F. Hanaoka, UV-induced ubiquitylation of XPC protein mediated by UV-DDB-ubiquitin ligase complex, Cell 121 (2005) 387–400.
[68] H. Wang, L. Zhai, J. Xu, H.Y. Joo, S. Jackson, H. Erdjument-Bromage, P. Tempst, Y. Xiong, Y. Zhang, Histone H3 and H4 ubiquitylation by the CUL4-DDB-ROC1 ubiquitin ligase facilitates cellular response to DNA damage, Mol. Cell 22 (2006) 383–394.
[69] M.G. Kapetanaki, J. Guerrero-Santoro, D.C. Bisi, C.L. Hsieh, V. Rapic-Otrin, A.S. Levine, The DDB1-CUL4ADDB2 ubiquitin ligase is deficient in xeroderma pigmentosum group E and targets histone H2A at UV-damaged DNA sites, Proc. Natl. Acad. Sci. U.S.A. 103 (2006) 2588–2593.
[70] B.J. Hwang, S. Toering, U. Francke, G. Chu, p48 activates a UV-damaged-DNA binding factor and is defective in xeroderma pigmentosum group E cells that lack binding activity, Mol. Cell. Biol. 18 (1998) 4391–4399.
[71] J.Y. Tang, B.J. Hwang, J.M. Ford, P.C. Hanawalt, G. Chu, Xeroderma pigmentosum p48 gene enhances global genomic repair and suppresses UV-induced mutagenesis, Mol. Cell 5 (2000) 737–744.
[72] M.E. Fitch, S. Nakajima, A. Yasui, J.M. Ford, In vivo recruitment of XPC to UV-induced cyclobutane pyrimidine dimers by the DDB2 gene product, J. Biol. Chem. 278 (2003) 46906–46910.
[73] J. Moser, M. Volker, H. Kool, S. Alekseev, H. Vrieling, A. Yasui, A.A. van Zeeland, L.H. Mullenders, The UV-damaged DNA binding protein mediates efficient targeting of the nucleotide excision repair complex to UV-induced photo lesions, DNA Repair 4 (2005) 571–582.
[74] J.T. Reardon, A. Sancar, Recognition and repair of the cyclobutane thymine dimer, a major cause of skin cancers, by the human excision nuclease, Genes Dev. 17 (2003) 2539–2551.
[75] H. Naegeli, L. Bardwell, E.C. Friedberg, The DNA helicase and adenosine triphosphatase activities of yeast Rad3 protein are inhibited by DNA damage, J. Biol. Chem. 267 (1992) 392–398.
[76] U. Camenisch, R. Dip, S.B. Schumacher, B. Schuler, H. Naegeli, Recognition of helical kinks by xeroderma pigmentosum group A protein triggers DNA excision repair, Nat. Struct. Mol. Biol. 13 (2006) 278–284.
[77] U. Camenisch, R. Dip, M. Vitanescu, H. Naegeli, Xeroderma pigmentosum complementation group A protein is driven to nucleotide excision repair sites by the electrostatic potential of distorted DNA, DNA Repair 6 (2007) 1819–1828.
[78] N. Buschta-Hedayat, T. Buterin, M.T. Hess, M. Missura, H. Naegeli, Recognition of nonhybridizing base pairs during nucleotide excision repair of DNA, Proc. Natl. Acad. Sci. U.S.A. 96 (1999) 6090–6095.

1.7. Introductory opinion:

DNA repair triggered by sensors of helical dynamics

1.7.1. Aims of the study

This opinion paper aims at explaining XPC protein's substrate versatility. It proposes a hypothesis by which NER factors are rapidly recruited to DNA damage by abnormal oscillations in the undamaged DNA strand opposite to base lesions. Furthermore, it points out the sequential assembly of the GGR factors.

1.7.2. Main conclusions

A novel mechanism of damage recognition shows that a local DNA bulge is crucial for NER activity. Additionally, DNA distortions are sensed through interactions with non-damaged flipped-out nucleotides opposite to lesions. This indirect conformational readout is facilitated by increased thermal fluctuations of the damaged double helix thereby enabling one single protein to recognize many different lesions.

1.7.3. Supplementary remarks

When we wrote this paper, the crystal structure of Rad4 was not known yet (*Min* and *Pavletich*, 2007). However, the findings that XPC recognizes helical distortion and destabilized base pairs opposite to DNA lesions has been reinforced by the co-crystallization of Rad4 protein with an oligonucleotide containing a CPD mismatch.
The idea of (aromatic) residues interacting with non-damaged nucleotides of the paper's figure 2 was approved by the structural analysis of Rad4, which showed that several conserved amino acids contact the unpaired bases opposite the lesion site. I picked up this fact in my work (*Clement et al*. 2010, see section 2.1.), where I showed the importance of four residues in damage recognition and hand-over.

The GGR pathway in box 1 is outdated regarding the damage excision. It is now accepted that the 5' incision by XPF takes place before the 3' incision by XPG, and that NER rather works as a 'cut-patch-cut-patch' mechanism since repair synthesis starts immediately after 5' incision (*Staresincic et al*. 2009). This protects the intact DNA strand from staying naked and prone to endonucleases.

The outstanding questions in box 2 are still not fully answered. As for UV-DDB-mediated recognition of CPDs, it is possible that there is a dynamic mechanism similar to XPC (see review in section 3.6.) but there is no evidence for this hypothesis.

1.7.4. Contribution to this paper

I had a share in literature research and in proof-reading of this opinion paper.

1.7.5. Reference

Maillard O, Camenisch U, **Clement FC**, Blagoev KB, and Naegeli H (2007) DNA repair triggered by sensors of helical dynamics. *Trends Bioc Sci* 32: 494-499.

1.7.6. Manuscript

Opinion TRENDS in Biochemical Sciences Vol.32 No.11

DNA repair triggered by sensors of helical dynamics

Olivier Maillard[1], Ulrike Camenisch[1], Flurina C. Clement[1], Krastan B. Blagoev[2] and Hanspeter Naegeli[1]

[1] Institute of Pharmacology and Toxicology, University of Zürich-Vetsuisse, Winterthurerstrasse 260, CH-8057 Zürich, Switzerland
[2] Theoretical Division, Los Alamos National Laboratory, Los Alamos, NM 87545, USA

Nucleotide excision repair is a constitutive stress response that eliminates DNA lesions induced by multiple genotoxic agents. Unlike the immune system, which generates billions of immunoglobulins and T cell receptors for antigen recognition, the nucleotide excision repair complex uses only a few generic factors to detect an astounding diversity of DNA modifications. New data favor an unexpected strategy whereby damage recognition is initiated by the detection of abnormal oscillations in the undamaged strand opposite to DNA lesions. Another core subunit recognizes the increased susceptibility of DNA to be kinked at injured sites. We suggest that early nucleotide excision repair factors gain substrate versatility by avoiding direct contacts with modified residues and exploiting instead the altered dynamics of damaged DNA duplexes.

Versatile DNA damage recognition

The genome is under permanent attack from ultraviolet (UV) radiation, environmental mutagens and endogenous metabolic byproducts that pose a continuous risk to DNA integrity. Given that genome stability represents a fundamental biological challenge, it is not surprising to find intricate networks of repair mechanisms that can cope with these manifold genetic insults. In particular, living organisms of all biological kingdoms are equipped with a multiprotein system that eliminates crosslinks between adjacent bases, primarily cyclobutane pyrimidine dimers, induced by exposure to the UV component of sunlight [1]. This repair pathway, generally known as nucleotide excision repair (NER), is in fact the only cellular mechanism available for the error-free removal of such DNA photoproducts in humans. In addition to intrastrand crosslinks, the same NER pathway also eliminates a wide diversity of base adducts caused by electrophilic chemicals and oxygen radicals [2,3], in addition to protein–DNA crosslinks [4], methylated bases and abasic sites [5]. These different lesions share no common chemical motif that might support a classical 'lock-and-key' recognition scheme, raising the question of how NER systems achieve their characteristic substrate versatility.

The 'cut-and-patch' NER pathway can be broken down into the following steps: (i) recognition of DNA distortions by XPC protein; (ii) verification of DNA lesions by transcription factor IIH (TFIIH), xeroderma pigmentosoum group A (XPA) and replication protein A (RPA); (iii) dual DNA incision; and (iv) DNA repair synthesis (Box 1). It has been demonstrated that four subunits (XPC, TFIIH, XPA and RPA) are necessary and sufficient to form a preincision complex that detects target sites for mammalian NER activity [6,7]. The mechanism by which the few subunits of this versatile recognition intermediate discriminate between damaged substrates and normal double-stranded DNA is an actively investigated area. There is also ongoing discussion regarding the role of an auxiliary factor, referred to as UV-damaged DNA-binding (UV-DDB), in facilitating the excision of cyclobutane pyrimidine dimers, which represent the most abundant type of UV lesion [7,8]. Recent developments in the characterization of XPC protein indicate that this early recognition subunit of the NER pathway operates in an indirect manner by acting as a molecular sensor of the increased dynamics of damaged DNA compared with the more rigid native double helix. In view of these new findings, we propose a counterintuitive hypothesis by which the rapid recruitment of NER factors to DNA damage in mammalian chromosomes is triggered by abnormal strand oscillations or other conformational fluctuations of the undamaged complementary sequence across lesion sites.

Preassembly, stepwise recruitment or random aggregation?

The order of arrival of NER factors has been a matter of intense debate [7,9–11], in part raised by the fact that none of the core proteins seems to display a great enough selectivity to function as a unique sensor of damaged substrates. A full incision complex comprising 20 polypeptides achieves a mass of >1 MDa, but the measurement of nuclear diffusion rates indicates that NER factors are present as separate subunits and not as part of a large repair 'machine'. Also, the fast translocation of these factors to hotspots of DNA damage is more consistent with a sequential recruitment of individual subunits [12]. This stepwise assembly has the advantage that multifunctional components such as TFIIH, RPA or XPF-ERCC1 (a protein dimer composed of xeroderma pigmentosum group F and excision repair cross-complementing 1) can shuttle between transcription, replication, recombination or other parallel pathways. In addition, the sequential recruitment of freely diffusing proteins might be more rapid and efficient than other strategies such as random

Corresponding author: Naegeli, H. (naegelih@vetpharm.unizh.ch).
Available online 25 October 2007.

 doi:10.1016/j.tibs.2007.08.008

Box 1. The human NER reaction and its core subunits

Many human NER proteins are encoded by genes that, when mutated, give rise to xeroderma pigmentosum (XP), an inherited disorder characterized by extreme photosensitivity and a 2000-fold increased incidence of sunlight-induced skin cancer [1,41]. The XP syndrome further involves a greater risk of contracting internal tumors and, in some cases, neurological complications, presumably reflecting the essential role of NER in the removal of endogenous DNA damage. The products of the *XPA–XPG* genes provide the core subunits of an excision complex that comprises approximately 20 polypeptide subunits.

The different NER steps, namely recognition of DNA distortions, verification of base lesions, dual DNA incision and repair synthesis, are illustrated in Figure I, where the substrate carries a benzo[*a*]pyrene diol epoxide adduct. The NER system excises such carcinogen–DNA adducts, in addition to UV photoproducts or other lesions, in the form of oligonucleotide segments that have a length of 24–32 residues [42]. This reaction is generally thought to proceed by a stepwise mechanism initiated by a heterotrimeric factor consisting of XPC, RAD23B (RAD, radiation-sensitive) and CETN2 (centrin-2) [13,14,43]. XPC protein possesses DNA-binding activity, whereas the RAD23B and CETN2 partners exert accessory functions by stabilizing the complex and stimulating its action in DNA repair. UV-damaged DNA-binding (UV-DDB) protein can accelerate the recognition of UV photoproducts [8]. After the initial association with damaged sites, XPC protein mediates the recruitment of transcription factor IIH (TFIIH), followed by replication protein A (RPA), XPA, XPG and, finally, XPF–ERCC1, which is a heterodimer composed of XPF and excision repair cross complementing-1 [44,45].

Four of these early factors (XPC, TFIIH, RPA and XPA) generate a unique recognition intermediate characterized by transient unwinding of the duplex substrate around the lesion. This open intermediate contains 'Y-shaped' double- to single-stranded DNA transitions, which provide a substrate for the junction-specific DNA endonucleases XPF–ERCC1 and XPG [46,47]. By cleaving the damaged strand at the 'Y-shaped' junctions, these two endonucleases act as 'scissors' to cut out DNA damage from the double helix. XPF–ERCC1 makes the 5′ and XPG the 3′ incision. Helical integrity is reconstituted by a downstream DNA synthesis complex consisting of an error-free DNA polymerase (primarily DNA polymerase ε), in conjunction with replication factor C (RFC) and proliferating cell nuclear antigen (PCNA). Subsequently, the newly synthesized DNA repair patches are joined to the pre-existing strands by the action of DNA ligase I [44,48].

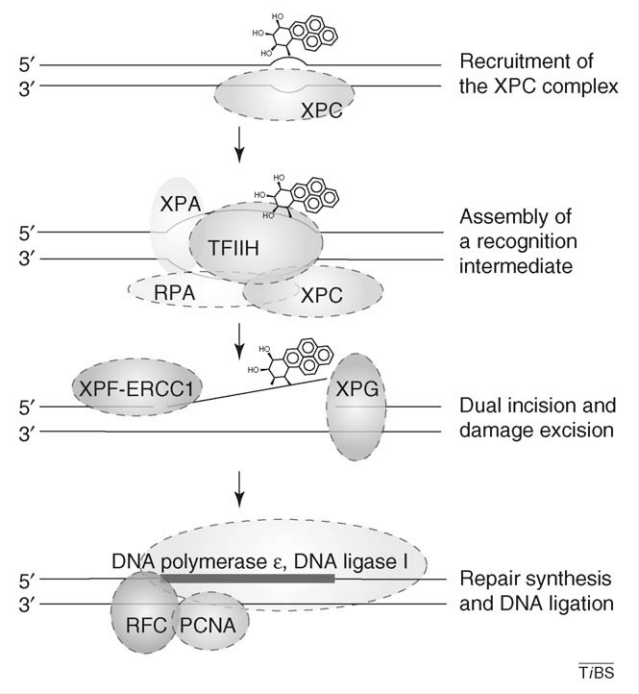

Figure I. The human NER pathway and its core subunits. The damaged strand of the DNA substrate carries a polycyclic aromatic hydrocarbon adduct. See text for abbreviations.

aggregation or the preassembly of large 'repairosome' complexes [12].

The 'XPC first' model is the most widely accepted scenario for the initiation of NER activity (Box 1). This model was instigated by reconstitution experiments aimed at determining the order in which NER proteins are recruited to lesion sites. In one study, damaged plasmids preincubated with XPC were repaired more rapidly in cell extracts than those preincubated with XPA and RPA [13]. Further support for the 'XPC first' model came from the energy dependence of specific NER intermediates [10,11]. ATP is not necessary for the simple association of XPC and TFIIH with damaged DNA fragments, but ATP hydrolysis is absolutely required for the recruitment of XPA and RPA. These observations indicate that the damage-specific binding of XPC is an early ATP-independent step and that DNA unwinding promoted by TFIIH, an energy-dependent process, is needed for the subsequent incorporation of the remaining subunits into the growing NER complex.

The order of assembly has also been examined by monitoring the nuclear trafficking of core NER subunits. For that purpose, cultured human cells were exposed to UV light through filters with small pores to induce localized foci of DNA damage. The mobility of XPC and XPA from unirradiated regions of the nuclei to these damaged foci was monitored by staining each factor with fluorescently tagged antibodies [9]. This approach established that XPC accumulates in DNA repair foci even in the absence of XPA. Instead, XPA, TFIIH, XPG (the 3′ endonuclease) and XPF–ERCC1 do not seem to move to damaged foci when XPC is missing, implying that the lesions have to be recognized by XPC before other subunits can be loaded onto the DNA substrate. Taken together, these different findings converge on the idea that the XPC subunit is the primary initiator of NER assembly.

An attraction for the undamaged side of the double helix

What characteristic feature of damaged DNA induces the recruitment of XPC protein? Hanawalt and Haynes [14] were the first to propose that the need for DNA repair is determined by comparing the conformation of damaged DNA with that of a normal double helix. It was later found that the recognition of different bulky base adducts correlates with the degree to which the duplex is thermodynamically destabilized [15]. More recently, Isaacs and Spielmann [16] concluded that damaged DNA is more easily bent and, therefore, postulated that a greater local flexibility could provide another generic determinant shared by all known NER substrates.

The preference for lesions that lower the melting temperature of duplex DNA has been exploited to test the particular orientation with which the NER subunits align themselves along the double-stranded nucleic acid

molecule. For that purpose, greatly defined DNA substrates were constructed by combining an artificial adduct, known to retain normal hydrogen bonding and stacking interactions [17], with different kinds of conformational distortions. The varying repairability of these synthetic duplexes in human cell extracts confirmed that destabilization of the double helix is a crucial molecular determinant for lesion recognition. In fact, excision was readily detected on composite substrates in which the 'nondistorting' adduct was combined with a DNA bulge generated by the insertion of mismatches or nucleotide loops (Figure 1a). This local disruption of base pairing led to excision regardless of whether the bulge included both strands of the duplex or only the undamaged complementary strand across the adduct (Figure 1a, substrates 2 and 4). More surprising, however, is the observation that no excision took place when the same adduct was combined with a one-sided bulge involving only the damaged strand (Figure 1a, substrate 3). Similarly, the duplex became refractory to excision when both strands at the site of distortion carried a bulky modification (Figure 1a, substrate 5). Thus, this novel approach not only confirmed that a local DNA bulge is indispensable for NER activity but also pointed to an unexpected mechanism in which the early sensing of DNA distortions occurs through an interaction with flipped-out nucleotides on the undamaged side of the double helix [18]. This goes against the conventional dogma asserting that DNA lesion recognition occurs primarily through contacts with damaged bases or at least some components of the damaged strand. Instead, the experiments of Figure 1a indicate that mammalian NER factors are initially loaded onto the opposite undamaged sequence of the double helix, from where the lesion is approached and subsequently repaired. Additional studies showed that the recognition of extruded bases in the undamaged complementary strand is also crucial for the analogous NER process in bacteria [19].

Damage-induced DNA oscillations

The model of conformational 'readout' on the undamaged side of the double helix, outlined in the previous section, raises the question of whether naturally arising DNA lesions can indeed destabilize the double helix to a sufficient degree to induce a local bulge with single-stranded character. New insights have come from mathematical models that describe the complex macromolecular dynamics of modified nucleic acid substrates. In fact, double-stranded DNA is not a static entity, and even the native double helix is constantly in motion as a result of thermal fluctuations. Normally, the two strands of duplex DNA oscillate with respect to each other in a sequence-dependent manner, such that the distance between complementary strands exhibits fast and small variations [20]. In the absence of DNA damage, however, the picosecond-to-nanosecond timescale of these spontaneous vibrations is too short to be recognized by repair factors. In contrast, normal base pairing and stacking interactions are weakened in the presence of DNA adducts, giving rise to much more prominent strand movements.

Recent mathematical calculations led to the prediction that even subtly distorting lesions, such as cyclobutane pyrimidine dimers, provoke longer-lived and larger openings between the two strands of the double helix relative to undamaged DNA [21]. The frequency of these large strand fluctuations is 25 times greater at photoproduct positions than in undamaged DNA sequences, and, as illustrated in Figure 1b, the amplitude of these oscillations is drastically increased relative to the undamaged control. Another important prediction is that these dynamic changes triggered by base damage are expected to involve mainly oscillations of the intact sequence opposing the lesion, because the strand containing base adducts is less flexible than native DNA [21].

To summarize, the paradigm of bipyrimidine photoproducts shows that DNA lesions have the ability to induce dynamic changes of the duplex, involving transient

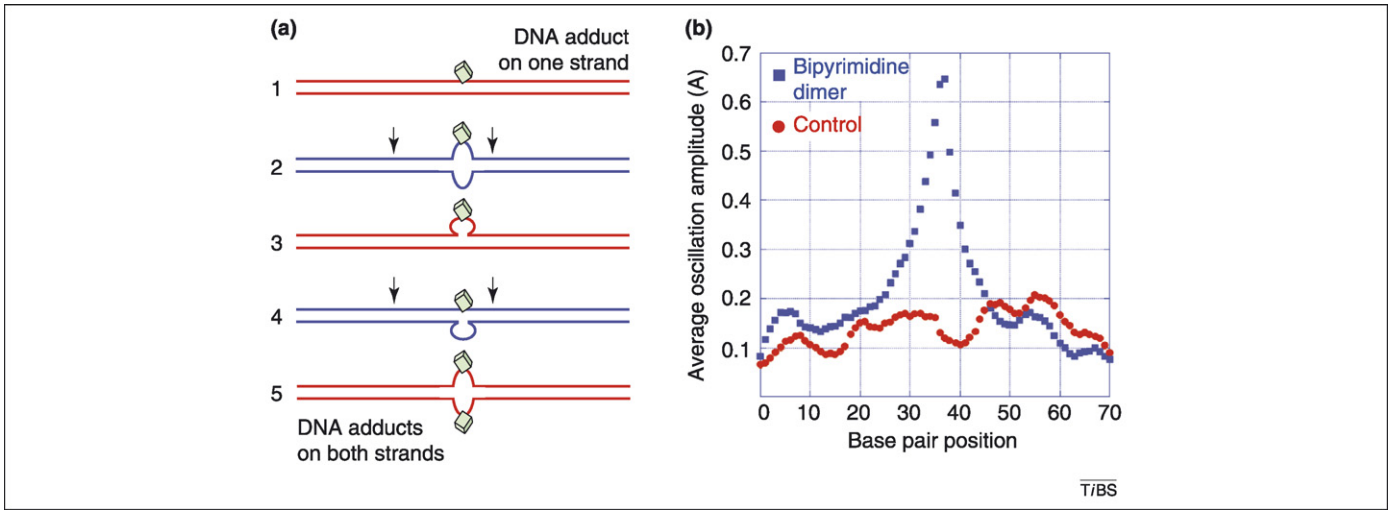

Figure 1. Recruitment of the NER complex to abnormally oscillating sites on the undamaged side of the DNA duplex. **(a)** Conformational requirement for excision of a 'nondistorting' DNA adduct located in one strand of the duplex (substrates 1–4). In the case of substrate 5, the same DNA adduct was placed in both strands simultaneously. Substrates 1, 3 and 5 are refractory to recognition by the NER complex. Only the adducts in substrates 2 and 4 are conveyed to the NER process. The sites of dual DNA incision are indicated by the arrows. These experimental findings [18] indicate that DNA damage recognition is initiated by the appearance of a bulge of native but single-stranded DNA opposite to the offending lesion. **(b)** Strand oscillations caused by a single bipyrimidine photoproduct. The average amplitude of strand openings is shown at different positions of a 70-bp fragment. Red circles, undamaged sequence; blue rectangles, DNA containing a cyclobutane pyrimidine dimer. Adapted from Ref. [21].

openings between complementary sequences, which result in strand oscillations particularly on the undamaged side of the double helix. The increased appearance of oscillations in the undamaged strand is consistent with a marked conformational heterogeneity observed across benzo[*a*]pyrene diol epoxide adducts [22]. In duplexes bearing an acetylaminofluorene adduct, only the undamaged sequence is susceptible to incision by endonuclease VII [23], an enzyme that cleaves distorted DNA, thus supporting the conclusion that more extensive dynamic changes occur in the complementary native strand.

XPC protein is a sensor of abnormal strand oscillations

One of the initiators of the mammalian NER reaction, XPC protein, has an intrinsic affinity for DNA molecules that deviate from the Watson–Crick geometry, including loops, mismatched bubbles or overhangs [24,25]. Accordingly, it has been suggested that XPC protein displays a general preference for conformational anomalies of the double helix, but the molecular basis of this unique recognition function has long remained elusive.

The human XPC sequence comprises a region of homology with the nucleic acid-binding domains of RPA and breast cancer susceptibility protein 2 (BRCA2) [26]. In the case of RPA and BRCA2, the single-stranded DNA-binding activity correlates with the presence of conserved aromatic side chains that mediate stacking interactions with closely spaced DNA bases [27]. The search for functionally analogous residues in human XPC protein revealed that two neighboring aromatics are essential for DNA-binding and NER activity [26]. XPC protein also displays a marked preference for single-stranded oligonucleotides, implying that it recognizes the local single-stranded character of damaged DNA. However, the presence of DNA lesions strongly reduces its binding to damaged single-stranded oligonucleotides compared with the more efficient interaction of XPC with undamaged counterparts [26,28].

In summary, the affinity for single-stranded oligonucleotides, in combination with an aversion to interact with damaged strands, indicates that XPC protein initiates the NER pathway by 'reading' the native strand of damaged duplexes. As illustrated in Figure 2, this mechanism fits with the large and long-lived oscillations across lesion sites, thus predicting that XPC protein operates by capturing the transient formation of single-stranded conformations in the complementary strand. The suggestion that a DNA damage sensor is attracted by the undamaged complementary strand might at first seem internally inconsistent. However, this newly discovered mechanism of DNA quality control has the advantage that the initial sensor does not rely on interactions with damaged bases, and in fact avoids such intimate contacts with abnormal residues, thus enhancing the range of modifications that can be conveyed to DNA repair. In this respect, XPC might use its affinity for oscillating DNA strands to serve as a more general platform that attracts the components of multiple repair pathways to damaged sites in chromatin. For example, recent data suggest that XPC protein could interact with subunits of the base

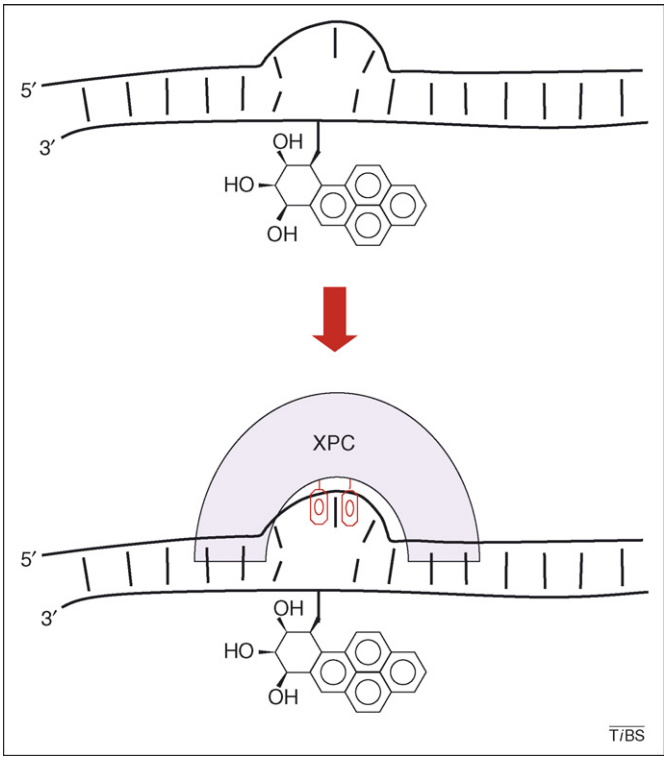

Figure 2. Scheme illustrating how human XPC protein might deploy a pair of aromatic side chains (shown in red) to capture DNA oscillations in the undamaged strand opposite to base lesions. This model predicts that unpaired deoxyribonucleotide residues located across the damaged site become sandwiched between aromatic side chains of XPC protein. The substrate versatility of this unique sensor of DNA oscillations is enhanced by avoiding direct contacts with adducted or otherwise defective residues in the damaged strand. Adapted from Ref. [26].

excision repair [29,30] and nonhomologous end-joining systems [31].

The mode of action of other NER recognition factors

Because of the deleterious consequences of strand breaks, the incision reaction must occur under extremely rigorous control. Lin and Sancar [32] predicted that a cascade of different DNA damage recognition steps of mediocre selectivity leads to an overall specificity that is comparable with that of transcription factors. For example, XPC protein, which interacts mainly with the undamaged strand, mediates the loading of TFIIH onto the damaged strand [33], such that the two DNA helicase components of TFIIH (XPB and XPD) function as tracking enzymes that locate the chemically damaged base [34,35].

XPA is another subunit of the ultimate lesion verification complex that, like XPC, has a preference for distorted DNA structures carrying mismatches, loops or bubbles, even if no actual DNA lesion has been introduced into the substrate [36]. Despite its low DNA-binding affinity, a damage 'verification' function has been proposed for XPA based on the observation that it interacts more avidly with DNA in conjunction with other NER partners [37]. XPA exhibits a distinctive preference for distorted DNA molecules, such as cisplatin-damaged duplexes or four-way DNA junctions, which share the architectural feature of presenting two double strands emerging from a central bend [36]. Indeed, the characterization of an XPA mutant, where neighboring lysines in a positively charged

Box 2. Outstanding questions

How does the degree of DNA oscillation relate to repair efficiency?
Nuclear magnetic resonance (NMR) spectroscopy and optical correlation spectroscopy (OCS) will be used to measure changes of helical dynamics resulting from the formation of DNA damage. These methods involve a magnetic label in the case of NMR, or fluorescent labels for OCS. The NMR analyses are limited to small nucleic acid molecules up to 30 bp in size, but OCS can also be applied to the study of larger DNA duplexes. The frequency and amplitude of strand oscillations can be modulated by isotope substitutions in the DNA base pairs. Thereafter, the degree of strand oscillations or other DNA fluctuations will be compared with the rates of NER assembly and efficiency of damage excision.

How does UV-DDB mediate the recognition of cyclobutane pyrimidine dimers?
An accessory factor (UV-DDB) is thought to facilitate the recognition of cyclobutane pyrimidine dimers, the most frequent photoproduct induced by exposure to sunlight [8]. Intriguingly, UV-DDB seems to be necessary for the recruitment of NER factors to cyclobutane pyrimidine dimers in intact cells but not in reconstituted *in vitro* systems [7]. Thus, although UV-DDB might represent the first factor that recognizes pyrimidine dimers in human cells, its mode of interaction with damaged sites, and the physical handover of DNA lesions from UV-DDB to the next NER factors, needs to be analyzed in the chromosomal context.

What is the role of protein ubiquitylation in the NER pathway?
UV-DDB is not only a damage recognition subunit but also a molecular adaptor that connects the Cul4A–Roc1 ubiquitin ligase complex to a wide repertoire of protein targets. Known substrates of this ubiquitylation machinery include, in addition to UV-DDB itself, various histones and XPC protein [49]. The ubiquitylation reaction seems to stimulate excision activity, but it is not clear why the presence of small polypeptide modifiers should be important for either damage recognition or the assembly of excision complexes.

How do the other NER subunits contribute to DNA damage recognition?
The NER pathway probably functions as a recognition cascade, in which a sequence of multiple steps of mediocre selectivity ultimately yields an excellent specificity for DNA lesions [9,32]. However, it is not yet clear how the downstream factors TFIIH, RPA, XPG or XPF–ERCC1 contribute to this selectivity cascade.

Damage recognition in the transcription-coupled pathway
XPC and UV-DDB are not always needed for NER activity, because these factors are dispensable for the transcription-coupled subpathway [1,50]. How the transcription complex mediates DNA damage recognition and recruits the repair machinery are other unsolved problems.

DNA-binding surface were replaced by glutamates, indicates that the assembly of active incision complexes is dependent on the close association of XPA protein with a narrow bending angle in the DNA substrate [38].

How does an affinity for kinked DNA contribute to damage recognition? Base stacking is the predominant energetic force leading to the intrinsic rigidity of DNA but the loss of base stacking, resulting in the formation of dynamic hinge points, is a common consequence of DNA lesions [16]. This property of damaged DNA implies that XPA protein could exploit its affinity for sharply bent DNA backbones to carry out a damage verification function by another indirect mechanism, that is, by probing the susceptibility of the DNA substrate to be kinked during assembly of the lesion verification complex [38].

Conclusions and perspectives

One of the most formidable challenges in molecular recognition is that faced by the initiators of the NER reaction as they locate damaged bases among a large excess of undamaged residues. This challenge is further complicated by the amazing diversity of target lesions, and it is evident that substrate recognition in the NER pathway must display great levels of versatility. An intriguing new aspect emerging from the molecular analysis of XPC and other mammalian NER subunits is that a subset of early recognition factors operate in an entirely indirect manner by detecting damage-induced alterations in DNA dynamics, including increased strand oscillations and the susceptibility of the DNA backbone to undergo site-specific kinks. The notion that generic DNA damage recognition factors can operate in a strictly indirect manner, thus avoiding close contacts with injured bases, is supported by recent studies on the prokaryotic NER system [19,39,40].

How does this novel concept of damage recognition guided by abnormal DNA dynamics, such as strand oscillations, change the direction of research in the NER field? Clearly, future experiments should not be limited to the analysis of static molecular complexes formed by DNA damage recognition factors and their nucleic acid substrates. Instead, new experimental approaches will be aimed at the measurement of dynamic changes induced by biologically significant DNA lesions (see Box 2). Quantitative relationships will be established between the type and degree of such dynamic changes and the efficiency of lesion recognition in addition to the rate of NER complex assembly. Advanced real-time methods will be employed in reconstituted systems and in intact cells to monitor the recruitment of NER factors and the specific reciprocal interactions arising between multiple subunits in response to alterations of DNA dynamics. Another important issue will be the examination of how reversible posttranslational modifications of NER subunits might facilitate the recognition of transient dynamic changes of the DNA substrate.

Acknowledgements

H.N. is supported by the Swiss National Science Foundation (grant 3100A0-113694) and by Oncosuisse (grant KLS-01827-02-2006). The work of K.B.B. is partly supported by the Center for Nonlinear Studies at the Los Alamos National Laboratory.

References

1 Friedberg, E.C. *et al.* (2006) *DNA Repair and Mutagenesis,* ASM Press
2 Reardon, J.T. *et al.* (1997) In vitro repair of oxidative DNA damage by human nucleotide excision repair system: possible explanation for neurodegeneration in xeroderma pigmentosum patients. *Proc. Natl. Acad. Sci. USA* 94, 9463–9468
3 Kuraoka, I. *et al.* (2000) Removal of oxygen free-radical-induced 5′, 8-purine cyclodeoxynucleosides from DNA by the nucleotide excision-repair pathway in human cells. *Proc. Natl. Acad. Sci. USA* 97, 3832–3837
4 Reardon, J.T. and Sancar, A. (2006) Repair of DNA-polypeptide crosslinks by human excision nuclease. *Proc. Natl. Acad. Sci. USA* 103, 4056–4061
5 Huang, J.C. *et al.* (1994) Substrate spectrum of human excinuclease: repair of abasic sites, methylated bases, mismatches and bulky adducts. *Proc. Natl. Acad. Sci. USA* 91, 12213–12217
6 Mu, D. *et al.* (1997) Characterization of reaction intermediates of human excision repair nuclease. *J. Biol. Chem.* 272, 28971–28979
7 Reardon, J.T. and Sancar, A. (2003) Recognition and repair of the cyclobutane thymine dimer, a major cause of skin cancers, by the human excision nuclease. *Genes Dev.* 17, 2539–2551

8 Tang, J.Y. *et al.* (2000) Xeroderma pigmentosum p48 gene enhances global genomic repair and suppresses UV-induced mutagenesis. *Mol. Cell.* 5, 737–744
9 Volker, M. *et al.* (2001) Sequential assembly of the nucleotide excision repair factors in vivo. *Mol. Cell* 8, 213–224
10 Evans, E. *et al.* (1997) Mechanism of open complex and dual incision formation by human nucleotide excision repair factors. *EMBO J.* 16, 6559–6573
11 Riedl, T. *et al.* (2003) The comings and goings of nucleotide excision repair factors on damaged DNA. *EMBO J.* 22, 5293–5303
12 Politi, A. *et al.* (2005) Mathematical modeling of nucleotide excision repair reveals efficiency of sequential assembly strategies. *Mol. Cell* 19, 679–690
13 Sugasawa, K. *et al.* (1998) Xeroderma pigmentosum group C protein complex is the initiator of global genome nucleotide excision repair. *Mol. Cell* 2, 223–232
14 Hanawalt, P.C. and Haynes, R.H. (1965) Repair replication of DNA in bacteria: irrelevance of chemical nature of base defect. *Biochem. Biophys. Res. Commun.* 19, 462–467
15 Gunz, D. *et al.* (1996) Recognition of DNA adducts by human nucleotide excision repair. Evidence for a thermodynamic probing mechanism. *J. Biol. Chem.* 271, 25089–25098
16 Isaacs, R.J. and Spielmann, H.P. (2004) A model for initial DNA lesion recognition by NER and MMR based on local conformational flexibility. *DNA Rep.* 3, 455–464
17 Marx, A. *et al.* (1997) 4′-acetylated thymidines: a new class of DNA chain terminators and photocleavable DNA building blocks. *J. Am. Chem. Soc.* 119, 1131–1132
18 Buterin, T. *et al.* (2005) DNA quality control by conformational readout on the undamaged strand of the double helix. *Chem. Biol.* 12, 913–922
19 Malta, E. *et al.* (2006) Base flipping in nucleotide excision repair. *J. Biol. Chem.* 281, 2184–2194
20 Alexandrov, B.S. *et al.* (2006) Bubble statistics and dynamics in double-stranded DNA. *Phys. Rev. E* 74, 05090
21 Blagoev, K.B. *et al.* (2006) Ultra-violet light induced changes in DNA dynamics may enhance TT-dimer recognition. *DNA Rep.* 5, 863–867
22 Cosman, M. *et al.* (1996) Solution conformation of the (–)-*cis*-*anti*-benzo[*a*]pyrenyl-dG adduct opposite dC in a DNA duplex: intercalation of the covalently attached BP ring into the helix with base displacement of the modified deoxyguanosine into the major groove. *Biochemistry* 35, 9850–9863
23 Bertrand-Burggraf, E. *et al.* (1994) Endonuclease VII of phage T4 nicks *N*-2-acetylaminofluorene-induced DNA structures in vitro. *Mutat. Res.* 314, 287–295
24 Batty, D. *et al.* (2000) Stable binding of human XPC complex to irradiated DNA confers strong discrimination for damaged sites. *J. Mol. Biol.* 300, 275–290
25 Sugasawa, K. *et al.* (2001) A multistep damage recognition mechanism for global genomic nucleotide excision repair. *Genes Dev.* 15, 507–521
26 Maillard, O. *et al.* (2007) An aromatic sensor with aversion to damaged strands confers versatility to DNA repair. *PLoS Biol.* 5, e79
27 Bochkarev, A. *et al.* (1997) Structure of the single-stranded-DNA-binding domain of replication protein A bound to DNA. *Nature* 385, 176–181
28 Trego, K.S. and Turchi, J.J. (2006) Pre-steady-state binding of damaged DNA by XPC-hHR23B reveals a kinetic mechanism for damage discrimination. *Biochemistry* 45, 1961–1969
29 Shimizu, Y. *et al.* (2003) Xeroderma pigmentosum group C protein interacts physically and functionally with thymine DNA glycosylase. *EMBO J.* 22, 164–173
30 D'Errico, M. *et al.* (2006) New functions of XPC in the protection of human skin cells from oxidative damage. *EMBO J.* 25, 4305–4315
31 Despras, E. *et al.* (2007) Long-term XPC silencing reduces DNA double-strand break repair. *Cancer Res.* 67, 2526–2534
32 Lin, J.J. and Sancar, A. (1992) (A)BC excinuclease: the *Escherichia coli* nucleotide excision repair enzyme. *Mol. Microbiol.* 6, 2219–2224
33 Yokoi, M. *et al.* (2000) The xeroderma pigmentosum group C protein complex XPC-HR23B plays an important role in the recruitment of transcription factor IIH to damaged DNA. *J. Biol. Chem.* 275, 9870–9875
34 Naegeli, H. *et al.* (1992) The DNA helicase and adenosine triphosphatase activities of yeast Rad3 protein are inhibited by DNA damage. *J. Biol. Chem.* 267, 392–398
35 Fan, L. *et al.* (2006) Conserved XPB core structure and motifs for DNA unwinding: implications for pathway selection of transcription or excision repair. *Mol. Cell* 22, 27–37
36 Missura, M. *et al.* (2001) Double-check probing of DNA bending and unwinding by XPA-RPA: an architectural function in DNA repair. *EMBO J.* 20, 3554–3564
37 Li, L. *et al.* (1995) An interaction between the DNA repair factor XPA and replication protein A appears essential for nucleotide excision repair. *Mol. Cell. Biol.* 15, 5396–5402
38 Camenisch, U. *et al.* (2006) Recognition of helical kinks by xeroderma pigmentosum group A protein triggers DNA excision repair. *Nat. Struct. Mol. Biol.* 13, 278–284
39 Truglio, J.J. *et al.* (2006) Structural basis for DNA recognition and processing by UvrB. *Nat. Struct. Mol. Biol.* 13, 360–364
40 Waters, T.R. *et al.* (2006) Damage detection by the UvrABC pathway: crystal structure of UvrB bound to fluorescein-adducted DNA. *FEBS Lett.* 580, 6423–6427
41 Kraemer, K.H. *et al.* (1984) DNA repair protects against cutaneous and internal neoplasia: evidence from xeroderma pigmentosum. *Carcinogenesis* 5, 511–514
42 Huang, J.C. *et al.* (1992) Human nucleotide excision nuclease removes thymine dimers from DNA by incising the 22nd phosphodiester bond 5′ and the 6th phosphodiester bond 3′ to the photodimer. *Proc. Natl. Acad. Sci. USA* 89, 3664–3668
43 Nishi, R. *et al.* (2005) Centrin 2 stimulates nucleotide excision repair by interacting with xeroderma pigmentosum group C protein. *Mol. Cell. Biol.* 25, 5664–5674
44 Aboussekhra, A. *et al.* (1995) Mammalian DNA nucleotide excision repair reconstituted with purified protein components. *Cell* 80, 859–868
45 Mu, D. *et al.* (1995) Reconstitution of human DNA repair excision nuclease in a highly defined system. *J. Biol. Chem.* 270, 2415–2418
46 Evans, E. *et al.* (1997) Open complex formation around a lesion during nucleotide excision repair provides a structure for cleavage by human XPG protein. *EMBO J.* 16, 625–638
47 Bessho, T. *et al.* (1997) Reconstitution of human excision nuclease with recombinant XPF-ERCC1 complex. *J. Biol. Chem.* 272, 3833–3837
48 Shivji, M.K. *et al.* (1995) Nucleotide excision repair DNA synthesis by DNA polymerase epsilon in the presence of PCNA, RFC, and RPA. *Biochemistry* 34, 5011–5017
49 Sugasawa, K. *et al.* (2005) UV-induced ubiquitylation of XPC protein mediated by UV-DDB-ubiquitin ligase complex. *Cell* 121, 387–400
50 Andressoo, J.O. and Hoeijmakers, J.H. (2005) Transcription-coupled repair and premature ageing. *Mutat. Res.* 577, 179–194

Chapter 2

Results

2.1. Dissection of the xeroderma pigmentosum group C protein function by site-directed mutagenesis

2.1.1. Aims of the study

In this study, I aimed at elucidating the function of four evolutionary conserved amino acids (N754, F756, F797, and F799), mapped to the BHD3 domain of XPC protein. Using site-directed mutagenesis, I substituted the residues with alanine and subjected these mutants to different experiments investigating their properties regarding DNA damage recognition and induction of DNA repair.

2.1.2. Results in brief

Each one of the tested residues (N754, F756, F797, and F799) plays an important role in DNA damage search on native DNA and the sequential assembly of an ultimate recognition machinery. N754, F756, F797 cooperate to sense damage-induced base displacements opposite to lesion sites, while F799 is important to stabilize XPC protein at the damaged site. F797 and F799 are crucial in engaging TFIIH into the repair complex since the mutation to alanine abrogated their ability to trigger GGR. N754 (and to a lesser extent also F797 and F799) contribute to XPC protein mobility, an important feature in the search of damaged DNA.

2.1.3. Contribution to this paper

For this work, I was profoundly involved in designing the experiments as well as in the writing of the paper. I performed all experiments except the multiphoton laser irradiation, which was carried out by Martin Tomas (figure 3 in the paper), and analyzed the data.

2.1.4. Reference

Clement FC, Kaczmarek N, Mathieu N, Tomas M, Leitenstorfer A, Ferrando-May E, and Naegeli H (2010) Dissection of the xeroderma pigmentosum group C protein function by site-directed mutagenesis. *Antioxid Redox Signal*, manuscript accepted.

2.1.5. Manuscript

Dissection of the xeroderma pigmentosum group C protein function by site-directed mutagenesis

FLURINA C. CLEMENT,[1] NINA KACZMAREK,[1] NADINE MATHIEU,[1] MARTIN TOMAS,[2] ALFRED LEITENSTORFER,[2] ELISA FERRANDO-MAY,[3] and HANSPETER NAEGELI[1]

[1]Institute of Pharmacology and Toxicology, University of Zürich-Vetsuisse, CH-8057 Zürich, Switzerland

[2]Department of Physics and Center for Applied Photonics, University of Konstanz, D-78464 Konstanz, Germany

[3]Bioimaging Center, University of Konstanz, D-78464 Konstanz, Germany

Running head: Mutational dissection of XPC function

Address reprint requests to:

Hanspeter Naegeli

University of Zürich-Vetsuisse, Institute of Pharmacology and Toxicology

Winterthurerstrasse 260

CH-8057 Zürich, Switzerland

Phone +41 44 635 87 63 Fax +41 44 635 89 10

E-mail: *naegelih@vetpharm.uzh.ch*

ABSTRACT

Xeroderma pigmentosum group C (XPC) protein is a sensor of helix-distorting DNA lesions whose function is to trigger the global genome repair (GGR) pathway. Previous studies demonstrated that XPC protein operates by detecting the single-stranded character of non-hydrogen-bonded bases opposing lesion sites. This mode of action is supported by structural analyses of the yeast Rad4 homolog that identified critical side chains making close contacts with a pair of extrahelical nucleotides. Here, alanine substitutions of the respective conserved residues (N754, F756, F797, F799) in human XPC were tested for DNA-binding activity, accumulation in tracks and foci of DNA lesions, nuclear protein mobility and the induction of downstream GGR reactions. This study discloses a dynamic interplay between XPC protein and DNA, whereby the association with one displaced nucleotide in the undamaged strand mediates the initial encounter with lesion sites. The additional flipping-out of an adjacent nucleotide is necessary to hand over the damaged site to the next GGR player. Surprisingly, this mutagenesis analysis also reveals that the rapid intranuclear trafficking of XPC protein depends on constitutive interactions with native DNA, implying that the search for base damage takes place in living cells by a facilitated diffusion process.

INTRODUCTION

Nucleotide excision repair is a fundamental cytoprotective system that removes bulky DNA adducts and intrastrand crosslinks generated by ultraviolet (UV) light, genotoxic chemicals, reactive metabolic intermediates, oxygen radicals as well as lipid peroxidation products (18, 19, 21, 35, 46). Two distinct subpathways of this versatile DNA repair process have been discerned depending on the genomic context. Transcription-coupled repair eliminates DNA lesions from the transcribed strand of active genes whereas global-genome repair (GGR) excises base damage from any sequence including non-transcribed strands and silent domains (17, 20). The relevance of an effective DNA repair surveillance is highlighted by the inherited disorder xeroderma pigmentosum (XP) where defects in the GGR pathway lead to a > 1000-fold increased incidence of sunlight-induced skin cancer. XP patients also have a higher risk of developing internal tumors and often suffer from neurological deterioration or other traits of premature aging attributable to oxidative stress (2, 6, 11). The disease can be classified into seven repair-deficient complementation groups designated XP-A through XP-G (12, 27).

XPC protein is the 940-amino acid DNA-binding constituent of a promiscuous sensor that associates with damaged sites to initiate the GGR reaction (4, 39, 44). The other two subunits of this initiator complex, Rad23B and centrin-2, have an accessory function in stabilizing XPC and stimulating its recognition function (31, 32). XPC protein provides a landing platform for transcription factor TFIIH (48), whose unwinding activity assisted by XPA and replication protein A (RPA) generates an open nucleoprotein intermediate in which the DNA is melted over 25-30 nucleotides (15, 45). The double- to single-stranded transitions at the borders of this open complex are cleaved by structure-specific endonucleases, thereby releasing the offending lesion by dual DNA incision (23, 33, 36). Finally, repair patch synthesis is carried out by the coordinated activity of DNA polymerases and ligases (3, 37).

Against the conventional dogma that DNA lesions are recognized through direct contacts with modified nucleotides, XPC protein distinguishes between damaged DNA and the native double helix by sensing the single-stranded character of non-hydrogen-bonded bases in the undamaged strand (7, 28, 42). This view was confirmed when a crystallographic analysis of the yeast Rad4 homolog revealed the bimodal binding scheme of this versatile factor (30). One part of Rad4 protein, involving its large transglutaminase homology domain and a short β–hairpin domain (BHD1), associates with 11 base pairs of duplex DNA flanking the lesion. A second part, comprised of β–hairpin domains BHD2 and BHD3, interacts with a 4-nucleotide segment of the undamaged strand opposing the lesion. Two of these undamaged nucleotides are displaced out of the double helix and accommodated into a hand-like Rad4 protein fold, where the DNA adopts the configuration of a single-stranded overhang (38). The amino acids making contacts with these extrahelical nucleotides are evolutionary conserved (Fig. 1A) and, therefore, it can be predicted from the Rad4 structure that N754 and F756 of human XPC interact with one flipped-out base, located on the 3' side, whereas F799 binds to the second flipped-out nucleotide on the 5' side and F797 interacts with both extrahelical residues simultaneously (Fig. 1B).

The presence of two fully extruded nucleotides in the Rad4–DNA complex is intriguing because most helix-distorting lesions, including those that are readily excised by the GGR system, cause the destabilization of just a single base pair. For example, UV light-induced (6-4) photoproducts interfere with the Watson-Crick hydrogen bonding pattern of only one modified pyrimidine while all surrounding base pairs retain their native double helical geometry (24, 25). Similarly, the rapidly excised (+)-*cis*-benzo[*a*]pyrene-N^2-dG or *N*-acetyl-2-aminofluorene-dG adducts disrupt only the Watson-Crick pairing between the modified guanines and their cytosine partner (13, 34). This discrepancy between the limited base pair destabilization induced by many GGR substrates and the more extensive base displacement

in the Rad4 co-crystal raises the twofold questions of how this factor and its human counterpart are able to find lesions embedded in native genomic DNA and what is the function of the extensive conformational changes observed in the Rad4 crystal complex.

To address these unresolved issues, residues N754, F756, F797 and F799 of the human XPC sequence, which are predicted to accommodate the two flipped-out nucleotides in their outward position, were subjected to site-directed mutagenesis. The biochemical properties of the resulting alanine mutants were tested both *in vitro* and in living cells to determine the contribution of each individual side chain to the molecular search process, the detection of lesions and formation of a stable recognition intermediate as well as the induction of downstream reactions. This report provides new insights into dynamic aspects of the genome-wide search mechanism by which XPC protein finds DNA damage and initiates the versatile GGR pathway.

MATERIALS AND METHODS

XPC constructs and mutants

The human *XPC* complementary DNA was cloned into pEGFP-N3 (Clontech, Mountain View, California, USA) using the restriction enzymes *Xma*I and *Kpn*I and into the pFastBac HTc vector (Invitrogen, Basel, Switzerland) with *Not*I and *Kpn*I. Mutations were generated by site-directed mutagenesis (QuickChange, Stratagene, Heidelberg, Deutschland) using the primers 5'-gaaggtgccccgggccgagtttgggaatgtgtac-3' (N754A), 5'-gaaggtgccccggaacgaggctgggaatgtgtac-3' (F756A), 5'-caggccatcactggcgctgatttccatggcggc-3' (F797A) and 5'-ccatcactggctttgatgcccatggcggctactcc-3' (F799A) from Microsynth (Balgach, Switzerland). All resulting clones were sequenced to exclude concomitant accidental mutations.

XPC expression in insect cells

The vector pFastBac HTc containing the human *XPC* sequence, fused to His_6 and maltose-binding protein (MBP) tags (28), was introduced into recombinant baculovirus using the BAC-TO-BAC Baculovirus Expression System (Invitrogen). *Sf*9 cells (2×10^6) were infected and cell lysates containing His_6-MBP-XPC fusion proteins were obtained as described (43). Each *Sf*9 cell lysate was analyzed by denaturing polyacrylamide gel electrophoresis, Coomassie staining and immunoblotting with antibodies against His_6 (Sigma, Buchs, Switzerland). The amount of human XPC protein was determined by comparing the intensity of the His_6-MBP-XPC band of ~170 kDa with that of a bovine serum albumin standard (Fluka, Basel, Switzerland).

DNA-binding assay

Double-stranded and junction DNA probes were produced by hybridization of a ^{32}P-labeled 135-mer with fully or partially complementary 135-mers (Microsynth) in 50 mM

Tris–HCl (pH 7.4), 10 mM $MgCl_2$ and 1 mM dithiothreitol (DTT). Complete hybridization of the radiolabeled strand was demonstrated by analysis of the duplex and junction DNA products on native 5% (w/v) polyacrylamide gels. The indicated concentrations of XPC protein, as part of *Sf*9 cell lysates (5-25 μl), were incubated with ^{32}P-labeled 135-mer substrates (2 nM) in 200 μl buffer A [25 mM Tris–HCl, pH 7.5, 0.3 M NaCl, 10% (v/v) glycerol, 0.01% (v/v) Triton X-100, 0.25 mM phenylmethane sulfonyl fluoride and 1 mM EDTA). After 1.5 h at 4°C, the reaction mixtures were supplemented with monoclonal antibodies against MBP linked to paramagnetic beads (0.2 mg; New England BioLabs, Bioconcept, Allschwil, Switzerland). Following another 1 h at 4°C, the beads were washed twice with 200 μl buffer A, and the radioactivity associated with the paramagnetic beads was quantified by liquid scintillation counting. All values were corrected for the background resulting from control incubations with a lysate from uninfected cells.

Cell culture

All cell culture media and supplements were from Invitrogen. Simian virus 40-transformed human XP-C fibroblasts (GM16093), derived from patient XP14BR, were obtained from the Coriell Institute for Medical Research (Camden, New Jersey, USA). These cells carry a homozygous C to T transition at codon 718 leading to a non-functional truncate (10). The XP-C fibroblasts were grown in a humidified incubator at 37°C and 5% CO_2 using Dulbecco's modified Eagle's medium (DMEM) supplemented with 10% heat-inactivated fetal calf serum (FCS), 100 units/ml penicillin G and 100 μg/ml streptomycin. Chinese hamster ovary (CHO) cells were cultured as the XP-C fibroblasts except that DMEM was replaced by F-12 Nutrient Mixture.

Transfections

500,000 XP-C or 250,000 CHO cells were seeded into 6-well plates. After 24 h, at a

confluence of 80-85%, the cells were transfected with 1 μg XPC-pEGFP-N3 or pEGFP-DDB2-C1 plasmids using 4 μl FuGENE HD transfection reagent (Roche, Basel, USA). Following a 4-h incubation, the transfection mixture was replaced by complete culture medium and the cells were incubated for another 18 h at 37°C. The expression of XPC-GFP constructs was assessed by immunoblotting using monoclonal antibodies against human XPC protein (Abcam, Cambridge, England).

High-resolution DNA damage induction

Multiphoton laser irradiation is a powerful tool to induce narrow areas of DNA damage in the nuclei of mammalian cells (29). CHO cells were grown in μ-Dish$^{35mm,\ high}$ (Ibidi, München, Germany) and, 18 h after transfection, the medium was replaced by phenol red-free DMEM supplemented with 10% FCS and 25 mM HEPES (pH 7.2). Single nuclei were irradiated along a 10-μm track with a multiphoton fiber laser coupled to a confocal microscope (LSM Pascal, Zeiss, Göttingen, Deutschland). The laser generates pulses of 775 nm with the duration of 290 femtoseconds and a repetition rate of 107 MHz (41). By multiphoton excitation, three colliding photons of low energy (775 nm wavelength) cause DNA lesions that would normally arise from the absorption of a single photon at higher energy (258 nm wavelength). The peak power density at the focal plane was 365 GW/cm^2 and the pixel dwell time was 44.2 ms, generating approximately 5000 UV lesions [cyclobutane pyrimidine dimers and (6-4) photoproducts] in each treated cell (8). The area of each irradiation track was < 10 μm^2 and its volume < 20 μm^3.

Induction of UV foci

CHO cells were grown on glass cover slips (20 mm diameter) and transfected with XPC-GPF constructs as described before. After 18-h incubations, the cell culture medium was removed and the cells were rinsed with phosphate-buffered saline (PBS). UV foci were

induced by irradiation through the 5-μm pores of polycarbonate filters (Millipore, Zug, Switzerland) using a UV-C source (254 nm, 150 J/m^2). Immediately after irradiation, the filters were gently removed and the cells incubated for the indicated periods at 37°C in complete DMEM.

Immunocytochemistry

All procedures were performed at room temperature, unless otherwise stated. At the indicated times after irradiation, cells were washed and fixed for 15 min using 4% (w/v) paraformaldehyde in PBS. The cells were permeabilized with PBS containing 0.1% (v/v) TWEEN 20 for 10 min and DNA was denatured with 0.07 M NaOH for 8 min. Subsequently, the samples were washed five times with 0.1% TWEEN 20 and blocked (30 min at 37°C) with 20% FCS in PBS. The samples were incubated (1 h at 37°C in PBS containing 5% FCS) with primary antibodies directed against (6-4) photoproducts (MBL International Corporation, Woburn, Massachusetts, USA) (dilution 1:1000) or against the p62 (Abcam) and p89 subunits of TFIIH (Santa Cruz Biotechnology, Santa Cruz, California, USA) (dilution 1:250). Next, the samples were washed with 0.1% TWEEN 20, blocked twice for 10 min with 20% FCS and incubated with Alexa Fluor 594-conjugated secondary antibodies (Invitrogen) (dilution 1:400) for 30 min at 37°C. After washing with 0.1% TWEEN 20 in PBS, the nuclei were stained for 10 min with Hoechst dye 33258 (200 ng/ml). Finally, the samples were washed three times with PBS and analyzed using an oil immersion objective.

Image analysis

Fluorescence measurements in UV tracks were carried out through a x40 oil immersion objective lens with a numerical aperture of 1.4 (EC-Plan-Neo-Fluar, Zeiss) using an Ar^+ source (488 nm wavelength). The selected parameters (laser power and magnification factor) were kept constant throughout all experiments. For real-time recordings, an image was taken

every five seconds for up to 105 seconds after irradiation and analyzed by the ImageJ software (http://rsb.info.nih.gov/ij) including corrections for bleaching (http://www.embl-heidelberg.de/eamnet/html/body_bleach_correction.html) and cell movements (http://bigwww.epfl.ch/thevenaz/stackreg). An initial control image was taken immediately before damage induction. The average fluorescence signals were corrected for the background levels and normalized to the mean intensity of the same nuclear region before irradiation. Foci of UV lesions or DNA repair factors in paraformaldehyde-fixed cells were quantified using the LAS AF lite v1.9 software (Leica, Wetzlar, Germany).

Protein dynamics in living cells

To carry out fluorescence recovery after photobleaching (FRAP) analyses, CHO cells were grown on glass cover slips and transfected as described above. Cells with low expression of GFP fusions were subjected to high-time resolution FRAP using a Leica TCS SP5 confocal microscope equipped with an Ar^+ laser (488 nm) and a x63 oil immersion lens (numerical aperture of 1.4). The assays were performed in a controlled environment at 37°C and with a CO_2 supply of 5%. A region of interest (ROI) of 4 mm^2 was photo-bleached for 2.3 s at 80% laser intensity. Fluorescence recovery within the ROI was monitored 200 times using 115-ms intervals followed by 30 frames at 250 ms and 20 frames at 500 ms. Simultaneously, a reference ROI of the same size was measured for each time point to correct for overall bleaching. Finally, the data were normalized to the prebleach intensity.

FRAP on local damage (FRAP-LD) was applied to test the stability of XPC interactions with damaged sites. In CHO cells transfected with GFP fusion constructs, ROIs corresponding to foci of XPC accumulation were defined 15-30 min after UV-C irradiation (254 nm, 150 J/m^2) through polycarbonate filters. These ROIs were photobleached until the fluorescence reached a level equivalent to that of the nuclei around the foci. Fluorescence recovery within each ROI was monitored through a x40 oil immersion objective lens with a

numerical aperture of 1.4. The measurements were conducted 10 times using 700-ms intervals followed by 10 frames of 5 s and 6 frames of 20 s. Simultaneously, a reference ROI of the same size was measured for each time point to correct for overall bleaching. The values were used to calculate ratios between the damaged area in the foci and the corresponding intensity before bleaching. In the data display, the first fluorescence measurement after photobleaching is set to 0 (1).

Host cell reactivation assay

pGL3 and phRL-TK vectors expressing firefly (*Photinus*) and *Renilla* luciferase were purchased from Promega (Dübendorf, Switzerland). The pGL3 DNA was UV-irradiated (257 nm, 1000 J/m^2) in 10 mM Tris-HCl (pH 8) and 1 mM EDTA. Human XP–C fibroblasts, grown to a confluence of 80% in 6-well plates, were transfected with 0.5 μg XPC-pEGFP expression vector, 0.45 μg irradiated pGL3 DNA and 0.05 μg phRL-TK. After a 4-h incubation, the transfection reagent was replaced by complete medium. The cells were lysed after a further 18-hour period using 0.5 ml Passive Lysis Buffer (Promega) following the manufacturer's instructions. *Photinus* and *Renilla* luciferase activity was determined in a Dynex microtiter plate luminometer using the Dual-Luciferase Assay System (Promega). Mean values were calculated from the ratios between *Photinus* and *Renilla* luciferase activity.

Statistical analysis

Results are expressed as mean ± SD or mean ± SEM of at least three independent experiments in each group. The statistical analysis was performed with InStat 3.0 Software for Macintosh (GraphPad Software) using the Student's *t* test for comparisons. A value of $p < 0.05$ was considered statistically significant.

RESULTS

DNA-binding activity in vitro

Human XPC was over-expressed in *Sf*9 insect cells, as a fusion with maltose-binding protein (MBP), and cell lysates containing quantitatively similar levels of wild-type and mutant MBP-XPC were identified by immunoblotting (Fig. 2A). The DNA-binding activity was determined in pull-down assays by incubation with radiolabeled substrates displaying the same length but different conformations, i.e., homoduplex fragments of 135 base pairs, single-stranded 135-mer oligonucleotides or junction molecules consisting of a duplex region of 71 base pairs with single-stranded overhangs of 64 nucleotides. Dose response experiments were conducted with increasing amounts of cell lysate (Fig. 2B) to determine a non-saturating concentration of wild-type XPC protein (1.7 nM) for comparisons with site-directed mutants containing single alanine substitutions.

This *in vitro* DNA-binding assay demonstrates that the tested amino acids are indeed critical for the interaction of XPC protein with DNA. With all substrate conformations, the three mutations N754A, F756A and F797A confer a more severe DNA-binding defect than the F799A substitution (Fig. 2C). However, all four mutants are essentially unable to interact with the single-stranded oligonucleotides. A surprising observation is that the four site-directed mutants also display a reduced binding to homoduplex DNA (Fig. 2C). Thus, residues N754, F756, F797 and F799, selected in view of their affinity for the single-stranded configuration of extrahelical nucleotides, also contribute in a substantial manner to the binding of XPC protein to undamaged DNA in its native double helical form.

DNA damage recognition in tracks of UV lesions

The ability to recognize DNA damage in living cells was tested by monitoring the accumulation of green-fluorescent protein (GFP) constructs along high-resolution tracks of

UV lesions. The XPC subunit is normally assisted in the recognition of UV photoproducts by an accessory factor known as UV-damaged DNA-binding (UV-DDB) protein (16). To avoid this stimulatory effect of UV-DDB and, hence, determine the intrinsic function of XPC protein in detecting DNA damage, nuclear relocation experiments were performed in Chinese hamster ovary (CHO) cells, which are devoid of UV-DDB activity because they fail to express its DNA-binding subunit DDB2 (40).

After transfection with appropriate vectors, individual CHO cells expressing low levels of XPC-GFP fusions, in the range of endogenous XPC in human fibroblasts (8), were identified by measuring the overall nuclear fluorescence. Next, 10-μm tracks of UV lesions were produced by application of a multiphoton laser that achieves high spatial resolution with minimal collateral damage (29, 41). The subsequent real-time redistribution of XPC-GFP was assessed by recording the local increase in fluorescence intensity along each laser track (Fig. 3A). Wild-type XPC protein responded to local irradiation by reallocating to the damaged areas with an accumulation half-life of ~15 seconds (Fig. 3B). Already after ~50 seconds, a plateau level was reached reflecting a steady-state condition with constant turnover. In contrast, the N754A, F756A, F797A and F799A single mutants relocated to the UV lesion tracks with prolonged half-lives of accumulation and markedly reduced plateau levels (Fig. 3B). These results demonstrate that all four tested amino acid side chains are required for the formation of a DNA damage recognition intermediate in the chromatin of living cells. The most severe reduction of local accumulation is caused by the N754A change.

DNA damage recognition in UV foci

In addition to UV photoproducts, irradiation by the multiphoton laser causes oxidative damage and DNA strand breaks. The nuclear relocation experiments were, therefore, confirmed by generating UV-C foci containing essentially only cyclobutane pyrimidine dimers and (6-4) photoproducts (8, 14, 26). For that purpose, CHO cells transfected with

XPC-GFP constructs were UV-irradiated (254 nm wavelength) through the pores of polycarbonate filters, thereby localizing the DNA damage to small nuclear spots. After a 15-min recovery at 37°C, the cells were subjected to paraformaldehyde fixation to visualize the co-localization of (6-4) photoproducts and XPC-GFP fusions. As shown in Fig. 4, wild-type XPC protein generated bright green foci with reduced overall nuclear fluorescence indicative of a strong accumulation in damaged sites with a concomitant depletion of the GFP fusion from undamaged regions. The XPC single mutants also relocated to the damaged foci but to a lower degree generating weaker green fluorescence signals over the surrounding nuclear area. An exact quantitative comparison between the mutations is limited by the wide heterogeneity of size, shape and photoproduct density of the foci but, on the average, the four mutants reached a local fluorescence intensity above background that was only ~30% of that observed with the wild-type control (N = 30). These results support the notion that all tested amino acids (N754, F756, F797 and F799) are required for the formation of a DNA damage recognition intermediate in living cells.

Overall nuclear dynamics of XPC protein

The interaction of XPC protein with genomic DNA before and after UV irradiation was examined by fluorescence recovery after photobleaching (FRAP), which is a powerful real-time method to probe the nuclear mobility of repair proteins (1, 22). In cells containing low levels of each XPC-GFP fusion, a 4-μm^2 area of the nucleus was bleached with a laser (488 nm wavelength, not producing DNA damage) to eliminate the fluorescence signal. Subsequently, the gradual recovery of fluorescence within the bleached area, due to the rapid diffusion of free XPC-GFP molecules, is recorded over time. In non-irradiated CHO cells, when the DNA contains no UV lesions, the bleached spot ultimately reaches a fluorescence intensity equal to that detected before the photobleaching process (Fig. 5A). After UV irradiation (20 J/m^2), this fluorescence recovery is significantly delayed, indicating that the

movements of XPC protein are restrained as a consequence of its binding to UV lesions. The UV dose of 150 J/m^2, used to saturate the XPC molecules with a high lesion density, further delays the recovery of fluorescence reflecting an immobilization of the fusion proteins in response to DNA damage (22).

The FRAP analysis was employed for a direct comparison of protein dynamics between wild-type XPC and the single mutants (N754A, F756A, F797A, F799A). In non-irradiated cells, i.e., in the absence of UV lesions, the alanine substitution N754A, and to a lesser extent the F797A and F799A mutations, retarded the fluorescence recovery (Fig. 5B). This unanticipated finding indicates that the DNA-binding defect of these mutants (see Fig. 2C) restricts their normal nuclear mobility in comparison to the wild-type control. When the cells were UV-irradiated, the nuclear dynamics of the four tested mutants was not affected by their encounters with DNA lesions (Figs. 5C–F), lending further support to the conclusion that the loss of one of the tested XPC side chains is sufficient to prevent the formation of a stable recognition complex.

XPC protein dynamics in UV foci

Among the tested mutants, F756A and F799A display the highest residual accumulation in the quantitative laser track assay of Fig. 3B. To compare the stability of the interactions that these mutants undergo with damaged genomic DNA, UV-induced foci containing the respective fusion proteins were analyzed by fluorescence recovery after photobleaching on local damage (FRAP-LD) (1). To that end, the green fluorescence of individual foci was photobleached until the signal reached the lower background level of the surrounding nuclear areas. The subsequent fluorescence recovery due to the exchange of bleached XPC molecules with non-bleached counterparts was again recorded over time, thus yielding distinct dissociation curves (Fig. 6). In particular, we observed that the fluorescence of the F756A and F799A mutants reached the pre-bleach intensity after ~30 seconds, indicating that they

readily dissociate from UV-irradiated sites. Instead, wild-type XPC protein forms a subset of stable complexes in the UV foci in a manner that the final plateau of fluorescence remains significantly below the pre-bleach signal (Fig. 6). Thus, this analysis of local protein dynamics confirms that, despite its more moderate contribution to DNA binding (see Fig. 2C), the side chain of F799 is nevertheless necessary for the anchoring of XPC protein onto damaged DNA.

XPC-dependent recruitment of TFIIH complexes

Once bound to damaged DNA, XPC protein serves as a platform for the loading of transcription factor TFIIH onto the substrate (39, 48). Therefore, we next tested how the different mutations affect the ability of XPC protein to recruit TFIIH to lesion sites. For that purpose, XP-C fibroblasts lacking functional *XPC* were complemented by transfection with XPC-GFP fusion vectors. Foci of UV lesions were generated by irradiation through micropore filters and, after 30 min, the cells were processed by immunocytochemistry to stain the TFIIH subunits p62 and p89 with a red-fluorescent dye. Finally, the UV-dependent co-localization of XPC protein and TFIIH was assessed by quantifying the green and red signals, respectively, in nuclear foci.

In the case of wild-type XPC, the accumulation of GFP fusion protein translates to the recruitment of p62 within the UV-irradiated areas. However, the redistribution of this TFIIH subunit is not observed in XP-C cells expressing the F799A mutant (Fig. 7A) or in XP-C cells transfected with the empty pEGFP vector (data not shown). To perform quantitative comparisons, the ratio of fluorescence over background was determined in each focus, whereby the green fluorescence stands for the accumulation of XPC protein and the red fluorescence represents the p62 (Fig. 7B) or p89 subunits (Fig. 7C). This quantitative analysis revealed that the N754A and F756A mutants fully retain the ability to engage TFIIH. Instead, the F797A and F799A mutations result in a decreased recruitment of the TFIIH complex to

lesion sites. This conclusion is supported by the observation that the F797A/F799A double mutant still accumulates in the UV foci of XP-C cells but, unlike the N754A/F756A double mutant, is unable to hand over the lesions to the downstream TFIIH machinery.

It should be pointed out that, in these experiments performed with human fibroblasts, the UV-dependent redistribution of the different mutants is slightly more effective than in the comparable assay of Fig. 4 carried out with CHO cells. This difference is attributable to the fact that CHO cells lack DDB2, the DNA-binding subunit of UV-DDB, which in human cells stimulates the relocation of XPC protein to UV foci produced by the micropore filter method (47). Therefore, we performed additional control experiments to show that the overexpression of DDB2-GFP alone, in the absence of XPC protein, is not sufficient to recruit the p62 and p89 subunits (Figs. 7B and 7C). Thus, the differential transfer of UV lesions to the TFIIH complex represents a genuine property of the tested XPC mutants and reflects the contribution of the respective amino acid side chains to the conformational rearrangements necessary for the loading of this downstream factor onto damaged DNA.

GGR activity in human cells

Finally, the repair proficiency of each mutant was tested by expressing XPC-GFP constructs in GGR-deficient XP-C fibroblasts (Fig. 8A). The degree of functional complementation was determined by a host-cell reactivation assay that has been developed to measure the cellular GGR activity (9) and which is performed by co-transfection with a dual luciferase system. The reporter plasmid, damaged by UV-C irradiation, carries a *Photinus* luciferase gene whereas the undamaged control codes for the *Renilla* luciferase (28). After an 18-h incubation, the activity of *Photinus* luciferase, whose expression depends on the repair of UV lesions, was measured in cell lysates and normalized against the accompanying *Renilla* counterpart. In XP-C fibroblasts transfected with the empty pEGFP vector, the luciferase expression is reduced to background levels consistent with the absence of GGR

activity in this cell line (Fig. 8B). Compared to wild-type XPC, all tested single mutants display a repair defect leading to reduced expression of the luciferase reporter. The mildest response was associated with the F756A substitution, consistent with the observation that this mutant is only partially impaired in its ability to relocate to tracks of UV lesions but is fully proficient in the subsequent TFIIH recruitment (see Figs. 3B and 7). In contrast, the most severe GGR defect was imposed by the F799A mutation, which is in line with the finding that this particular amino acid is very critical for the recruitment of TFIIH to lesion sites.

DISCUSSION

The present analysis of human XPC protein, based on site-directed mutagenesis, was instigated by the intriguing configuration of DNA found in crystal complexes of the yeast Rad4 homolog with a model substrate (30). In this previous structural study, Rad4 protein binds to damaged duplexes by interacting with a double-stranded to single-stranded DNA transition around the lesion site, whereby two neighboring nucleotides in the undamaged strand are completely displaced out of the double helix. Conserved amino acids (N754, F756, F797 and F799) predicted to make close contacts with these flipped-out nucleotides have been identified in the human XPC sequence and challenged by alanine substitutions (Fig. 1). The results of our study demonstrate that the four tested residues indeed play a key role in the formation of a recognition intermediate that transfers the DNA lesions to downstream GGR factors.

The most crucial outcome of this study is that the examined side groups drive a sequence of distinguishable nucleoprotein transitions starting from the default search mode, by which XPC protein finds DNA damage in the genome, to an initial (unstable) encounter complex at lesion sites and, finally, the installation of an ultimate (stable) recruitment platform. The variable effects of alanine substitutions at different XPC positions imply that the respective amino acid residues exert diverging functions during the aforementioned transitions. In the *in vitro* assay, the interaction with DNA is more sensitive to N754A, F756A and F797A substitutions than to the corresponding change at position F799. The most prominent difference between the N754A, F756A and F797A mutations, on the one hand, and the F799A substitution on the other hand, was observed with the junction DNA molecule (Fig. 2C) used as a model substrate to probe the affinity of XPC protein for unpaired bases in a duplex context. The common binding partner of residues N754, F756 and F797 is the flipped-out base on the 3' side of the undamaged strand (Fig. 1B), suggesting that these three

side chains of XPC protein cooperate to sense damage-induced base displacements opposite to lesion sites. Conversely, the F799A mutation conveys a more severe reduction in the binding to single-stranded DNA relative to junction molecules indicating that this residue is nevertheless important to stabilize XPC protein onto the displaced undamaged strand. This view is supported by FRAP-LD analyses indicating that the F799A mutant is unable to anchor itself onto UV-irradiated DNA in living cells (Fig. 6).

A separation of function between the tested amino acid residues was also evident when we monitored the subsequent TFIIH recruitment. Both the N754A and F756A mutations diminish the relocation to UV foci, but the fraction of these XPC mutants that did accumulate at lesion sites was as effective as the wild-type control in engaging TFIIH into the nascent GGR complex. Instead, the F797A and, particularly, the F799A mutation interfered with TFIIH recruitment (Fig. 7). The common binding partner of F797 and F799 is the flipped-out residue on the 5' side (Fig. 1), thus indicating that the extrusion of this additional nucleotide is essential for the transfer of DNA lesions from XPC protein to TFIIH. These findings are consistent with a previous truncation study indicating that the detection of damaged sites is mainly mediated by a dynamic interface of XPC protein that includes amino acids 607-766, whereas an adjacent protein segment (amino acids 767-833) is required for the following stabilization of a GGR-initiating complex on the target substrate (8).

Surprisingly, our mutagenesis analysis revealed that the side chains of XPC protein that interact with the flipped-out nucleotides in the ultimate recognition complex also contribute to the default binding to native double-stranded DNA (Fig. 2C). This finding is at first sight counterintuitive because it may have been expected that an amino acid substitution that reduces the affinity for the native duplex, and hence suppresses the interaction with genomic DNA, would cause an increased nuclear mobility in FRAP experiments. However, when this prediction was tested in undamaged living cells, we found that the N754A change actually

limits the movements of XPC protein (Fig. 5B). Although less pronounced, a diminished nuclear mobility compared to wild-type was also found for the F797A and F799A mutants. A likely scenario that accommodates this surprising observation is that XPC protein searches for DNA lesions by a facilitated diffusion procedure whereby protein movements within living cells are guided by interactions with DNA filaments. Facilitated protein diffusion may occur by a "sliding" mode, i.e., by movements along linear molecules, or by a "hopping" mode that involves continuous association-dissociation cycles from one site to another on DNA. In either case, by reducing the dimensionality of the search process, facilitated diffusion is thought to enhance the efficiency of target site location by several orders of magnitude (5, 49). Support for the involvement of N754 in a facilitated search process comes from the observation that the low mobility conferred by the exchange of this residue with alanine (Fig. 5B) correlates with the weakest accumulation of all mutants in UV lesion tracks (Fig. 3B).

To summarize, this study describes how four critical amino acid side chains of human XPC protein interact with multiple DNA conformations to drive the genome-wide search process, the formation of a dynamic (unstable) encounter complex and the installment of a stable recognition intermediate that promotes TFIIH recruitment. The GGR proficiency of the tested XPC mutants reflects the cumulative effect of the respective amino acid substitutions on these distinguishable but interrelated activities of XPC protein. Further studies will be devoted to analyze the contribution of UV-DDB and chromatin remodeling complexes in this genome-wide lesion recognition mechanism.

ACKNOWLEDGEMENTS

We thank A. Lenisa, M. Träxler, and D. Hermann for excellent technical assistance, G. Marra (University of Zürich) for the gift of CHO cells and S. Linn (University of California, Berkeley) for the DDB2-GFP expression vector.

AUTHOR DISCLOSURE STATEMENT

No competing financial interests exist.

ABBREVIATIONS

CHO = Chinese hamster ovary

DMEM = Dulbecco's modified Eagle's medium

EGFP = enhanced green-fluorescent protein

FCS = fetal calf serum

FRAP = fluorescence recovery after photobleaching

FRAP-LD = FRAP on local damage

GFP = green-fluorescent protein

GGR = global-genome repair

MBP = maltose-binding protein

PBS = phosphate-buffered saline

RPA = replication protein A

SD = standard deviation

SEM = standard error of the mean

TFIIH = transcription factor IIH

UV = ultraviolet

UV-DDB = UV-damaged DNA-binding

XP = xeroderma pigmentosum

REFERENCES

1. Alekseev S, Luijsterburg, MS, Pines A, Geyerts B, Mari PO, Giglia-Mari G, Lans H, Houtsmuller AB, Mullenders LH, Hoeijmakers JH, and Vermeulen W. Cellular concentrations of DDB2 regulate dynamic binding of DDB1 at UV-induced DNA damage. *Mol Cell Biol* 28:7402-7413, 2008.
2. Andressoo JO, Hoeijmakers JH, and Mitchell JR. Nucleotide excision repair disorders and the balance between cancer and aging. *Cell Cycle* 5: 2886–2888, 2006.
3. Araujo SJ, Tirode F, Coin F, Pospiech H, Syväoja JE, Stucki M, Hübscher U, Egly JM, and Wood RD. Nucleotide excision repair of DNA with recombinant human proteins: definition of the minimal set of factors, active forms of TFIIH, and modulation by CAK. *Genes Dev* 14: 349-359, 2000.
4. Batty D, Rapic'-Otrin V, Levine AS, and Wood RD. Stable binding of human XPC complex to irradiated DNA confers strong discrimination for damaged sites. *J Mol Biol* 300: 275-290, 2000.
5. Berg OG, Winter RB, and van Hippel PH. Diffusion-driven mechanisms of protein translocation on nucleic acids. 1. Models and theory. *Biochemistry* 20: 6929-6948, 1981.
6. Brooks PJ. The case for 8,5'-cyclopurine-2'-deoxynucleosides as endogenous DNA lesions that cause neurodegeneration in xeroderma pigmentosum. Neuroscience 145: 1407-1417, 2007.
7. Buterin T, Meyer C, Giese B, and Naegeli H. DNA quality control by conformational readout on the undamaged strand of the double helix. *Chem Biol* 12: 913-922, 2005.
8. Camenisch U, Träutlein D, Clement FC, Fei J, Leitenstorfer A, Ferrando-May E, and Naegeli H. Two-stage dynamic DNA quality check by xeroderma pigmentosum group C protein. *EMBO J* 28: 2387-99, 2009.

9. Carreau M, Quilliet X, Eveno E, Salvetti A, Danos O, Heard JM, Mezzina M, and Sarasin A. Functional retroviral vector for gene therapy of xeroderma pigmentosum group D patients. *Hum Gene Ther* 6: 1307-1315, 1995.

10. Chavanne F, Broughton BC, Pietra D, Nardo T, Browitt A, Lehmann AR, and Stefanini M. Mutations in the XPC gene in families with xeroderma pigmentosum and consequenced at the cell, protein and transcription level. *Cancer Res* 60: 1974–1982, 2000.

11. Cleaver JE. Cancer in xeroderma pigmentosum and related disorders of DNA repair. *Nat Rev Cancer* 5: 564–573, 2005.

12. Cleaver JE, Thompson LH, Richardson AS, and States JC. A summary of mutations in the UV-sensitive disorders: xeroderma pigmentosum, Cockayne syndrome, and trichothiodystrophy. *Hum Mutat* 14: 9–22, 1999.

13. Cosman M, Fiala R, Hingerty BE, Laryea A, Lee H, Amin S, Geacintov NE, Broyde S, and Patel D. Solution conformation of the (+)-trans-anti[BPh]dA adduct opposite dT in a DNA duplex: intercalation of the covalently attached benzo[c]phenanthrene to the 5'-side of the adduct site without disruption of the modified base pair. *Biochemistry* 32: 12488-12497, 1993.

14. Dinant C, de Jager M, Essers J, van Cappellen WA, Kanaar R, Houtsmuller AB, and Vermeulen W. Activation of multiple DNA repair pathways by subnuclear damage induction methods. *J Cell Sci* 120: 2731–2740, 2007.

15. Evans E, Moggs JG, Hwang JR, Egly JM, and Wood RD. Mechanism of open complex and dual incision formation by human nucleotide excision repair factors. *EMBO J* 16: 6559-6573, 1997.

16. Fitch ME, Nakajima S, Yasui A, and Ford JM. In vivo recruitment of XPC to UV-induced cyclobutane pyrimidine dimers by the DDB2 gene product. *J Biol Chem* 278:

46906-46910, 2003.

17. Friedberg EC. How nucleotide excision repair protects against cancer. *Nat Rev Cancer* 1: 22–33, 2001.

18. Friedberg EC, Walker GC, Siede W, Wood RD, Schultz RA, and Ellenberger T. *DNA Repair and Mutagenesis*. Washington, DC: ASM Press, 2006, p. 698.

19. Gillet LC and Schärer OD. Molecular mechanisms of mammalian global genome nucleotide excision repair. *Chem Rev* 106: 253–276, 2006.

20. Hanawalt PC and Spivak G. Transcription-coupled DNA repair: two decades of progress and surprises. *Nat Rev Mol Cell Biol* 9: 958–970, 2008.

21. Hoeijmakers JH. DNA damage, aging, and cancer. *N Engl J Med* 361: 1475-1485, 2009.

22. Hoogstraten D, Bergink S, Verbiest VH, Luijsterburg MS, Geverts B, Raams A, Dinant C, Hoeijmakers JH, Vermeulen W, and Houtsmuller AB. Versatile DNA damage detection by the global genome nucleotide excision repair protein XPC. *J Cell Sci* 121: 2850–2859, 2008.

23. Huang JC, Svoboda DL, Reardon JT, and Sancar A. Human nucleotide excision nuclease removes thymine dimers from DNA by incising the 22nd phosphodiester bond 5' and the 6th phosphodiester bond 3' to the photodimer. *Proc Natl Acad Sci USA* 89: 3664-3668, 1992.

24. Kim JK, Soni SD, Arakali AV, Wallace JC, and Alderfer JL. Solution structure of a nucleic acid photoproduct of deoxyfluorouridylyl-(3'-5')-thymidine monophosphate (d-FpT) determined by NMR and restrained molecular dynamics: structural comparison of two sequence isomer photoadducts (d-U5p5T and d-T5p5U). *Nucleic Acids Res* 23: 1810-1815, 1995.

25. Kim JK and Choi BS. The solution structure of DNA duplex-decamer containing the

(6-4) photoproduct of thymidylyl(3'-->5')thymidine by NMR and relaxation matrix refinement. *Eur J Biochem* 228: 849-854, 1995.

26. Lan L, Nakajima S, Oohata Y, Takao M, Okano S, Masutani M, Wilson SH, and Yasui A. In situ analysis of repair processes for oxidative DNA damage in mammalian cells. *Proc Natl Acad Sci USA* 101: 13738–13743, 2004.
27. Lehmann AR. DNA repair-deficient diseases, xeroderma pigmentosum, Cockayne syndrome and trichothiodystrophy. *Biochimie* 85: 1101–1111, 2003.
28. Maillard O, Solyom S, and Naegeli H. An aromatic sensor with aversion to damaged strands confers versatility to DNA repair. *PLoS Biol* 5: e79, 2007.
29. Meldrum RA, Botchway SW, Wharton CW, and Hirst GJ. Nanoscale spatial induction of ultraviolet photoproducts in cellular DNA by three-photon near-infrared absorption. *EMBO Rep* 4: 1144–1149, 2003.
30. Min JH and Pavletich NP. Recognition of DNA damage by the Rad4 nucleotide excision repair protein. *Nature* 449: 570-575, 2007.
31. Ng JM, Vermeulen W, van der Horst GT, Bergink S, Sugasawa K, Vrieling H, and Hoeijmakers JH. A novel regulation mechanism of DNA repair by damage-induced and RAD23-dependent stabilization of xeroderma pigmentosum group C protein. *Genes Dev* 17: 1630–1645, 2003.
32. Nishi R, Okuda Y, Watanabe E, Mori T, Iwai S, Masutani C, Sugasawa K, and Hanaoka F. Centrin 2 stimulates nucleotide excision repair by interacting with xeroderma pigmentosum group C protein. *Mol Cell Biol* 25: 5664–5674, 2005.
33. O'Donovan A, Davies AA, Moggs JG, West SC, and Wood RD. XPG endonuclease makes the 3' incision in human DNA nucleotide excision repair. *Nature* 371: 432-435, 1994.
34. O'Handley SF, Sanford DG, Xu R, Lester CC, Hingerty BE, Broyde S, and Krugh TR.

Structural characterization of an N-acetyl-2-aminofluorene (AAF) modified DNA oligomer by NMR, energy minimization, and molecular dynamics. *Biochemistry* 32: 2481-2497, 1993.

35. Sancar A. DNA excision repair. *Annu Rev Biochem* 65: 43–81, 1996.

36. Sijbers AM, de Laat WL, Ariza RR, Biggerstaff M, Wei YF, Moggs JG, Carter KC, Shell BK, Evans E, de Jong MC, Rademakers S, de Rooij J, Jaspers NG, Hoeijmakers JH, and Wood RD. Xeroderma pigmentosum group F caused by a defect in a structure-specific DNA repair endonuclease. *Cell* 86: 811-822, 1996.

37. Staresincic L, Fagbemi FA, Enzlin JH, Gourdin AM, Wijgers N, Dunand-Sauthier I, Giglia-Mari G, Clarkson SG, Vermeulen W, and Schärer OD. Coordination of dual incision and repair synthesis in human nucleotide excision repair. *EMBO J* 28: 1111-1120, 2009.

38. Sugasawa K. Regulation of damage recognition in mammalian global genome nucleotide excision repair. *Mutat Res* 685: 29-37, 2010.

39. Sugasawa K, Ng JM, Masutani C, Iwai S, van der Spek PJ, Eker AP, Hanaoka F, Bootsma D, and Hoeijmakers JH. Xeroderma pigmentosum group C protein complex is the initiator of global genome nucleotide excision repair. *Mol Cell* 2: 223–232, 1998.

40. Tang JY, Hwang BJ, Ford JM, Hanawalt PC, and Chu G. Xeroderma pigmentosum p48 gene enhances global gemomic repair and suppresses UV-induced mutagenesis. *Mol Cell* 5: 737–744, 2000.

41. Träutlein D, Adler F, Moutzouris K, Jeromin A, Leitenstorfer A, and Ferrando-May E. Highly versatile confocal microscopy system based on a tunable femtosecond Er:fiber source. *J Biophoton* 1: 53–61, 2008.

42. Trego KS and Turchi JJ. Pre-steady-state binding of damaged DNA by XPC-hHR23B reveals a kinetic mechanism for damage discrimination. *Biochemistry* 45: 1961–1969,

2006.

43. Uchida A, Sugasawa K, Masutani C, Dohmae N, Araki M, Yokoi M, Ohkuma Y, and Hanaoka F. The C-terminal domain of the XPC protein plays a crucial role in nucleotide excision repair through interactions with transcription factor IIH. *DNA Rep* 1: 449–461, 2002.

44. Volker M, Mone MJ, Karmakar P, van Hoffen A, Schul W, Vermeulen W, Hoeijmakers JH, van Driel R, van Zeeland AA, and Mullenders LH. Sequential assembly of the nucleotide excision repair factors in vivo. *Mol Cell* 8: 213–224, 2001.

45. Wakasugi M and Sancar A. Assembly, subunit composition, and footprint of human DNA repair excision nuclease. *Proc Natl Acad Sci USA* 95: 6669–6674, 1998.

46. Wood RD. DNA repair in eukaryotes. *Annu Rev Biochem* 65: 135-167, 1996.

47. Yasuda G, Nishi R, Watanabe E, Mori T, Iwai S, Orioli D, Stefanini M, Hanaoka F, and Sugasawa K. In vivo destabilization and functional defects of the xeroderma pigmentosum C protein caused by a pathogenic missense mutation. *Mol Cell Biol* 27: 6606–6614, 2007.

48. Yokoi M, Masutani C, Maekawa T, Sugasawa K, Ohkuma Y, and Hanaoka F. The xeroderma pigmentosum group C protein complex XPC-HR23B plays an important role in the recruitment of trans- cription factor IIH to damaged DNA. *J Biol Chem* 275: 9870–9875, 2000.

49. Zharkov D and Grollmann AP. The DNA trackwalkers: principles of lesion search and recognition by DNA glycosylases. *Mutat Res* 577: 24-54, 2005.

FIGURE LEGENDS

FIG. 1. Conserved amino acids interacting with flipped-out nucleotides. (A) Sequence comparison centered on the protein domain of eukaryotic XPC homologs (residues 750-833 of the human polypeptide) predicted to interact with flipped-out nucleotides. The asterisks denote amino acid side chains of Rad4 protein that interact directly with DNA (Min & Pavletich 2007). The residues targeted for site-directed mutagenesis are indicated in orange. (B) Ribbon diagram of the predicted XPC domain that associates with two flipped-out nucleotides. N754 and F756 interact with the displaced nucleotide on the 3'side, F799 with the displaced nucleotide on the 5' side and F797 interacts with both residues simultaneously. CPD, cyclobutane pyrimidine dimer. The figure was made with the PyMol Molecular Viewer using the coordinates PDB 2QSG. (For interpretation of the reference to color in this figure legend, the reader is referred to the web version of this article at www.liebertonline.com/ars)

FIG. 2. DNA-binding defect of XPC mutants in vitro. (A) Immunoblot of *Sf*9 cell lysates (50 μg of total protein) demonstrating similar amounts of MBP-XPC fusions. Control, lysate from uninfected cells; Wt, wild-type. (B) Binding of XPC protein to single-stranded, double-stranded or junction DNA. The indicated concentrations of MBP-XPC in cell lysate were incubated with ^{32}P-labeled 135-mer substrates (2 nM). The DNA captured by XPC protein was separated from the free oligonucleotides and quantified in a scintillation counter. The bound fraction is reported as the percentage of total input DNA. Asterisks denote statistically significant differences between the binding to junction and single-stranded oligonucleotides and the homoduplex control (mean ± SD, *$p < 0.001$, **$p < 0.0001$, $N = 3$). (C) Comparison of DNA-binding activity of wild-type and mutant XPC protein (1.7 nM) in the presence of

the indicated substrates. Asterisks denote statistically significant differences of the mutants from wild-type protein (mean ± SD, *$p < 0.05$, **$p < 0.0001$, $N = 3$).

FIG. 3. Real-time accumulation in tracks of UV lesions. (A) Representative images illustrating the differential accumulation of wild-type and mutant XPC protein at lesion sites. CHO cells expressing low levels of XPC-GFP were laser-treated to generate 10-μm tracks of UV lesions. The black bars indicate the position of the 10-μm irradiation track. (B) Real-time kinetics of DNA damage recognition. The accumulation of XPC-GFP (wild-type or mutants) at different time points is plotted as a percentage of the average fluorescence before irradiation. Asterisks indicate the statistically significant differences of wild-type XPC compared to the mutants (mean ± SEM, *$p < 0.05$, $N = 10$). (For interpretation of the references to color in this figure legend, the reader is referred to the web version of this article at www.liebertonline.com/ars)

FIG. 4. Acccumulation in foci of UV lesions. Representative images illustrating that the site-directed mutants are defective in the reallocation to UV foci relative to the wild-type control. CHO cells were irradiated through the pores of polycarbonate filters and fixed 15 min after treatment to monitor the co-localization of the GFP fusion constructs (green) and (6-4) photoproducts (red). Hoechst, DNA staining visualizing the nuclei. (For interpretation of the references to color in this figure legend, the reader is referred to the web version of this article at www.liebertonline.com/ars)

FIG. 5. Analysis of protein dynamics in the nuclei of living cells. In CHO cells expressing the indicated XPC-GFP constructs, a nuclear area of 4 μm^2 is bleached with a 488-nm wavelength laser. The subsequent fluorescence recovery depends on the diffusion rate and

macromolecular interactions (8, 22). (A) Response of wild-type XPC protein to UV irradiation. Asterisks denote statistically significant differences of UV-irradiated compared to non-irradiated cells (mean ± SEM, *p < 0.05, **p < 0.0001, N = 12). (B) Differential movements of wild-type and mutant XPC protein in non-irradiated cells. The order of protein mobility is as follows: Wt = F756A > F799A > F797A > N754A. The asterisks mark statistically significant differences of N754A compared to the wild-type control (mean ± SEM, *p < 0.05, **p < 0.0001, N = 10). (C-F) The nuclear mobility of the indicated XPC mutants is not retarded by UV irradiation (N = 12, ± SEM).

FIG 6. Dissociation from sites of UV damage in living cells. The green signal representing XPC-GFP fusion proteins in the UV foci of CHO cells was bleached to reach the overall fluorescence intensity of the surrounding nuclear area. The differential recovery of fluorescence in the bleached spots indicates that only wild-type XPC forms stable recognition complexes. Asterisks denote statistically significant differences of the mutants from wild-type control (mean ± SEM, *p < 0.001, **p < 0.0001, N = 10).

FIG 7. Recruitment of TFIIH. (A) Representative images illustrating that wild-type XPC but not the F799A mutant is able to recruit the p62 subunit of TFIIH to UV foci. (B and C) Quantitative assessments of green and red signals representing the accumulation of XPC-GFP and the indicated TFIIH subunits, respectively, in XP-C fibroblasts. Foci of DNA damage were generated by UV-C irradiation through micropore filters. The recruitment of p62 and p89 is determined by immunocytochemistry. Asterisks indicate statistically significant differences between the accumulation of p62 and p89, respectively, and the accumulation of XPC protein (mean ± SEM, *p < 0.05, **p < 0.0001, N = 30). (For interpretation of the

references to color in this figure legend, the reader is referred to the web version of this article at www.liebertonline.com/ars)

FIG 8. GGR activity. (A) Representative immunoblot to compare the expression of XPC-GFP fusion proteins in XP-C fibroblasts. (B) The repair of UV lesions was determined by means of a host-cell reactivation assay. The asterisks denote statistically significant differences from the wild-type protein control (mean ± SD, *$p < 0.0001$, $N = 9$). Reactivation of the luciferase reporter is plotted as the percentage of controls determined by transfecting cells with the vector coding for wild-type XPC-GFP; pEGFP, background luciferase expression in cells transfected with the empty vector.

A

```
                                      *  *                                                   *  *  ******* *
S. cerevisiae       550 EITKNTFGNIEVFAPTMIPGNCCLVENPVAIKAARFLGVEFAPAVTSFKFERGSTVKPVLSGIVVAKWLREAIETAIDGIEFI
H. sapiens          750 KVPRNEFGNVYLFLPSMMPIGCVQLNLPNLHRVARKLDIDCVQAITGFDFHG-GYSHPVTDGYIVCEEFKDVLLTAWENEQAV
M. musculus         742 KVPRNEFGNVYLFLPSMMPVGCVQMTLPNLNRVARKLGIDCVQAITGFDFHG-GYCHPVTDGYIVCEEFRDVLLAAWENEQAI
G. gallus           746 KVPRNEYGNVYLFLPSMLPIGCVQLRLPNLNRLARKLDIDCAQAVTGFDFHG-GYSHAVTDGYVVCEEYKEVLIAAWENEQAE
A. meleagris        608 KVPRNDYGNVYLFKPCMLPVGCAHLRLSNLHRVAKKLSIDAAPAVTGFDFHG-GYSHAVTDGYVVCEEFEEILRAAWVEEQEL
D. melanogaster    1176 IVPRNAYGNVELFKDCMLPKKTVHLRLPGLMRICKKLNIDCANAVVGFDFHQ-GACHPMYDGFIVCEEFREVVTAAWEEDQQV
P. annelida         943 KIPHNEYGNVYMFNENMCPLDCTYLKLSGLVQISRKLGKQCIPAVVGWAFDG-GFTHPVIDGAIVLEKDAIDFINAWEKLESG
A. nidulans         600 RIPKNAFGNLDVYVPSMVPAGGIHITHLDAARAARILGIDYADAVTGFSFKG-RHGTAIIKGVVVASEYKEAVEEVLKALEEE
S. pombe            522 IVPKNAYGNIDLYVPSMLPYGAYHCRKRCALAAAKFLEIDYAKAVVGFDFQR-KYSKPKLEGVVVSKRYEEAIDLIAEEIDQE
C. glabrata         561 EIETNTFGNIEVFVPSMIPANCCLVESPVAIKAASFIRIKFAKAVTAFKFEKGRSVKPSITGVVVALWFRDALVAAIDGITQA
K. waltii           588 EVPTNVYGNIDIYTSSMIPRGSCLIESPVAVKAAACLGIEFAKAVTGFKFEKKRVAKPQITGIVVSQEYREAVESMIDGVEYS
S. mikatae          549 EITKNAFGNIEVFVPTMIPGNCCLIESSVAIKATRFLGVEFAPAVTSFKFERGSTVKPVISGVVVAKWLREAIEVTIDGIEFI
```

B

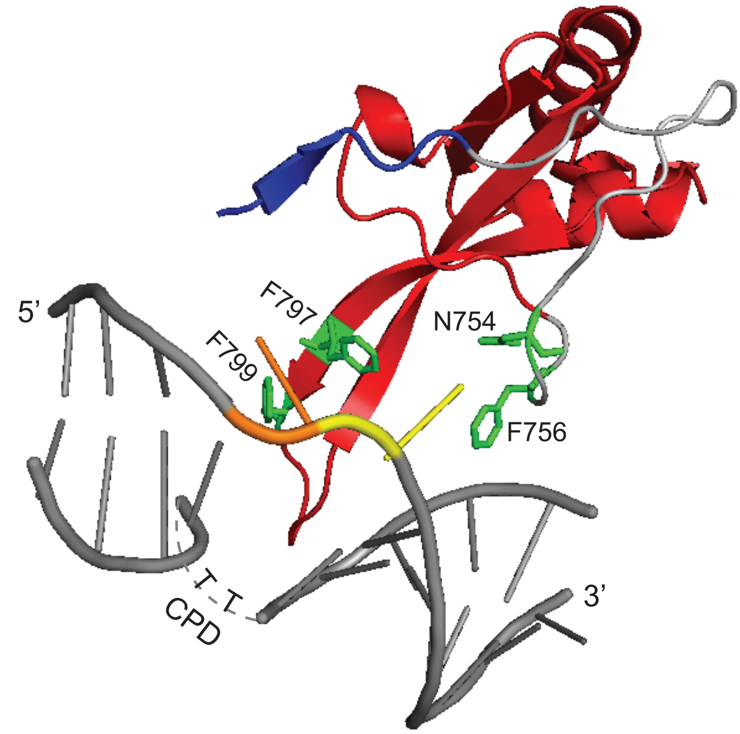

Fig. 1

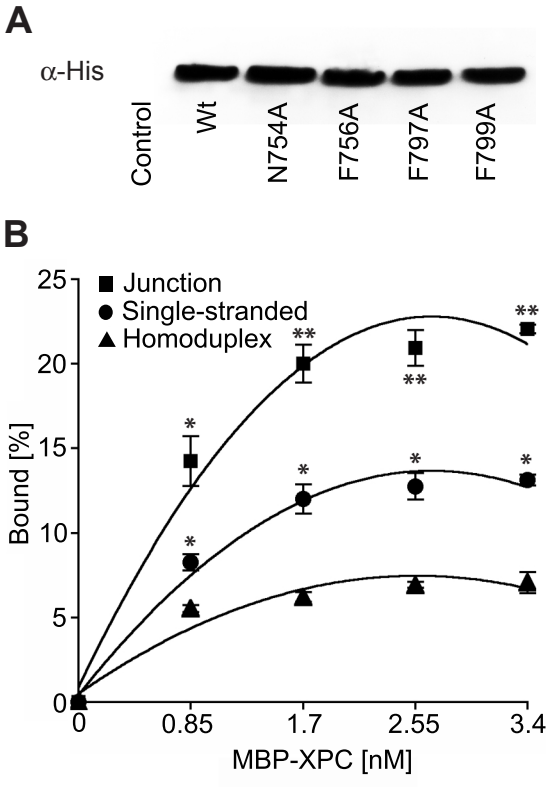
A
α-His
Control
Wt
N754A
F756A
F797A
F799A
B
Junction
Single-stranded
Homoduplex
Bound [%]
MBP-XPC [nM]
0
0.85
1.7
2.55
3.4
C
Wt
N754A
F756A
F797A
F799A
Bound [%]
Homoduplex
Junction
Single-stranded

Fig. 2

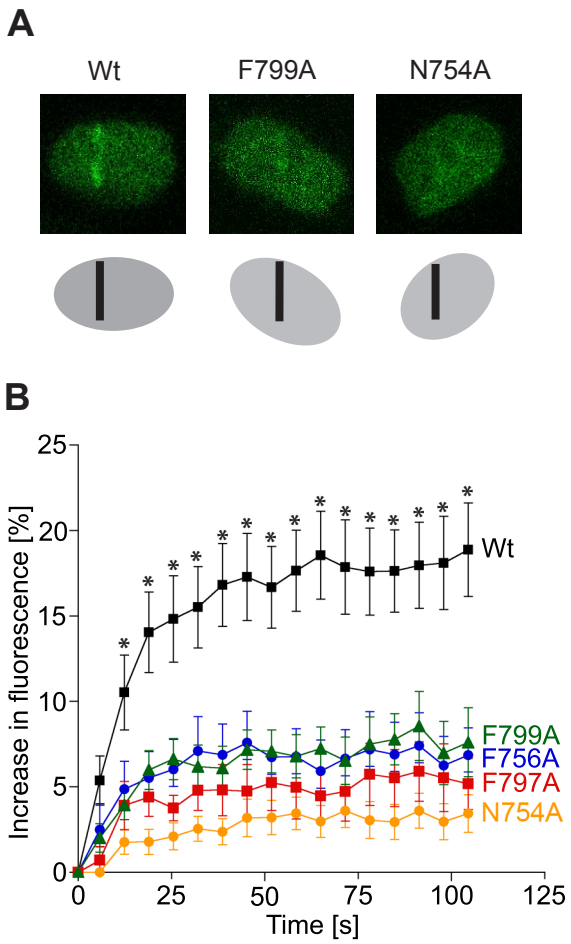
A
Wt
F799A
N754A
B
Increase in fluorescence [%]
Time [s]
Wt
F799A
F756A
F797A
N754A

Fig. 3

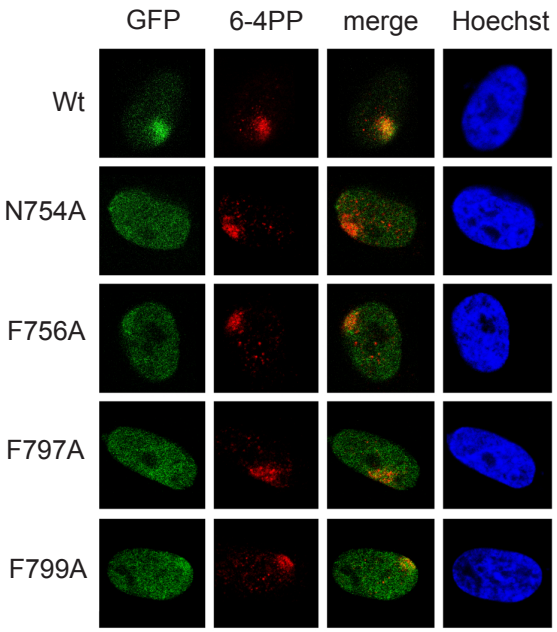

Fig. 4

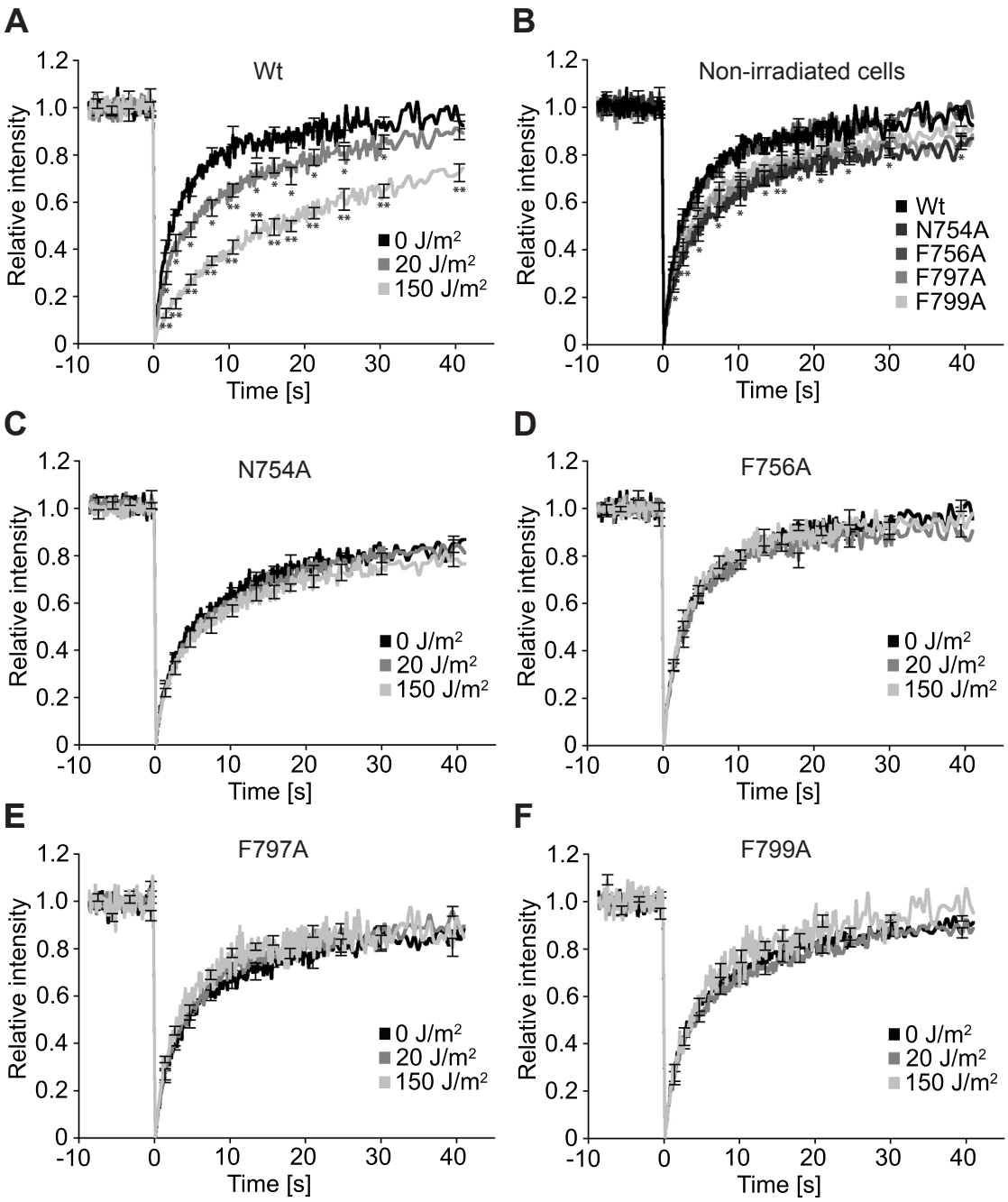
A
Wt
Relative intensity
Time [s]
0 J/m²
20 J/m²
150 J/m²
B
Non-irradiated cells
Wt
N754A
F756A
F797A
F799A
C
N754A
D
F756A
E
F797A
F
F799A

Fig. 5

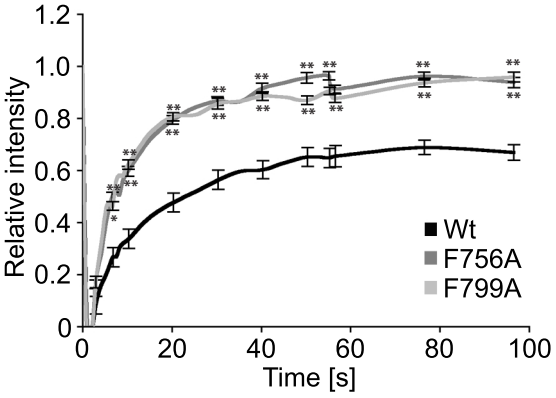
1.2
1.0
0.8
0.6
0.4
0.2
0
Relative intensity
0
20
40
60
80
100
Time [s]
Wt
F756A
F799A

Fig. 6

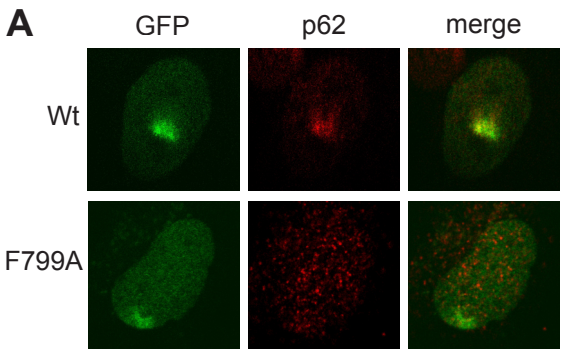
A
GFP
p62
merge
Wt
F799A

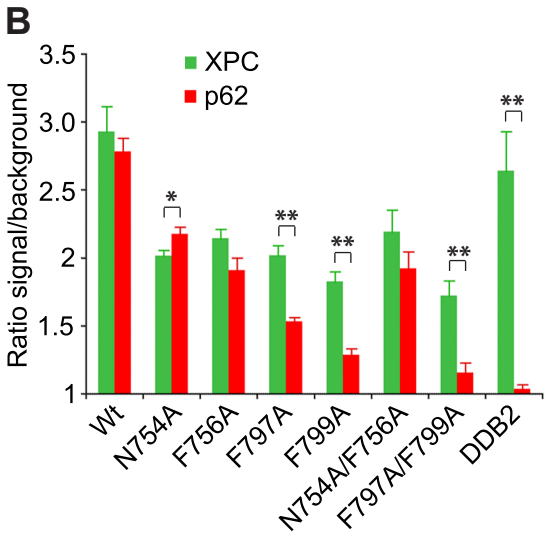
B
XPC
p62
Ratio signal/background
3.5
3.0
2.5
2
1.5
1
*
**
**
**
**
**
Wt
N754A
F756A
F797A
F799A
N754A/F756A
F797A/F799A
DDB2

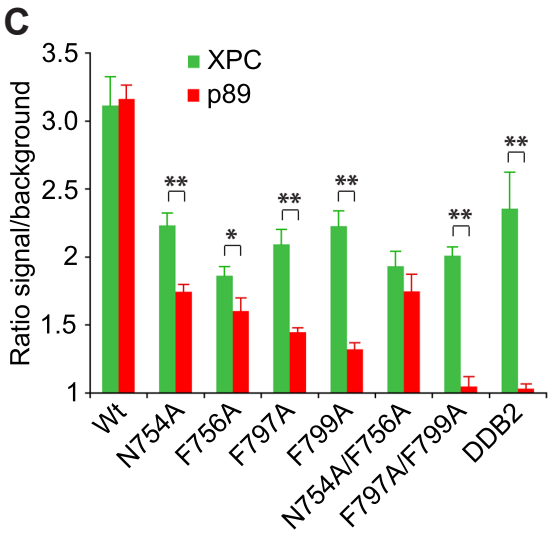
C
XPC
p89
Ratio signal/background
3.5
3.0
2.5
2
1.5
1
**
*
**
**
**
**
Wt
N754A
F756A
F797A
F799A
N754A/F756A
F797A/F799A
DDB2

Fig. 7

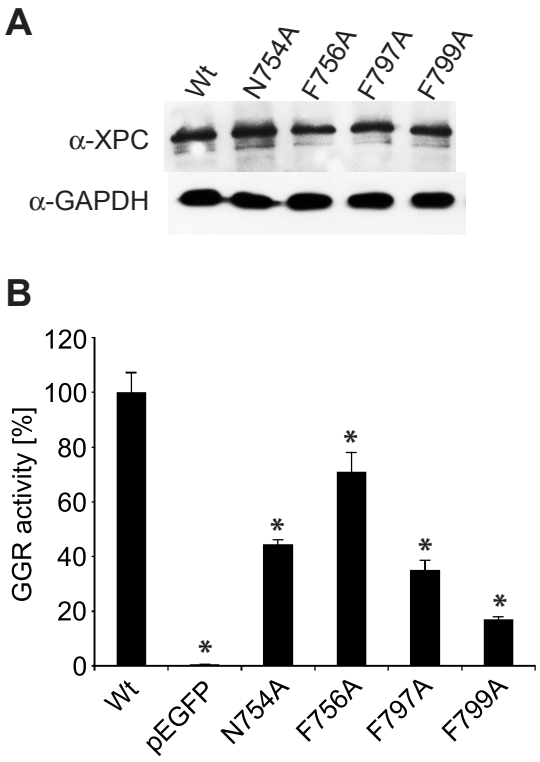
A
Wt
N754A
F756A
F797A
F799A
α-XPC
α-GAPDH
B
GGR activity [%]
120
100
80
60
40
20
0
Wt
pEGFP
N754A
F756A
F797A
F799A

Fig. 8

2.2. Two-stage dynamic DNA quality check by xeroderma pigmentosum group C protein

2.2.1. Aims of the study

The main question of this work was to study how XPC protein finds damaged lesion sites within an enormous background of native genomic DNA. Truncated XPC-GFP fusion constructs were created and their real-time redistribution after high-resolution DNA damage induction was studied using life-cell imaging.

2.2.2. Results in brief

In living cells, DNA damage was instantaneously recognized by XPC protein. Evolutionary conserved aromatic residues were mutated to alanine or serine and tested for their *in vitro* DNA binding ability, which was diminished for each of the mutants compared to wild-type protein. Based on these results and on truncation studies, $XPC_{607-766}$ was identified as the minimal DNA damage sensor also comprising residue W690 which (according to a patient showing a W690S mutation) is important for DNA binding. This indicates that BHD3 is not required for DNA damage recognition. In FRAP experiments a fraction of $XPC_{607-831}$ is immobilized in a damage-specific manner demonstrating that BHD3 is crucial for the installation of a stable repair complex upon lesion recognition. A single E755K mutation within $XPC_{607-766}$ reduces the DNA-repellent effect of the β-turn structure, a feature that is important for damage recognition. These findings lead to the conclusion that XPC exerts its function in a two-stage dynamic process: first by rapid interrogation of the double helix via DNA-attractive and DNA-repulsive motifs, then forming a static repair-initiating complex.

2.2.3. Contribution to this paper

I participated in the cloning of the XPC protein truncations as well as their purification and performed the *in vitro* DNA-binding assays.

2.2.4. Reference

Camenisch U, Träutlein D, **Clement FC**, Fei J, Leitenstorfer A, Ferrando-May E, and Naegeli H (2009) Two-stage dynamic DNA quality check by xeroderma pigmentosum group C protein. *EMBO J* 28: 2387-2399.

2.2.5. Manuscript and supplementary information

The EMBO Journal (2009) 28, 2387–2399 | © 2009 European Molecular Biology Organization | All Rights Reserved 0261-4189/09
www.embojournal.org

THE EMBO JOURNAL

Two-stage dynamic DNA quality check by xeroderma pigmentosum group C protein

Ulrike Camenisch[1,4], Daniel Träutlein[2,4], Flurina C Clement[1], Jia Fei[1], Alfred Leitenstorfer[2], Elisa Ferrando-May[3] and Hanspeter Naegeli[1,*]

[1]Institute of Pharmacology and Toxicology, University of Zürich-Vetsuisse, Zürich, Switzerland, [2]Department of Physics and Center for Applied Photonics, University of Konstanz, Konstanz, Germany and [3]Bioimaging Center, University of Konstanz, Konstanz, Germany

Xeroderma pigmentosum group C (XPC) protein initiates the DNA excision repair of helix-distorting base lesions. To understand how this versatile subunit searches for aberrant sites within the vast background of normal genomic DNA, the real-time redistribution of fluorescent fusion constructs was monitored after high-resolution DNA damage induction. Bidirectional truncation analyses disclosed a surprisingly short recognition hotspot, comprising ~15% of human XPC, that includes two β-hairpin domains with a preference for non-hydrogen-bonded bases in double-stranded DNA. However, to detect damaged sites in living cells, these DNA-attractive domains depend on the partially DNA-repulsive action of an adjacent β-turn extension that promotes the mobility of XPC molecules searching for lesions. The key function of this dynamic interaction surface is shown by a site-directed charge inversion, which results in increased affinity for native DNA, retarded nuclear mobility and diminished repair efficiency. These studies reveal a two-stage discrimination process, whereby XPC protein first deploys a dynamic sensor interface to rapidly interrogate the double helix, thus forming a transient recognition intermediate before the final installation of a more static repair-initiating complex.

The EMBO Journal (2009) **28,** 2387–2399. doi:10.1038/emboj.2009.187; Published online 16 July 2009
Subject Categories: genome stability & dynamics
Keywords: DNA repair; genome stability; protein dynamics

Introduction

Nucleotide excision repair (NER) is a fundamental protective system that promotes genome stability by eliminating a wide range of DNA lesions (Gillet and Schärer, 2006). In addition to (6-4) photoproducts and cyclobutane pyrimidine dimers (CPDs) caused by ultraviolet (UV) light, the NER pathway removes DNA adducts generated by electrophilic chemicals as well as intrastrand DNA cross-links, DNA-protein cross-links and a subset of oxidative lesions (Huang *et al*, 1994; Kuraoka *et al*, 2000; Reardon and Sancar, 2006). The NER system operates through the cleavage of damaged strands on either side of injured sites, thus releasing defective bases as the component of oligomeric DNA fragments (Evans *et al*, 1997). Subsequently, the excised oligonucleotides are replaced by repair patch synthesis before DNA integrity is restored by ligation. Hereditary defects in this NER process cause devastating syndromes such as xeroderma pigmentosum (XP), a recessive disorder presenting with photosensitivity, a >1000-fold increased risk of skin cancer and, occasionally, internal tumours and neurological complications (Cleaver, 2005; Andressoo *et al*, 2006; Friedberg *et al*, 2006). XP patients are classified into seven repair-deficient complementation groups designated XP-A through XP-G (Cleaver *et al*, 1999; Lehmann, 2003).

In the NER pathway, the initial detection of DNA damage occurs by two alternative mechanisms. One subpathway, referred to as transcription-coupled repair, takes place when the transcription machinery is blocked by obstructing lesions in the transcribed strand (Hanawalt and Spivak, 2008). The second subpathway, known as global genome repair (GGR), is triggered by the binding of a versatile recognition complex, composed of XPC, Rad23B and centrin 2, to damaged DNA anywhere in the genome (Sugasawa *et al*, 1998; Nishi *et al*, 2005). XPC protein, which is the actual damage sensor of this initiator complex, displays a general preference for DNA substrates that contain helix-destabilizing lesions including (6-4) photoproducts (Batty *et al*, 2000; Sugasawa *et al*, 2001). In the particular case of CPDs, this recognition function depends on an auxiliary protein discovered by virtue of its characteristic UV-damaged DNA-binding (UV-DDB) activity (Nichols *et al*, 2000; Fitch *et al*, 2003). The affinity of this accessory factor for UV-irradiated substrates is conferred by a DNA-binding subunit (DDB2) mutated in XP-E cells (Scrima *et al*, 2008).

To achieve its outstanding substrate versatility, XPC protein interacts with an array of normal nucleic acid residues surrounding the lesion in a way that no direct contacts are made with the damaged bases themselves (Buterin *et al*, 2005; Trego and Turchi, 2006; Maillard *et al*, 2007). This exceptional binding strategy has been confirmed by structural analyses of Rad4 protein, a yeast orthologue that shares ~40% similarity with the human XPC sequence. In co-crystals, Rad4 protein associates with DNA through a large transglutaminase-homology domain (TGD) flanked by the three β-hairpin domains BHD1, BHD2 and BHD3 (Supplementary Figure 1; Min and Pavletich, 2007). In view of the position of these structural elements relative to the accompanying model substrate, a recognition mechanism has been proposed in which BHD3 would 'sample the DNA's conformational space to detect a lesion' (Min and Pavletich, 2007).

These earlier studies describing the features of an ultimately stable XPC/Rad4–DNA complex explain its ability

*Corresponding author. Institute of Pharmacology and Toxicology, University of Zurich-Vetsuisse, Winterthurerstrasse 260, Zurich 8057, Switzerland. Tel.: +41 44 635 87 63; Fax: +41 44 635 89 10; E-mail: naegelih@vetpharm.uzh.ch
[4]These authors contributed equally to this work

Received: 3 February 2009; accepted: 17 June 2009; published online: 16 July 2009

to serve as a molecular platform for the recruitment of transcription factor IIH (TFIIH) or other downstream NER players (Yokoi *et al*, 2000; Uchida *et al*, 2002). However, one of the most challenging issues in the DNA repair field is the question of how a versatile sensor-like XPC/Rad4 examines the Watson–Crick double helix and faces the task of actually finding base lesions among a large excess of native DNA in a typical mammalian genome (Schärer, 2007; Sugasawa and Hanaoka, 2007). To address this long-standing question, we exploited fluorescence-based imaging techniques (Houtsmuller *et al*, 1999; Houtsmuller and Vermeulen, 2001; Politi *et al*, 2005) to visualize the mobility of XPC protein at work in the chromatin context of living cells. Our results point to a two-stage discrimination process, in which the rapid DNA quality check driven by a dynamic sensor of non-hydrogen-bonded bases precedes the final engagement of BHD3 with lesion sites.

Results

Instantaneous recognition of DNA lesions in human cells

Damage-induced changes of molecular dynamics in the nuclear compartment have been followed by C-terminal conjugation of the human XPC polypeptide with green-fluorescent protein (GFP). The time-dependent relocation of this fusion product was tested by transfection of repair-deficient XP-C fibroblasts that lack functional *XPC* because of a mutation leading to premature termination at codon 718 (Chavanne *et al*, 2000). Individual nuclei containing low levels of XPC-GFP (similar to the XPC expression in wild-type fibroblasts) were identified on the basis of their overall fluorescence (Supplementary Figure 2). To induce lesions, the nuclei were subjected to near-infrared irradiation using a pulsed multiphoton laser, thereby generating spatially confined and clearly detectable patterns of DNA damage with minimal collateral effects (Meldrum *et al*, 2003). The resulting laser tracks contained (6-4) photoproducts (Figure 1A) and CPDs (Figure 1B), representing the major UV lesions processed by the NER system. As expected, wild-type XPC-GFP was rapidly concentrated at nuclear sites containing such photolesions (Figure 1A and B). As earlier studies showed that the UV-induced accumulation of XPC is stimulated by DDB2 protein (Fitch *et al*, 2003; Moser *et al*, 2005), we applied the same procedure to XP-E cells, in which an R273H mutation generates a DDB2 product that is inactive in DNA binding and fails to be expressed to detectable levels (Nichols *et al*, 2000; Itoh *et al*, 2001). In this XP-E background, XPC-GFP is nevertheless effectively relocated to UV-irradiated tracks (Figure 1C), consistent with the known ability of XPC protein to detect (6-4) photoproducts in the absence of UV-DDB activity (Batty *et al*, 2000; Kusumoto *et al*, 2001).

To determine the kinetics of protein redistribution, DNA photoproducts were formed along a single 10-μm line crossing the nucleus of XP-C cells. Maximal accumulation of XPC protein was detected after treatment with a near-infrared radiation of 300–360 $GW \cdot cm^{-2}$ (Supplementary Figure 3). Subsequently, DNA damage was induced with 314 $GW\,cm^{-2}$ to generate ~5000 UV lesions in each cell or, on the average, 1 UV lesion in $\sim 1.6 \times 10^6$ base pairs (see Materials and methods). Under these conditions, the local fluorescence in irradiated areas increased nearly instantaneously leading to a clearly distinguishable relocation of XPC fusion protein already 3 s after irradiation (Supplementary Movie 1). With progressive accumulation of wild-type XPC, a half-maximal increase in local fluorescence intensity was reached after ~40 s (Figure 1D). A plateau level of fluorescence in the irradiation tracks, reflecting a steady-state situation with constant turnover, was detected after ~300 s.

Concordance of relocation and DNA-binding activity

Besides the truncating *XPC* mutation, the XP-C fibroblasts used in this study (GM16093) are characterized by a

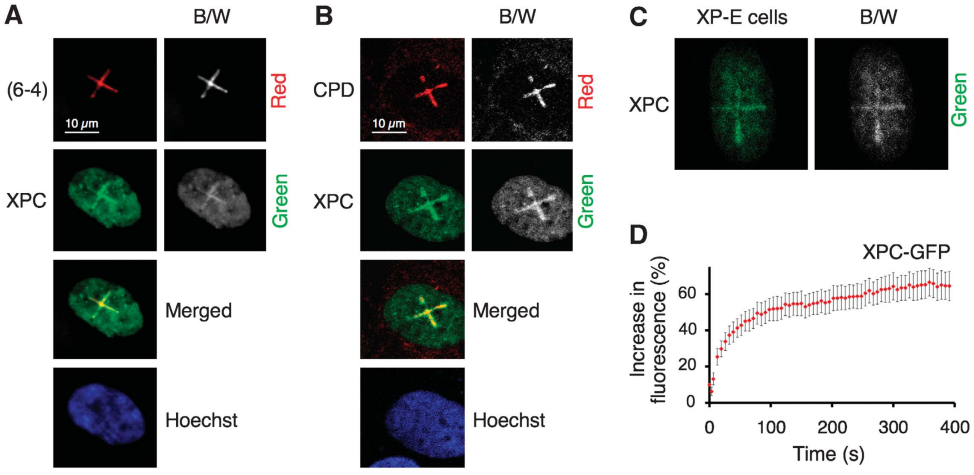

Figure 1 Instantaneous recognition of DNA damage by XPC protein in living cells. (**A**) High-resolution patterns of DNA damage and XPC-GFP accumulation. XP-C fibroblasts expressing low levels of XPC-GFP were laser treated to generate ~5000 UV lesions along each linear irradiation track. The cells were fixed after 6 min and (6-4) photoproducts were detected by immunochemical staining using the red dye Alexa 546. B/W, black-and-white images illustrating the pattern of UV lesions (*upper panel*) and the accumulation of XPC-GFP (*lower panel*). Merged, superimposed images in which the relocation of XPC-GFP matches the pattern of DNA damage. Hoechst, DNA staining visualizing the nuclei. (**B**) Co-localization of XPC-GFP and CPDs. (**C**) Efficient relocation of XPC-GFP to UV irradiation tracks in XP-E cells devoid of UV-DDB activity. (**D**) Real-time kinetics of DNA damage recognition. A single 10-μm line of UV photoproducts was generated across each nucleus of XP-C cells. The accumulation of XPC-GFP at different time points is plotted as a percentage of the average fluorescence before irradiation ($n = 7$). Error bars, standard errors of the mean.

comparably low level of DDB2 protein (Supplementary Figure 4). This reduced DDB2 expression suggested that the GM16093 fibroblasts may provide a cellular context in which, in contrast to an earlier report (Yasuda *et al*, 2007), the damage recognition defect of XPC mutants becomes evident without preceding DDB2 down-regulation. This view was confirmed by testing the nuclear dynamics of a repair-deficient W690S mutant with minimal DNA-binding affinity (Bunick *et al*, 2006; Maillard *et al*, 2007; Hoogstraten *et al*, 2008). In conjunction with the GFP fusion partner, this pathogenic mutant is expressed in similar amounts as the wild-type control and also localizes to the nuclei. However, in the XP-C fibroblasts of this study, the single W690S mutation causes >five-fold reduction in the relocation to UV-damaged areas (Figure 2A; Supplementary Movie 2). These findings were confirmed when another technique was used to inflict genotoxic stress, that is by UV-C irradiation (254 nm wavelength) through the pores of polycarbonate filters (Moné *et al*, 2004). In fact, compared with wild-type XPC, the W690S mutant exhibits only a marginal tendency to accumulate in UV-C radiation-induced foci (data not shown). Oligonucleotide-binding assays with XPC protein expressed in insect cells confirmed that this W690S mutation and the corresponding alanine substitution (W690A) abrogate the interaction with DNA (Figure 2B).

The same analysis was extended to further repair-deficient XPC mutants targeting conserved aromatic residues (Maillard *et al*, 2007). A nearly complete loss of DNA binding is conferred by the F733A mutation, whereas the W531A and W542A substitutions are associated with more moderate defects (Figure 2B). When tested in GM16093 fibroblasts as GFP fusions, the damage-dependent redistribution of these different mutants correlates closely with the respective DNA-binding properties. In fact, the W690S, W690A and F733A derivatives display a poor ability to concentrate at damaged sites. In contrast, the residual DNA-binding activity of W531A and W542A leads to an intermediary level of accumulation in areas containing UV photoproducts (Figure 2C). From this tight correspondence between DNA binding and nuclear redistribution, we concluded that the rapid relocation of XPC protein to UV lesion sites reflects the intrinsic capacity of this sensor subunit to detect DNA damage through direct interactions with the nucleic acid substrate.

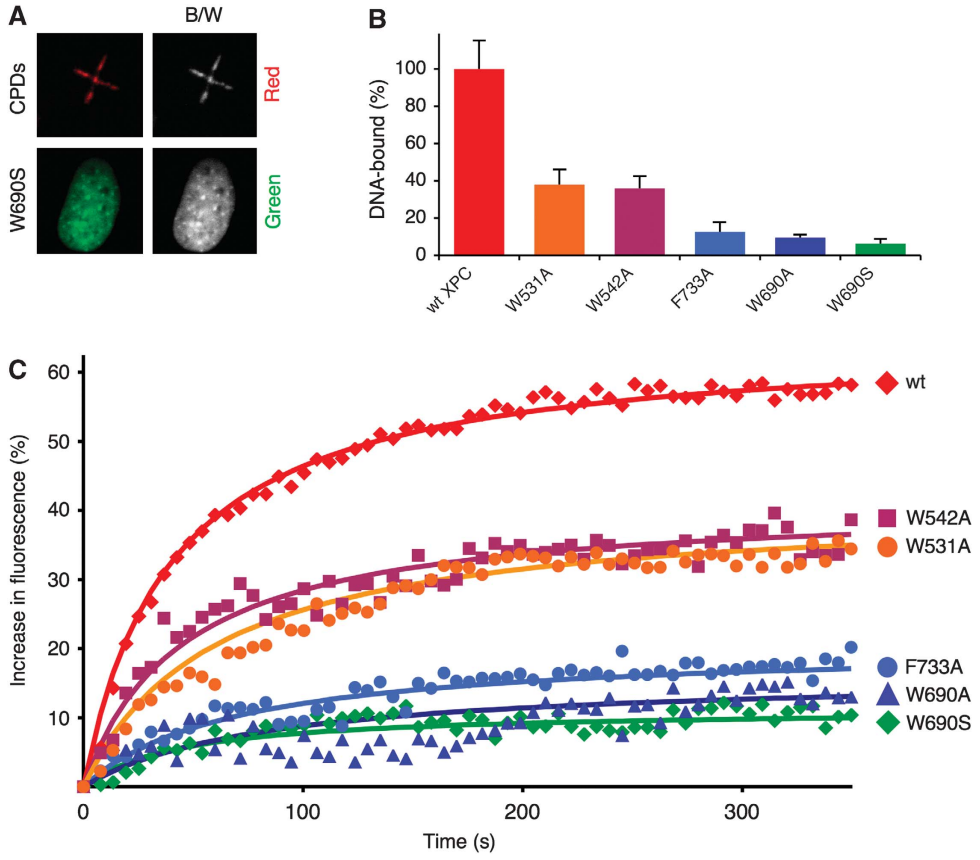

Figure 2 Dependence on intrinsic DNA-binding activity. (**A**) Representative image (in colour and black-and-white) showing the low residual accumulation of the W690S mutant 6 min after irradiation. DNA lesions were counterstained by antibodies against CPDs. (**B**) DNA-binding activity determined by direct pull down. Wild-type (wt) XPC or mutants were expressed in *Sf*9 cells as fusion constructs with maltose-binding protein (MBP). Cell lysates containing similar amounts of XPC protein (Maillard *et al*, 2007) were incubated with a single-stranded 135-mer oligonucleotide. Subsequently, radiolabelled DNA molecules captured by XPC protein were separated from the free probes using anti-MBP antibodies linked to magnetic beads, and the radioactivity in each fraction was quantified in a scintillation counter. DNA binding is represented as the percentage of radioactivity immobilized by wt XPC protein after deduction of a background value determined with empty beads ($n=3$). Error bars, standard deviation. (**C**) Correlation between DNA binding and the kinetics of XPC accumulation in XP-C cells ($n=7$). See legend to Figure 1D for details.

Role of the transglutaminase-like domain

As the transglutaminase-like region maps to the N-terminal part of human XPC (Figure 3A), we generated N-terminal truncations ($XPC_{118-940}$, $XPC_{427-940}$ and $XPC_{607-940}$) to test how the TGD sequences contribute to DNA damage recognition in living cells. The positions 118 and 607 were selected for these truncations to allow for comparisons with an earlier *in vitro* study monitoring the DNA-, Rad23B- and TFIIH-binding activity of XPC fragments (Uchida *et al*, 2002). Another truncate (XPC_{1-495}) was included as a negative control that lacks the entire C-terminal half. The functionality of these constructs, conjugated to GFP at their C-terminus, was compared in a host-cell reactivation assay that has been developed to measure the cellular GGR activity (Carreau *et al*, 1995). Briefly, XP-C fibroblasts were transfected with a dual luciferase reporter system along with an expression vector coding for full-length or truncated XPC fusions. The reporter plasmid, which carries a *Photinus* luciferase gene, was damaged by exposure to UV-C light and supplemented with an undamaged vector that expresses the *Renilla* luciferase. GGR efficiency was assessed after 18-h incubations by determining *Photinus* luciferase activity in cell lysates, followed by normalization against the *Renilla* control.

The full-length protein (XPC_{1-940}) and an $XPC_{118-940}$ derivative, isolated by functional complementation (Legerski and Peterson, 1992), were proficient in correcting the repair defect of XP-C cells (Figure 3B), thus showing that gene reactivation is determined by the ability of the GGR pathway to excise offending UV lesions. However, this repair activity could not be rescued by $XPC_{427-940}$ and $XPC_{607-940}$ (Figure 3B), implying that the N-terminal part of XPC protein is essential for the GGR reaction. All tested fragments were detected in transfected fibroblasts in similar amounts as the full-length control or the functional $XPC_{118-940}$ derivative

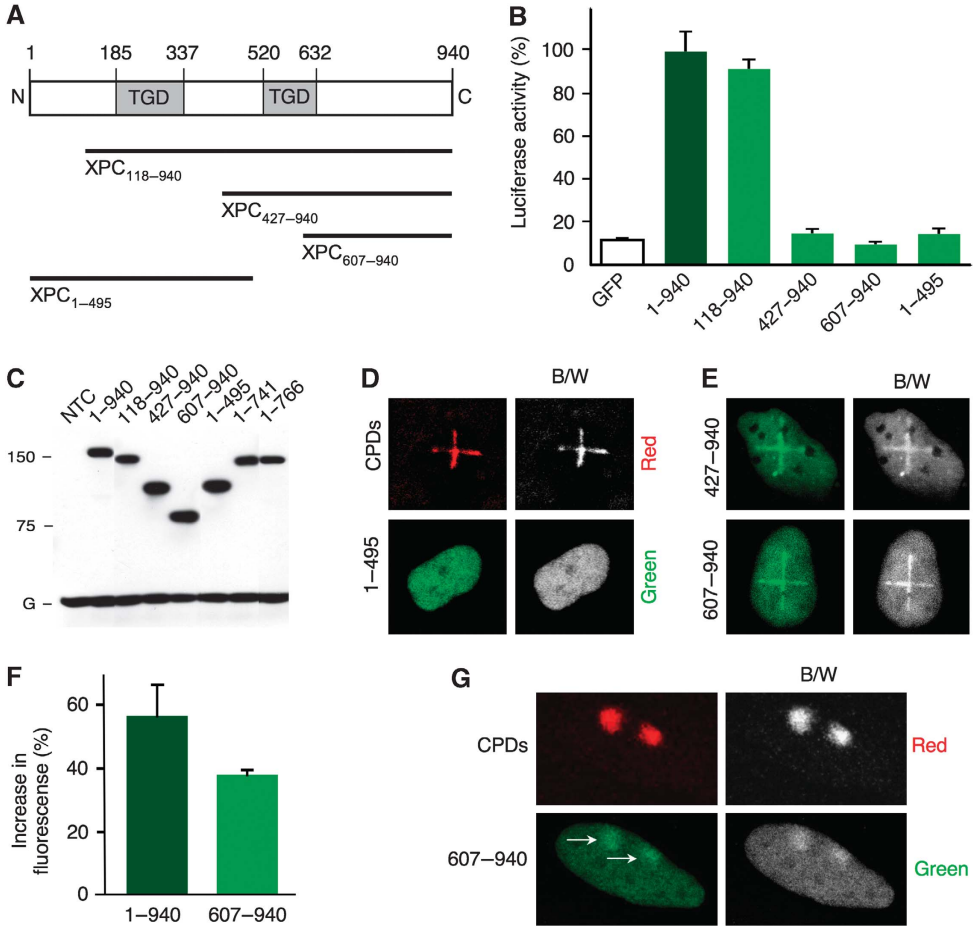

Figure 3 Mapping of the damage sensor domain to the C-terminal part of human XPC. (**A**) Scheme illustrating the position of the TGD sequences relative to the N-terminal XPC truncates. (**B**) GGR activity determined by host-cell reactivation assay ($n = 5$; error bars, standard deviation). (**C**) Immunoblot analysis of XP-C cells transfected with expression vectors coding for the indicated fusions. The protein level was probed using anti-GFP antibodies. G, endogenous GAPDH control. (**D**) Representative image showing that an XPC fragment lacking the C-terminus (XPC_{1-495}) fails to accumulate in laser-damaged areas. The XP-C fibroblasts were fixed 6 min after irradiation. B/W, black-and-white images showing that the tracks of DNA damage (*upper panel*) do not induce an accumulation of truncated XPC fusions (*lower panels*). (**E**) Representative images (in colour and black and white) showing that $XPC_{427-940}$ and $XPC_{607-940}$ accumulate in damaged areas of XP-C fibroblasts. The distribution of fluorescent fusion products was monitored 6 min after irradiation. (**F**) Local increase of fluorescence resulting from the damage-induced redistribution of full-length XPC or $XPC_{607-940}$. A 10-μm line of UV photoproducts was generated across each nucleus and the resulting accumulation of fusion proteins (after a 6-min incubation) is plotted as a percentage of the average fluorescence before irradiation ($n = 7$). Error bars, standard errors of the means. (**G**) Representative image illustrating that $XPC_{607-940}$ accumulates in foci generated by UV-C irradiation (100 J m^{-2}) through the pores of polycarbonate filters. The XP-C cells were fixed 15 min after treatment and CPDs were detected by immunochemical staining. The position of $XPC_{607-940}$ foci is indicated by the arrows.

(Figure 3C), indicating that their repair deficiency does not result from reduced expression or enhanced degradation.

Next, all GGR-deficient truncates were tested for their damage recognition proficiency in XP-C fibroblasts. Neither XPC_{1-495} (Figure 3D) nor XPC_{1-718} (Supplementary Figure 4) were redistributed to sites of photoproduct formation in the irradiated nuclei of living cells, confirming that the C-terminal half of XPC protein is necessary for lesion recognition. However, unlike these C-terminal truncations, fragment $XPC_{427-940}$ retains the ability to concentrate in laser-irradiated areas (Figure 3E). Even more surprising was the observation that the smaller fragment $XPC_{607-940}$ readily accumulates at sites containing UV photolesions (Figure 3E). The quantification of defined 10-μm tracks showed that $XPC_{607-940}$ is only ~30% less efficient than full-length XPC in relocating to damaged sites (Figure 3F). Thus, a large N-terminal part of human XPC (65% of the full-length protein including its TGD regions) stimulates DNA damage recognition, but is not absolutely required for the sensing process itself. This conclusion is confirmed by the accumulation of $XPC_{607-940}$ in UV-C foci generated by irradiation through the pores of polycarbonate filters (Figure 3G).

Differential contribution of β-hairpin domains

According to the Rad4 crystal, three consecutive β-hairpin domains (BHD1, BHD2 and BHD3) mediate the interaction with damaged DNA (see Supplementary Figure 1). In the homologous XPC sequence, these structural elements range from residue 637 (start of BHD1) to residue 831 (end of BHD3). To examine how each of these domains contributes to DNA damage recognition in living cells, we generated the C-terminal truncations XPC_{1-741} (comprising BHD1 and BHD2) and XPC_{1-831}, which includes all three BHDs (Figure 4A). Again, the truncation position 741 was chosen to allow for comparisons with an earlier *in vitro* study (Uchida *et al*, 2002). The constructs were conjugated to GFP at their C-terminus and tested for their ability to initiate the GGR reaction. In the case of XPC_{1-741}, the repair function is reduced to a background level observed with empty GFP vector (Figure 4B). However, the reporter gene was reactivated to ~40% of control in the presence of XPC_{1-831}, indicating that despite its C-terminal truncation, this large fragment retains in part the ability to recruit NER factors to lesion sites. Although attempting to delineate the borders of a minimal sensor domain, we surprisingly found that essentially the same GGR activity was induced by XPC_{1-766}, that is by adding only 25 amino acids to XPC_{1-741} (Figure 4B). A comparison with the Rad4 orthologue indicates that these 25 amino acids (residues 742–766) belong to an N-terminal extension of BHD3, which folds into a β-turn structure (see Figure 4A).

The UV-induced relocation of truncated XPC derivatives was tested in XP-C fibroblasts expressing similar low levels of each GFP construct (Supplementary Figure 5). Consistent with its distinctive functionality in the GGR assay, we observed that XPC_{1-766} accumulates more effectively than XPC_{1-741} to the 10-μm tracks of photolesions generated by laser irradiation (Figure 4C). An unequivocal pattern of XPC_{1-766} accumulation along the radiation tracks was also recorded in XP-E fibroblasts, that is in the absence of UV-DDB activity (Figure 4D). A quantitative comparison in both XP-C and XP-E cells highlights the increase in damage recognition when the truncation was introduced at residue 766 as compared with the truncation at position 741 (Figure 4E), thus showing that the damage-specific accumulation of XPC truncates as well as the effect of the β-turn structure takes place in the absence of DDB2 protein. A clear difference between XPC_{1-766} and XPC_{1-741} was reproduced when foci of fluorescence were monitored after UV-C irradiation through the pores of polycarbonate filters (Figure 4F). Taken together, this efficient redistribution of XPC_{1-766}, irrespective of the cell type or technique used to inflict DNA damage, establishes for the first time that most of BHD3 is not required for the initial damage-sensing process.

The β-turn structure enhances XPC dynamics

The GGR and relocation assays of Figure 4 revealed a striking difference between XPC_{1-741} and XPC_{1-766} because of the 25-amino-acid β-turn extension. To analyse the function of this β-turn structure, we compared the nuclear mobility of different truncates using fluorescence recovery after photobleaching (FRAP; Houtsmuller and Vermeulen, 2001). In cells that express similarly low levels of GFP fusion constructs, a nuclear area of $4\,\mu m^2$ was bleached and, subsequently, protein movements were tested by recording the recovery of local fluorescence, which is dependent on the ability of the GFP fusions to move rapidly within the nuclear compartment.

The control experiment of Figure 5A shows how, in the absence of a fusion partner, the GFP moiety moves freely inside the cells. Instead, the nuclear mobility of full-length XPC-GFP is restrained by its larger size and propensity to undergo macromolecular interactions, as reported earlier (Hoogstraten *et al*, 2008). Surprisingly, in a direct comparison between XPC_{1-741}, XPC_{1-766} and XPC_{1-831}, a larger size correlated with increased nuclear mobility (Figure 5B). The FRAP curves obtained with these different truncates were used to calculate effective diffusion coefficients (D_{eff}; Supplementary Table I). It was unexpected to find that, in undamaged cells, XPC_{1-766} (containing BHD1, BHD2 and the β-turn structure) and XPC_{1-831} (containing all three BHDs) move more rapidly inside the nucleus ($D_{eff} = 0.44$ and $0.49\,\mu m^2\,s^{-1}$, respectively) than the shorter polypeptide XPC_{1-741} lacking the β-turn ($D_{eff} = 0.34\,\mu m^2\,s^{-1}$). We concluded that these C-terminal truncations disclose the existence of a dynamic interface, residing within the β-turn structure, which enhances the constitutive nuclear mobility of XPC protein in the absence of genotoxic stress.

Subsequently, the FRAP approach was used to assess the corresponding responses to UV-C irradiation. In accord with its poor accumulation along DNA damage tracks (Figure 4C), the mobility of XPC_{1-741} is only marginally affected by the induction of photolesions (Figure 5C). In contrast, the diffusion rates of XPC_{1-766} (Figure 5D) and XPC_{1-831} (Figure 5E), which accumulate in UV lesion tracks, are significantly reduced (the respective D_{eff} values are listed in Supplementary Table I). In the case of XPC_{1-831}, the induction of DNA damage had a two-fold effect. First, UV lesions decreased the initial rate of protein diffusion exactly as observed with XPC_{1-766}. Second, similar to the response of full-length XPC (Hoogstraten *et al*, 2008), the overall fluorescence recovery is less complete on UV irradiation (Figure 5E), indicating that a fraction of XPC_{1-831} is immobilized in a damage-specific manner. In summary, these

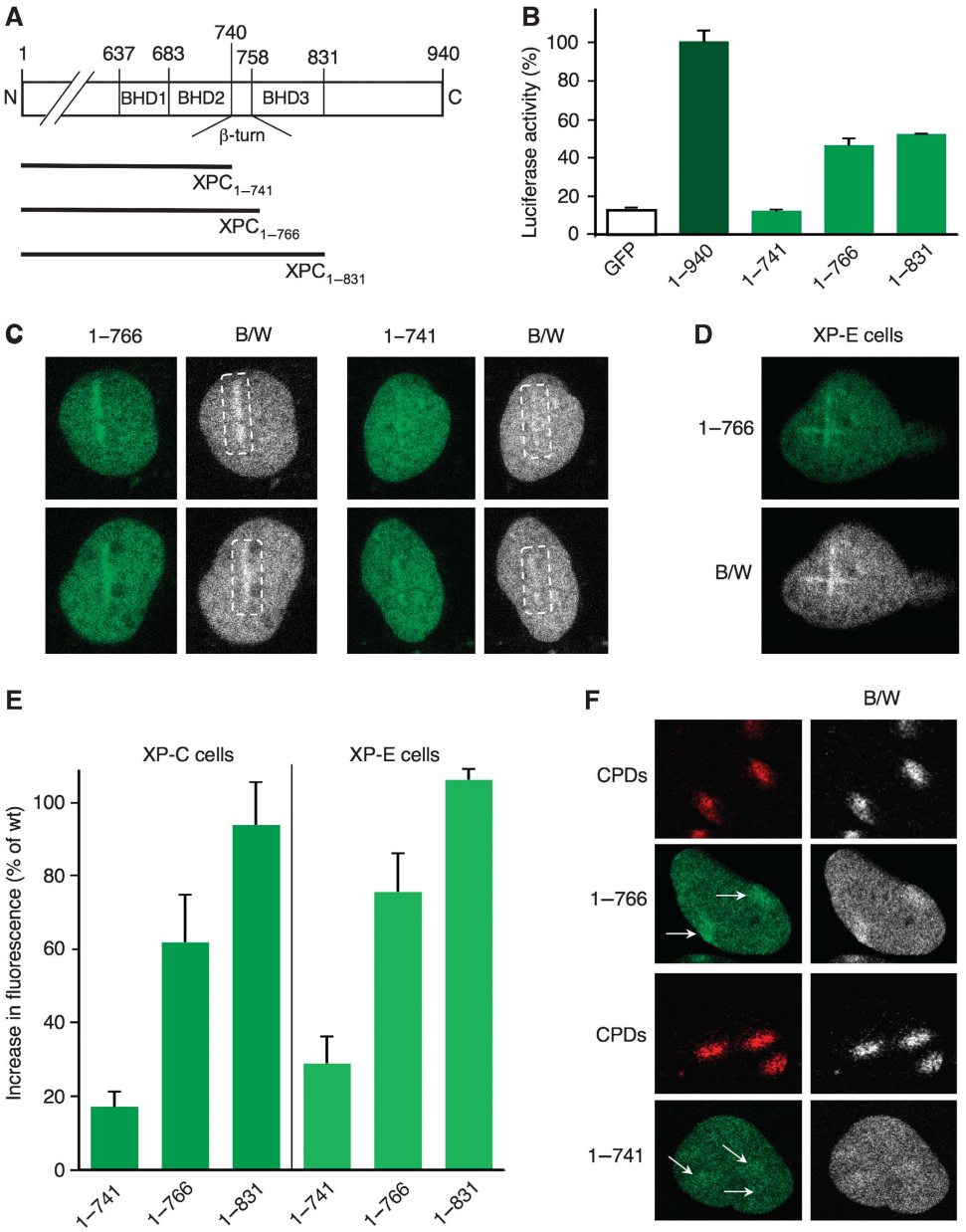

Figure 4 BHD3 is not required for DNA damage detection. (**A**) Scheme illustrating the location of BHD and β-turn sequences relative to the C-terminal XPC truncates of this study. (**B**) GGR activity determined by host-cell reactivation assay in XP-C fibroblasts ($n = 5$; error bars, standard deviation). (**C**) Representative images (taken 6 min after irradiation) comparing the accumulation of XPC_{1-766} and XPC_{1-741} at damaged sites. In the black-and-white representation, the linear irradiation tracks are surrounded by a dashed rectangle. (**D**) Representative image illustrating the accumulation of XPC_{1-766} along UV radiation tracks generated in XP-E fibroblasts devoid of UV-DDB activity. (**E**) The local increase in fluorescence, because of damage-induced redistributions of XPC truncates, was measured in XP-C and XP-E cells and plotted as the percentages of wt control as outlined in Figure 1D ($n = 5$; error bars, standard errors of the mean). (**F**) XPC_{1-766} is also more efficient than XPC_{1-741} in accumulating in DNA damage foci generated by UV-C irradiation through the pores of polycarbonate filters (see Figure 3G for details). XPC_{1-766} (*top*) and XPC_{1-741} foci (*bottom*) are indicated by the arrows.

protein mobility studies show that BHD3 induces the formation of a stable nucleoprotein complex once the lesion has been detected.

Antagonistic composition of the dynamic sensor domain

The truncation studies of Figures 4 and 5 suggested that residues 607–766 may be sufficient to find lesion sites in the genome. This hypothesis was confirmed by expressing short protein fragments in XP-C fibroblasts (Figure 6A). In the case of $XPC_{607-766}$ (consisting of BHD1/BHD2 and the β-turn structure), a clear pattern of damage-induced accumulation was detected immediately after laser irradiation (Figure 6B). In contrast, $XPC_{607-741}$ (lacking the β-turn) failed to accumulate in the tracks of UV lesions. $XPC_{607-741}$ was unable to relocate to damaged areas regardless of whether the GFP moiety was placed at the C- (Figure 6C) or at the N-terminus (data not shown). These results support the conclusion that $XPC_{607-766}$ displays a minimal sensor surface with damage recognition activity in living human cells.

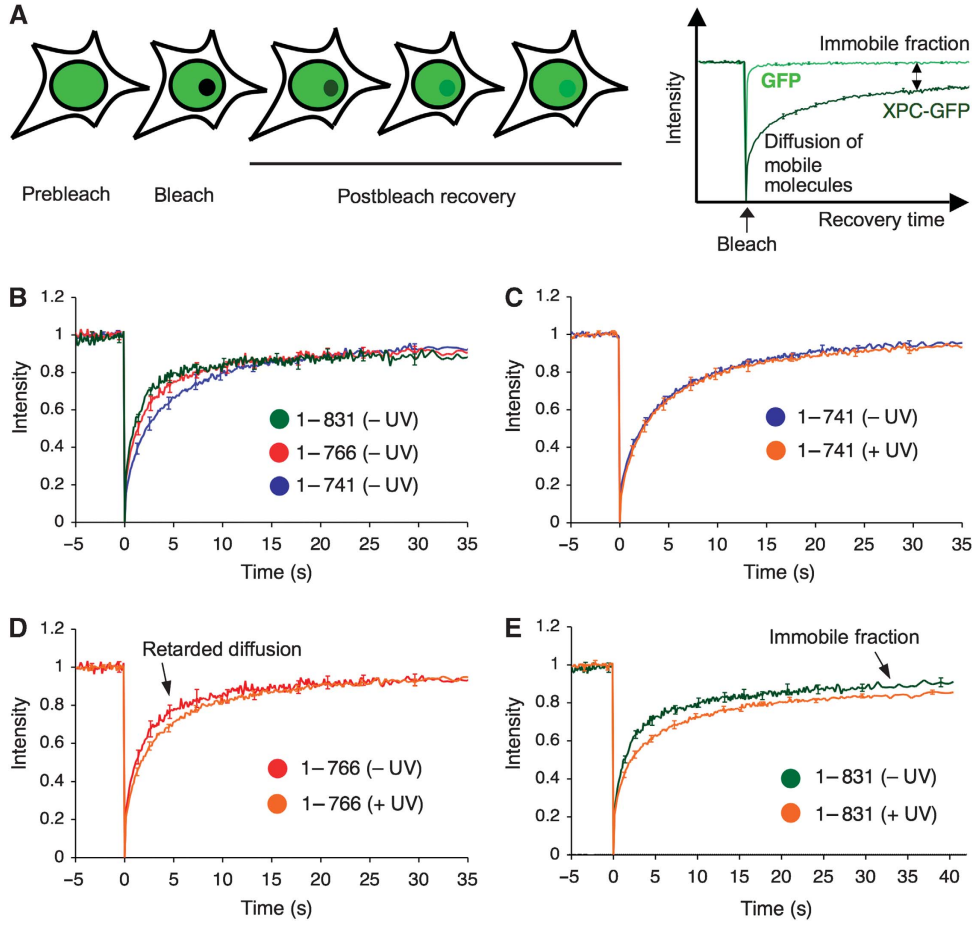

Figure 5 Identification of a dynamic core and two-stage damage recognition. (**A**) Principle of FRAP analysis. An area of 4 μm^2 in the nuclei of XP-C fibroblasts expressing a particular GFP construct is bleached with a 488-nm wavelength laser. The kinetics and extent of fluorescence recovery (shown for GFP and XPC-GFP) depends on diffusion rate, molecular interactions as well as the fraction of immobile molecules. (**B**) Recovery plots of XPC truncates normalized to prebleach intensity ($n = 12$). Error bars, standard errors of the mean. The difference between XPC_{1-766} and XPC_{1-831} is not significant. (**C**) The nuclear mobility of XPC_{1-741} remains unaffected by UV-C irradiation at a dose of 10 J m^{-2} ($n = 12$). (**D**) The initial diffusion of XPC_{1-766} is reduced by UV light (10 J m^{-2}, $n = 12$), reflecting transient molecular interactions during stage 1 of the damage recognition process. (**E**) A fraction of XPC_{1-831} is stably immobilized after UV irradiation (10 J cm^{-2}, $n = 12$), reflecting stage 2 of the damage recognition process.

The fragments $XPC_{607-741}$, $XPC_{607-766}$ and $XPC_{607-831}$ have been isolated to assess their DNA-binding properties using 135-mer DNA substrates. All three fragments were expressed and purified as soluble polypeptides without any signs of aggregation or precipitation that would be indicative of defective protein folding (Figure 6D). We compared their binding with three different DNA conformations: homoduplexes, heteroduplexes with three contiguous base mismatches or single-stranded oligonucleotides of the same length. Although $XPC_{607-741}$ (containing BHD1 and BHD2) is unable to find DNA lesions in living cells, this fragment displays a preference for unpaired bases embedded in double-stranded DNA. In fact, $XPC_{607-741}$ binds with higher affinity to heteroduplex DNA relative to homoduplexes or single-stranded oligonucleotides (Figure 6E).

A similar preference for hetero- over homoduplexes is retained by $XPC_{607-766}$, which includes both BHD1/BHD2 and the β-turn structure (Figure 6F), thus supporting the notion that this minimal sensor is active in living cells by searching for destabilized base pairs. A side-by-side comparison of dose-dependent DNA-binding activities with $XPC_{607-741}$ and $XPC_{607-766}$ showed that the β-turn structure leads to a substantial reduction in nucleic acid binding (Figure 6F). In particular, we found that the association constant representing the interaction with homoduplex DNA decreases nearly 10-fold from $2.7 \times 10^9\,M^{-1}$ for $XPC_{607-741}$ to $2.8 \times 10^8\,M^{-1}$ for $XPC_{607-766}$. This drop in binding to the native double helix implies that the enhanced nuclear mobility conferred by amino acids 742–766 (Figure 5B) results from an antagonistic DNA-repulsive effect.

Finally, to test the contribution of BHD3, the same 135-mer substrates were used to monitor the DNA-binding properties of a longer fragment ($XPC_{607-831}$) comprising all three BHDs. Figure 6G shows that this larger fragment has the characteristics of a single-stranded DNA-binding protein, indicating that BHD3 itself confers a pronounced selectivity for single-stranded conformations. The characteristic DNA-binding profile of this larger fragment $XPC_{607-831}$ corresponds roughly to that detected when identical reactions were carried out with full-length XPC protein (Supplementary Figure 6).

Design of an XPC mutant with retarded nuclear mobility

We postulated that part of the DNA-repulsive action mediated by the β-turn structure (Figure 6F) arises from negatively charged side chains that clash with the phosphates of the nucleic acid backbone. This hypothesis predicts that it should

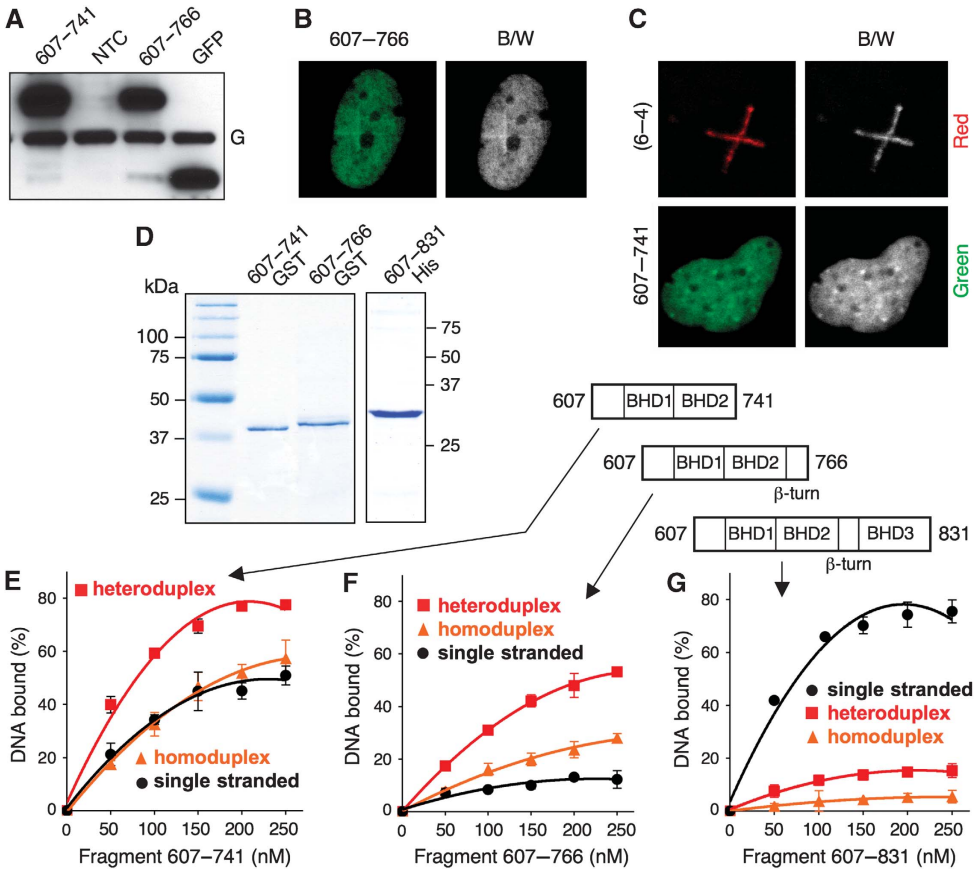

Figure 6 Antagonistic composition of the minimal damage sensor. (**A**) Immunoblot analysis of XP-C fibroblasts after transfection with vectors coding for the indicated XPC-GFP sequences. The expression was probed using anti-GFP antibodies. NTC, non-transfected cells; GFP, cells transfected with the GFP sequence alone; G, GAPDH control. (**B**) Representative image illustrating that fragment $XPC_{607-766}$ readily accumulates in damaged areas containing DNA photolesions. The distribution of fluorescent fusion products was monitored 1 min after laser irradiation. B/W, black-and-white image. (**C**) $XPC_{607-741}$ is unable to recognize UV lesions in living cells. Fibroblasts were subjected to fixation 1 min after irradiation and (6-4) photoproducts were detected by immunochemical staining. B/W, black-and-white images showing that UV lesions (*upper panel*) did not lead to accumulation of the fusion protein (*lower panel*). (**D**) Gel electrophoretic analysis of purified XPC fragments expressed as glutathione-*S*-transferase (GST) fusions in *E. coli* or with a histidine (His) tag in *Sf*9 cells. (**E**) DNA binding of $XPC_{607-741}$ determined by oligonucleotide capture. The indicated concentrations of XPC-GST fragments were incubated with radiolabelled 135-mer oligonucleotides (3-mismatch heteroduplexes, homoduplexes and single strands). Thereafter, DNA molecules immobilized by XPC fragments were separated from the free oligonucleotides using glutathione-Sepharose beads, followed by the quantification of radioactivity associated with the beads. DNA binding is represented as the percentage of total input radioactivity captured by XPC fragments after deduction of a background value determined with empty beads ($n = 6$; error bars, standard deviation). (**F**) DNA-binding profile of the minimal damage sensor ($XPC_{607-766}$) determined as described in the legend to Figure 6E. (**G**) Contribution of BHD3. The DNA-binding profile of $XPC_{607-831}$ was determined as outlined in the legend to Figure 6E, except that pull downs were performed with Ni-NTA agarose beads.

be possible to mitigate this DNA-repellent effect by replacing negatively charged amino acids with positively charged analogues. We identified a glutamate moiety at position 755 of the human β-turn motif that is conserved among higher eukaryotes (Figure 7A) and inverted the charge of this particular side chain by substitution with lysine.

The consequence of this engineered charge inversion was first tested by comparing the interaction with native double-stranded DNA in biochemical assays. For that purpose, the lysine substitution was introduced into $XPC_{607-766}$, thus generating a mutated fragment of 160 amino acids ($E755K_{607-766}$) that, similar to its wild-type counterpart ($XPC_{607-766}$), is amenable to expression and purification as a soluble polypeptide. DNA homoduplexes of 135 base pairs were used to determine the DNA-binding capacity of this mutated fragment in relation to the wild-type control. As illustrated in the comparison of Figure 7B, the E755K mutation was able to partially reverse the drop in DNA binding resulting from the presence of the β-turn structure in $XPC_{607-766}$. Binding saturation studies with homoduplex DNA indicates that the association constant increased from $2.8 \times 10^8\,M^{-1}$ for $XPC_{607-766}$ containing the wild-type sequence (determined in the earlier section) to $7.4 \times 10^8\,M^{-1}$ for the $E755K_{607-766}$ derivative, which carries the single charge inversion.

These findings led us to generate a mutant GFP fusion construct to confirm that the effect of the β-turn structure in enhancing the XPC dynamics, observed with truncated derivatives (Figure 5B), is retained in the full-length protein context. Unlike other repair-defective XPC mutants (W531A, W542A, W690A, W690S and F733A), all of which display a higher nuclear mobility than the wild-type control (Hoogstraten *et al*, 2008 and data not shown), the novel E755K mutant is characterized by a strikingly reduced nuclear mobility (Figure 7C) accompanied by a significant GGR defect (Figure 7D). Collectively, these effects induced by a

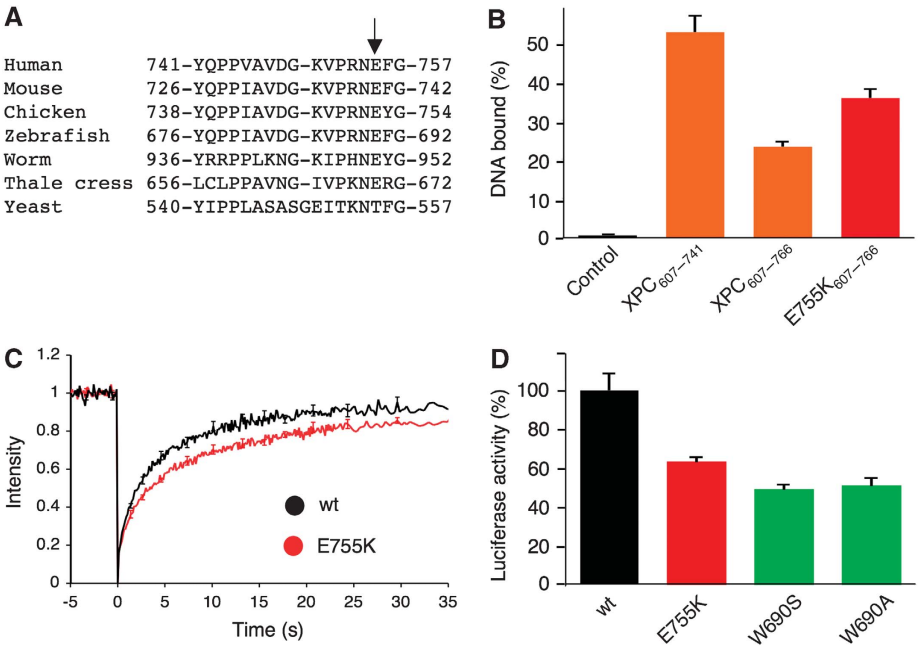

Figure 7 Analysis of the dynamic interface by site-directed mutagenesis. (**A**) Identification of a conserved glutamate (*arrow*) in the β-turn motif of higher eukaryotes. This residue is not conserved in the Rad4 sequence, suggesting that the yeast orthologue may have different dynamic properties. (**B**) A single E755K mutation reduces the DNA-repellent effect of the β-turn structure. The association of $XPC_{607-741}$, $XPC_{607-766}$ and $E755K_{607-766}$ with homoduplex DNA was compared at a polypeptide concentration of 150 nM, as outlined in the legend to Figure 6E. DNA binding is represented as the percentage of total input radioactivity captured by XPC fragments ($n=6$; error bars, standard deviation). A control reaction was carried out with empty beads. (**C**) FRAP analysis showing that, in undamaged cells, the nuclear mobility of the full-length E755K mutant is retarded relative to the wt control ($n=12$; error bars, standard error of the mean). (**D**) Host-cell reactivation assay showing that the E755K mutation confers a significant GGR defect. All results were corrected for the background activity in XP-C cells transfected with the GFP vector ($n=5$; error bars, standard deviation).

single site-directed mutation confirm that the dynamic properties of its minimal sensor surface, conferred by the β-turn structure, are critical for the ability of human XPC protein to act as a sensor of DNA damage.

Discussion

We elucidated the mechanism by which XPC protein scrutinizes DNA quality in living cells. The most outstanding finding is the identification of a two-stage discrimination process triggered by a dynamic sensor interface that detects DNA damage without the involvement of a prominent DNA-binding domain (BHD3), which was thought to represent the primary lesion recognition module on the basis of the Rad4 crystal structure (Min and Pavletich, 2007). The newly identified sensor interface serves to rapidly screen the double helix for the presence of unpaired bases, thus localizing damaged target sites that are amenable to the subsequent installation of an ultimate repair-initiating complex.

Dynamic molecular dialogue with the DNA double helix

According to the aforementioned Rad4 structure, the TGD region cooperates with BHD1 to associate with a portion of double-stranded DNA flanking the lesion (see Supplementary Figure 1). However, we observed that a large N-terminal segment (65% of the human sequence including most TGD sequences) has a stimulatory role, but is not directly required for the relocation of XPC protein to focus on DNA lesions (Figure 3). In the absence of this TGD segment, a strong interaction with the normal duplex is nevertheless mediated by the earlier described (Uchida *et al*, 2002) minimal DNA-binding fragment $XPC_{607-741}$, which consists of BHD1 and BHD2 (Figure 6E). Instead, a longer fragment covering all three BHDs displays a comparably low affinity for the normal duplex (Figure 6G), indicating that the double-stranded DNA-binding activity of BHD1/BHD2 is opposed by the neighbouring BHD3 sequence. The further dissection of this critical XPC region revealed that a short β-turn extension of BHD3 is sufficient to mediate in part such an antagonistic effect (Figure 6F).

Several observations in living cells support the notion that the addition of this β-turn extension conveys a true gain of function rather than causing the destabilization of adjacent structural elements in the respective XPC constructs. First, XPC_{1-766} and XPC_{1-831} display a residual GGR function that is missing in the case of XPC_{1-741}, which lacks the β-turn structure (Figure 4B). The fact that XPC_{1-766} and XPC_{1-831} exert a similarly low complementing activity is likely because of the absence of at least some components of the TFIIH-recruiting domain in their C-terminal region (Uchida *et al*, 2002). Second, a side-by-side comparison of the same C-terminal truncates shows that the enhanced nuclear mobility conferred by the β-turn structure (Figure 5B) correlates with a more efficient relocation to UV lesions (Figure 4E). Third, the nuclear mobility of XPC_{1-766}, but not XPC_{1-741}, is retarded by UV damage (Figure 5C and D), confirming that the former detects DNA lesions more effectively. Fourth, in living cells, the damage-induced accumulation of an earlier defined minimal DNA-binding fragment ($XPC_{607-741}$) is strictly dependent on the presence of the β-turn structure (Figure 6B). Finally,

the critical role of this dynamic β-turn subdomain is supported by a site-directed E755K substitution that reverts in part its DNA-repellent action. The increased affinity of this novel mutant for the native double helix results in decreased nuclear mobility and markedly reduced repair activity (Figure 7). According to the Rad4 structure, the critical position 755 maps to an amino-acid sequence that is in close contact with the DNA substrate (Min and Pavletich, 2007). Thus, our findings indicate that the β-turn structure displays both DNA-attractive and DNA-repulsive forces that dictate the dynamic interplay with duplex DNA such that, in the full genome context, this subdomain facilitates damage recognition by providing sufficient mobility to the XPC molecules searching for lesions.

Identification of a transient recognition intermediate

On binding to damaged substrates, XPC protein induces local DNA melting and kinking (Evans *et al*, 1997; Janicijevic *et al*, 2003; Mocquet *et al*, 2007). A structural basis for these rearrangements is again provided by the Rad4 crystal, in which the β-hairpin of BHD3 is inserted through the DNA duplex, causing two base pairs to entirely flip out of the double helix (see Supplementary Figure 1). In view of these features of the Rad4–DNA complex, it was unexpected to find that most of BHD3 including the protruding β-hairpin is actually not necessary to sense DNA damage in living cells. In fact, an XPC fragment that contains the β-turn structure, but is devoid of the remaining BHD3 sequence because of a truncation at position 766 (XPC_{1-766}), accumulates in UV foci with remarkable efficiency (~60% of the full-length control; Figure 4E), but without forming stable nucleoprotein complexes (Figure 5D). Similar to the W690S mutant, this truncated XPC_{1-766} derivative is even able to induce GGR activity (Figure 4B), although to moderate levels that are not sufficient to complement the repair defect of XP-C cells. A damage-specific accumulation of XPC_{1-766} was also detected in DDB2-deficient XP-E fibroblasts (Figure 4D and E) and V79 hamster cells (data not shown), thus excluding that the BHD3-independent relocation occurs in an indirect manner by association with UV-DDB. Finally, the conclusion that XPC protein forms a transient damage recognition intermediate without the involvement of BHD3 is supported by the finding that a small fragment ($XPC_{607-766}$) consisting only of BHD1/BHD2 and the β-turn structure (together ~15% of the human XPC sequence) still functions as a cellular DNA damage sensor (Figure 6B). This minimal sensor surface displays a binding preference for duplexes containing non-hydrogen-bonded bases, a generic feature of damaged DNA, and hence functions as a molecular caliper of thermodynamic base-pair stability.

A two-stage quality-control inspection

Although the BHD3 segment (residues 767–831) and its β-hairpin are not required to attract XPC protein to lesion sites, this additional domain favours the subsequent formation of stable nucleoprotein complexes, resulting in an immobile fraction of XPC protein in response to DNA damage (Figure 5E). The biochemical analysis of purified fragments shows that, unlike the BHD1/BHD2/β-turn minimal sensor, which displays a preference for duplexes with unpaired bases, BHD3 confers an exquisite selectivity for single-stranded DNA conformations (Figure 6G). In conjunction with the earlier mentioned Rad4 structure, these findings indicate that BHD3 does not participate in the early and transient recognition intermediate, but, instead, facilitates the subsequent stabilization of a repair-initiating complex using its single-stranded DNA-binding activity to encircle the undamaged strand across lesion sites.

To conclude, this is the first report providing evidence for a two-stage discrimination mechanism by which XPC protein carries out its versatile recognition function (Figure 8). This two-stage process obviates the difficulty of probing every genomic base pair for its susceptibility to undergo a BHD3-mediated β-hairpin insertion. Instead, the energetically less demanding search conducted by the dynamic BHD1/BHD2/β-turn interface is likely to precede more extensive BHD3-dependent structural adjustments. This initial search leads to the detection of non-hydrogen-bonded residues that are more prone than native base pairs to be flipped out of the double helix and, hence, become an interaction partner for the single-stranded DNA-binding activity of BHD3. A critical step of this two-stage quality-control process is the transition from an initially labile sensor intermediate to the more stable ultimate recognition complex. Two constitutive interaction partners of XPC protein, Rad23B and centrin 2, are thought to exert an accessory function not only by inhibiting XPC degradation, but also by stimulating its DNA-binding activity (Ng *et al*, 2003; Xie *et al*, 2004; Nishi *et al*, 2005). Such an auxiliary role is supported for Rad23B by the observation that $XPC_{607-940}$, a fragment that fails to associate with Rad23B (Uchida *et al*, 2002), has a reduced DNA damage recognition capacity in living cells (Figure 3F). In addition, the two-step discrimination process identified in this study raises the possibility that Rad23B, centrin 2 or other binding partners may facilitate the installation of an ultimate XPC–DNA complex by lowering the energetic cost of critical nucleoprotein rearrangements required for the final β-hairpin insertion.

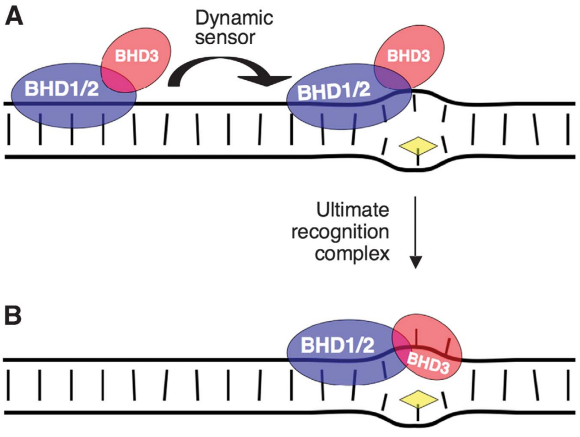

Figure 8 Two-stage detection of DNA lesions by XPC protein. Model depicting the switch from a dynamic damage sensor intermediate to the ultimate recognition complex. (**A**) This study identifies a minimal sensor interface that rapidly scrutinizes base-pair integrity. This initial search, carried out by BHD1/BHD2 in conjunction with the β-turn structure, results in the formation of a labile nucleoprotein intermediate. (**B**) The single-stranded DNA-binding activity of BHD3 promotes the subsequent transition to a stable recognition complex by capturing extruded nucleotides in the undamaged strand.

Materials and methods

XPC constructs

The human *XPC* complementary DNA was cloned into pEGFP-N3 (Clontech) using the restrictions enzymes *Kpn*I and *Xma*I. The same enzymes were used to generate the truncated XPC fragments. Primers for the insertion of restrictions sites and site-directed mutagenesis (QuickChange, Stratagene) are listed in the Supplementary Table II. All clones were sequenced (Microsynth) to exclude accidental mutations.

Cell culture

Simian virus 40-transformed human XP-C fibroblasts (GM16093) and untransformed XP-E fibroblasts (GM02415), derived from patients XP14BR and XP2RO, respectively, were purchased from the Coriell Institute for Medical Research (Camden, New Jersey, USA). The XP-C cells carry a homozygous C→T transition at position 2152 of the *XPC* sequence (Chavanne *et al*, 2000). The GM02415 cells carry a G→A transition in the *DDB2* sequence generating an inactive R273H mutant that is not expressed to detectable levels (Nichols *et al*, 2000; Itoh *et al*, 2001). These fibroblasts, as well as V79 hamster cells deficient in UV-DDB activity (Tang *et al*, 2000) were cultured in Dulbecco's modified Eagle's medium (DMEM; Gibco), supplemented with 10% fetal calf serum (FCS), penicillin G (100 units ml^{-1}) and streptomycin (100 μg ml^{-1}). The cells were maintained at 37°C in a humidified incubator containing 5% CO_2.

Transfections

One day before transfection, 600 000 cells were seeded into 6-well plates containing glass cover slips. At a confluence of 90–95%, the cells were transfected with 1 μg XPC-pEGFP-N3 (or truncated constructs) using 4 μl FuGENE HD reagent (Roche) and incubated for another 18 h. Expression of XPC polypeptides was monitored by western blotting (Maillard *et al*, 2007).

High-resolution DNA damage induction

The growth medium was replaced by phenol red-free DMEM (Gibco) supplemented with 10% FCS and 25 mM HEPES (pH 7.2). Single cells were irradiated with a femtosecond fibre laser (Träutlein *et al*, 2008) coupled to a confocal microscope (LSM Pascal, Zeiss) that generates pulses of 775 nm (duration 230 fs, repetition rate 107 MHz). The peak power density at the focal plane was 350 GW cm^{-2} and the pixel dwell time was 44.2 ms. Nuclei were irradiated along a single track or two intersecting lines. The area of each irradiation track was $<10\,\mu m^2$ and its volume $<20\,\mu m^3$.

By multiphoton excitation, three photons of low energy (775 nm wavelength) cause DNA lesions normally produced by the absorption of a single photon of higher energy (equivalent to 258 nm wavelength). Irradiation in the near-infrared range induces CPDs, (6-4) photoproducts and oxidative lesions (Lan *et al*, 2004; Dinant *et al*, 2007). In an earlier report (Meldrum *et al*, 2003), it has been calculated that three-photon irradiation with a peak power density of 350 GW cm^{-2} generates ~7000 UV lesions in each treated cell. Taking into account our slightly modified parameters, we calculated that in this study, the same power density produced ~5000 UV lesions along each linear 10-μm track.

Image analysis

Fluorescence measurements were carried out through a ×40 oil immersion objective lens with a numerical aperture of 1.4 (EC-Plan-Neo-Fluar, Zeiss) using an Ar^+ source (488 nm). The selected parameters, including laser power and magnification factor, were kept constant throughout all experiments. To monitor the distribution of fluorescent fusions, at least 60 images were taken for up to 10 min after irradiation and analysed using the ImageJ software (http://rsb.info.nih.gov/ij). An initial-control image was taken immediately before damage induction. Signals were corrected for bleaching (http://www.embl-heidelberg.de/eamnet/html/body_bleach_correction.html) and cell movements (http://bigwww.epfl.ch/thevenaz/stackreg). For every time point, the average fluorescence intensities were measured in the area of accumulation and, as a background reference, in a neighbouring area of identical size. Finally, the background-corrected values were normalized to the mean intensity of the same nuclear region before irradiation.

Induction of UV foci

After removal of the culture medium, the cells were rinsed with phosphate-buffered saline (PBS), covered by a polycarbonate filter (Millipore) with 5-μm pores and irradiated using a UV-C source (254 nm, 100 J m^{-2}). Subsequently, the filter was removed and the cells were returned to complete DMEM for 15 min at 37°C before paraformaldehyde fixation.

Immunocytochemistry

All wash steps and incubations were performed in PBS. At the indicated times after irradiation, cells were washed and fixed for 15 min at room temperature using 4% (v/v) paraformaldehyde. The cells were then permeabilized twice with 0.1% (v/v) TWEEN 20 for 10 min and DNA was denatured with 0.07 M NaOH for 8 min. Subsequently, the samples were washed five times with 0.1% TWEEN 20 and incubated (30 min at 37°C) with 20% FCS to inhibit unspecific binding. The samples were incubated (1 h at 37°C in 5% FCS) with primary antibodies (MBL International Corporation) directed against CPDs (TDM-2, dilution 1:3000) or (6-4) photoproducts (64M-2, dilution 1:1000). Next, the samples were washed with 0.1% TWEEN 20, blocked twice for 10 min with 20% FCS and treated with Alexa Fluor 546 dye-conjugated secondary antibodies (Invitrogen, dilution 1:400) for 30 min at 37°C. After washing with 0.1% TWEEN 20, the nuclei were stained for 10 min with Hoechst dye 33258 (200 ng ml^{-1}). Finally, the samples were washed three times and analysed using an oil immersion objective.

GGR assay

Triplicate samples of XP-C fibroblasts, at a confluence of 90–95%, were transfected in a 6-well plate. The total amount of plasmid DNA (1 μg) included 0.45 μg pGL3 (UV irradiated at 1000 J m^{-2}, coding for *Photinus* luciferase), 0.05 μg phRL-TK (unirradiated, coding for *Renilla* luciferase) and 0.5 μg of XPC-pEGFP expression vector. After 4 h, the transfection mixture was replaced by complete culture medium. After another 18 h, the cells were disrupted in 500 μl Passive Lysis Buffer (Promega). The lysates were cleared by centrifugation and the ratio of *Photinus* and *Renilla* luciferase activity was determined in a Dynex microtiter luminometer using the Dual-Luciferase assay system (Promega).

FRAP analysis

Protein mobility was analysed at high time resolution using a Leica TCS SP5 confocal microscope equipped with an Ar^+ laser (488 nm, not inducing DNA lesions) and a ×60 oil immersion lens (numerical aperture of 1.4). The assays were performed in a controlled environment at 37°C and CO_2 supply of 5%. A region of interest (ROI) covering 4 μm^2 was photobleached for 2.3 s at 100% laser intensity. Fluorescence recovery within the ROI was monitored 200 times using 115-ms intervals followed by 30 frames at 250-ms and 10 frames at 500 ms. Simultaneously, a reference ROI of the same size was measured for each time point to correct for overall bleaching. All data were normalized to the prebleach intensity and the effective diffusion model (Sprague *et al*, 2004) was used to estimate diffusion coefficients (see Supplementary Table I).

DNA-binding assays

Full-length MBP-XPC fusions were expressed in *Sf*9 cells (Maillard *et al*, 2007). Insect cell lysates (5–20 μl) were incubated with ^{32}P-labelled 135-mer oligonucleotides (4 nM) in 200 μl buffer A (25 mM Tris–HCl, pH 7.5, 0.3 M NaCl, 10% glycerol, 0.01% Triton X-100, 0.25 mM phenylmethane sulfonyl fluoride and 1 mM EDTA). After 1 h at 4°C, the reaction mixtures were supplemented with monoclonal antibodies against MBP linked to paramagnetic beads (0.2 mg, New England BioLabs). After another 2 h at 4°C, the beads were washed four times with 200 μl buffer A and the oligonucleotides associated with paramagnetic beads were quantified by liquid scintillation counting. All values were corrected for the background radioactivity resulting from unspecific binding to empty beads. The amount of immobilized XPC protein was controlled by denaturing gel electrophoresis.

GST-$XPC_{607-741}$, GST-$XPC_{607-766}$ and GST-$K755E_{607-766}$ (expressed in *Escherichia coli*) as well as His-$XPC_{607-831}$ (expressed in *Sf*9 cells) were purified as described (Uchida *et al*, 2002). The indicated concentrations of XPC fragments were incubated with radiolabelled 135-mer oligonucleotides (4 nM) in 200 μl buffer B (25 mM Tris–HCl, pH 7.5, 0.15 M NaCl, 10% glycerol, 0.01% Triton X-100, 0.25 mM phenylmethane sulfonyl fluoride and 1 mM EDTA).

After 1 h at 4°C, the reaction mixtures were supplemented with glutathione-Sepharose (10 μl, Amersham) or Ni-NTA agarose beads (10 μl, Qiagen). After another 1 h at 4°C, the beads were washed twice with 200 μl buffer B and the immobilized oligonucleotides were quantified by liquid scintillation counting. All values were corrected for the background radioactivity resulting from unspecific binding to empty beads. To estimate binding constants, the data from saturation experiments (50–250 nM protein) were subjected to Scatchard analysis by plotting the ratio of bound and free XPC fragments as a function of the fraction of bound protein (Husain and Sancar, 1987). The double-stranded homoduplex or heteroduplex probes were obtained by hybridization of complementary 135-mers in 50 mM Tris–HCl (pH 7.4), 10 mM $MgCl_2$ and 1 mM dithiothreitol. Equal amounts of each oligonucleotide were heated at 95°C for 10 min followed by slow cooling (3 h at 25°C).

Supplementary data
Supplementary data are available at *The EMBO Journal* Online (http://www.embojournal.org).

Acknowledgements

We thank D Hermann, A Lenisa, M Träxler and M Vitanescu for excellent technical assistance and W Vermeulen for introduction into the FRAP technique. We also thank CT Craescu, A Scrima and N Thomä for critical reading and discussion of the manuscript. This work was supported by the Swiss National Science Foundation (grant 3100A0-113694), Oncosuisse (grant KLS-01827-02-2006), the German Research Foundation (grant DFG MA/2385/2-3) and the Ministry of Science, Research and the Arts of Baden-Württemberg.

References

Andressoo JO, Hoeijmakers JH, Mitchell JR (2006) Nucleotide excision repair disorders and the balance between cancer and aging. *Cell Cycle* **5:** 2886–2888

Batty D, Rapic'-Otrin V, Levine AS, Wood RD (2000) Stable binding of human XPC complex to irradiated DNA confers strong discrimination for damaged sites. *J Mol Biol* **300:** 275–290

Bunick CG, Miller MR, Fuller BE, Fanning E, Chazin WJ (2006) Biochemical and structural domain analysis of xeroderma pigmentosum complementation group C protein. *Biochemistry* **45:** 14965–14979

Buterin T, Meyer C, Giese B, Naegeli H (2005) DNA quality control by conformational readout on the undamaged strand of the double helix. *Chem Biol* **12:** 913–922

Carreau M, Eveno E, Quilliet X, Chevalier-Lagent O, Benoit A, Tanganelli B, Stefanini M, Vermeulen W, Hoeijmakers JH, Sarasin A, Mezzina M (1995) Development of a new easy complementation assay for DNA repair deficient human syndromes using cloned repair genes. *Carcinogenesis* **16:** 1003–1009

Chavanne F, Broughton BC, Pietra D, Nardo T, Browitt A, Lehmann AR, Stefanini M (2000) Mutations in the XPC gene in families with xeroderma pigmentosum and consequenced at the cell, protein and transcription level. *Cancer Res* **60:** 1974–1982

Cleaver JE (2005) Cancer in xeroderma pigmentosum and related disorders of DNA repair. *Nat Rev Cancer* **5:** 564–573

Cleaver JE, Thompson LH, Richardson AS, States JC (1999) A summary of mutations in the UV-sensitive disorders: xeroderma pigmentosum, Cockayne syndrome, and trichothiodystrophy. *Hum Mutat* **14:** 9–22

Dinant C, de Jager M, Essers J, van Cappellen WA, Kanaar R, Houtsmuller AB, Vermeulen W (2007) Activation of multiple DNA repair pathways by subnuclear damage induction methods. *J Cell Sci* **120:** 2731–2740

Evans E, Moggs JG, Hwang JR, Egly JM, Wood RD (1997) Mechanism of open complex and dual incision formation by human nucleotide excision repair factors. *EMBO J* **16:** 6559–6573

Fitch ME, Nakajima S, Yasui A, Ford JM (2003) *In vivo* recruitment of XPC to UV-induced cyclobutane pyrimidine dimers by the DDB2 gene product. *J Biol Chem* **278:** 46906–46910

Friedberg EC, Walker GC, Siede W, Wood RD, Schultz RA, Ellenberger T (2006) *DNA Repair and Mutagenesis*. Washington DC: ASM Press

Gillet LC, Schärer OD (2006) Molecular mechanisms of mammalian global genome nucleotide excision repair. *Chem Rev* **106:** 253–276

Hanawalt PC, Spivak G (2008) Transcription-coupled DNA repair: two decades of progress and surprises. *Nat Rev Mol Cell Biol* **9:** 958–970

Hoogstraten D, Bergink S, Verbiest VH, Luijsterburg MS, Geverts B, Raams A, Dinant C, Hoeijmakers JH, Vermeulen W, Houtsmuller AB (2008) Versatile DNA damage detection by the global genome nucleotide excision repair protein XPC. *J Cell Sci* **121:** 2850–2859

Houtsmuller AB, Rademakers S, Nigg AL, Hoogstraten D, Hoeijmakers JH, Vermeulen W (1999) Action of DNA repair endonuclease ERCC1/XPF in living cells. *Science* **284:** 958–961

Houtsmuller AB, Vermeulen W (2001) Macromolecular dynamics in living cell nuclei revealed by fluorescence redistribution after photobleaching. *Histochem Cell Biol* **115:** 13–21

Huang JC, Hsu DS, Kazantsev A, Sancar A (1994) Substrate spectrum of human excinuclease: repair of abasic sites, methylated bases, mismatches and bulky adducts. *Proc Natl Acad Sci USA* **91:** 12213–12217

Husain I, Sancar A (1987) Binding of E. coli DNA photolyase to a defined substrate containing a single T<>T dimer. *Nucleic Acids Res* **15:** 1109–1120

Itoh T, Nichols A, Linn S (2001) Abnormal regulation of DDB2 gene expression in xeroderma pigmentosum group E strains. *Oncogene* **20:** 7041–7050

Janicijevic A, Sugasawa K, Shimizu Y, Hanaoka F, Wijgers N, Djurica M, Hoeijmakers JH, Wyman C (2003) DNA bending by the human damage recognition complex XPC-HR23B. *DNA Rep* **2:** 325–336

Kuraoka I, Bender C, Romieu A, Cadet J, Wood RD, Lindahl T (2000) Removal of oxygen free-radical-induced 5′,8-purine cyclodeoxynucleosides from DNA by the nucleotide excision-repair pathway in human cells. *Proc Natl Acad Sci USA* **97:** 3832–3837

Kusumoto R, Masutani C, Sugasawa K, Iwai S, Araki M, Uchida A, Mizukoshi T, Hanaoka F (2001) Diversity of the damage recognition step in the global genomic nucleotide excision repair *in vitro*. *Mutat Res* **485:** 219–227

Lan L, Nakajima S, Oohata Y, Takao M, Okano S, Masutani M, Wilson SH, Yasui A (2004) *In situ* analysis of repair processes for oxidative DNA damage in mammalian cells. *Proc Natl Acad Sci USA* **101:** 13738–13743

Legerski R, Peterson C (1992) Expression cloning of a human DNA repair gene involved in xeroderma pigmentosum group C. *Nature* **359:** 70–73

Lehmann AR (2003) DNA repair-deficient diseases, xeroderma pigmentosum, Cockayne syndrome and trichothiodystrophy. *Biochimie* **85:** 1101–1111

Maillard O, Solyom S, Naegeli H (2007) An aromatic sensor with aversion to damaged strands confers versatility to DNA repair. *PLoS Biol* **5:** e79

Meldrum RA, Botchway SW, Wharton CW, Hirst GJ (2003) Nanoscale spatial induction of ultraviolet photoproducts in cellular DNA by three-photon near-infrared absorption. *EMBO Rep* **4:** 1144–1149

Min J-H, Pavletich NP (2007) Recognition of DNA damage by the Rad4 nucleotide excision repair protein. *Nature* **449:** 570–575

Mocquet V, Kropachev K, Kolbanovskiy M, Kolbanovskiy A, Tapias A, Cay Y, Broyde S, Geacintov NE, Egly JM (2007) The human DNA repair factor XPC-HR23B distinguishes stereoisomeric benzo[a]pyrenyl-DNA lesions. *EMBO J* **26:** 2923–2932

Moné JJ, Bernas T, Dinant C, Goedvree FA, Manders EM, Volker M, Houtsmuller AB, Hoeijmakers JH, Vermeulen W, van Driel R (2004) *In vivo* dynamics of chromatin-associated complex formation in mammalian nucleotide excision repair. *Proc Natl Acad Sci USA* **101:** 15933–15937

Moser J, Volker M, Kool H, Alekseev S, Vrieling H, Yasui A, van Zeeland AA, Mullenders LH (2005) The UV-damaged DNA binding protein mediates efficient targeting of the nucleotide excision repair complex to UV-induced photo lesions. *DNA Rep* **4:** 571–582

Ng JM, Vermeulen W, van der Horst GT, Bergink S, Sugasawa K, Vrieling H, Hoeijmakers JH (2003) A novel regulation mechanism of DNA repair by damage-induced and RAD23-dependent stabi-

lization of xeroderma pigmentosum group C protein. *Genes Dev* **17:** 1630–1645

Nichols AF, Itoh T, Graham JA, Liu W, Yamaizumi M, Linn S (2000) Human damage-specific DNA-binding protein p48. *J Biol Chem* **275:** 21422–21428

Nishi R, Okuda Y, Watanabe E, Mori T, Iwai S, Masutani C, Sugasawa K, Hanaoka F (2005) Centrin 2 stimulates nucleotide excision repair by interacting with xeroderma pigmentosum group C protein. *Mol Cell Biol* **25:** 5664–5674

Politi A, Moné MJ, Houtsmuller AB, Hoogstraaten D, Vermeulen W, Heinrich R, van Driel R (2005) Mathematical modeling of nucleotide excision repair reveals efficiency of sequential assembly strategies. *Mol Cell* **19:** 679–690

Reardon JT, Sancar A (2006) Repair of DNA-polypeptide crosslinks by human excision nuclease. *Proc Natl Acad Sci USA* **103:** 4056–4061

Schärer OD (2007) Achieving broad substrate specificity in damage recognition by binding accessible nondamaged DNA. *Mol Cell* **28:** 184–185

Scrima A, Konickova R, Czyzewski BK, Kawasaki Y, Jeffrey PD, Groisman R, Nakatani Y, Iwai S, Pavletich NP, Thomä NH (2008) Structural basis of UV DNA-damage recognition by the DDB1-DDB2 complex. *Cell* **135:** 1213–1223

Sprague BL, Pego RL, Stavreva DA, McNally JG (2004) Analysis of binding reactions by fluorescence recovery after photobleaching. *Biophys J* **86:** 3473–3495

Sugasawa K, Hanaoka F (2007) Sensing of DNA damage by XPC/Rad4: one protein for many lesions. *Nat Struct Mol Biol* **14:** 887–888

Sugasawa K, Ng JM, Masutani C, Iwai S, van der Spek PJ, Eker AP, Hanaoka F, Bootsma D, Hoeijmakers JH (1998) Xeroderma pigmentosum group C protein complex is the initiator of global genome nucleotide excision repair. *Mol Cell* **2:** 223–232

Sugasawa K, Okamoto T, Shimizu Y, Masutani C, Iwai S, Hanaoka F (2001) A multistep damage recognition mechanism for global genomic nucleotide excision repair. *Genes Dev* **15:** 507–521

Tang JY, Hwang BJ, Ford JM, Hanawalt PC, Chu G (2000) Xeroderma pigmentosum p48 gene enhances global gemomic repair and suppresses UV-induced mutagenesis. *Mol Cell* **5:** 737–744

Träutlein D, Adler F, Moutzouris K, Jeromin A, Leitenstorfer A, Ferrando-May E (2008) Highly versatile confocal microscopy system based on a tunable femtosecond Er:fiber source. *J Biophoton* **1:** 53–61

Trego KS, Turchi JJ (2006) Pre-steady-state binding of damaged DNA by XPC-hHR23B reveals a kinetic mechanism for damage discrimination. *Biochemistry* **45:** 1961–1969

Uchida A, Sugasawa K, Masutani C, Dohmae N, Araki M, Yokoi M, Ohkuma Y, Hanaoka F (2002) The C-terminal domain of the XPC protein plays a crucial role in nucleotide excision repair through interactions with transcription factor IIH. *DNA Rep* **1:** 449–461

Xie Z, Liu S, Zhang Y, Wang Z (2004) Roles of Rad23 protein in yeast nucleotide excision repair. *Nucl Acids Res* **15:** 5981–5990

Yasuda G, Nishi R, Watanabe E, Mori T, Iwai S, Orioli D, Stefanini M, Hanaoka F, Sugasawa K (2007) *In vivo* destabilization and functional defects of the xeroderma pigmentosum C protein caused by a pathogenic missense mutation. *Mol Cell Biol* **27:** 6606–6614

Yokoi M, Masutani C, Maekawa T, Sugasawa K, Ohkuma Y, Hanaoka F (2000) The xeroderma pigmentosum group C protein complex XPC-HR23B plays an important role in the recruitment of transcription factor IIH to damaged DNA. *J Biol Chem* **275:** 9870–9875

SUPPLEMENTARY INFORMATION

Two-stage dynamic DNA quality check by xeroderma pigmentosum group C protein

Ulrike Camenisch[1,4], Daniel Träutlein[2,4], Flurina C. Clement[1], Jia Fei[1], Alfred Leitenstorfer[2], Elisa Ferrando-May[3] and Hanspeter Naegeli[1,*]

[1]Institute of Pharmacology and Toxicology, University of Zürich-Vetsuisse, CH-8057 Zürich, Switzerland

[2]Department of Physics and Center for Applied Photonics, University of Konstanz, D-78457 Konstanz, Germany

[3]Bioimaging Center, University of Konstanz, D-78457 Konstanz, Germany

[4]These authors contributed equally to this work

TABLE OF CONTENTS

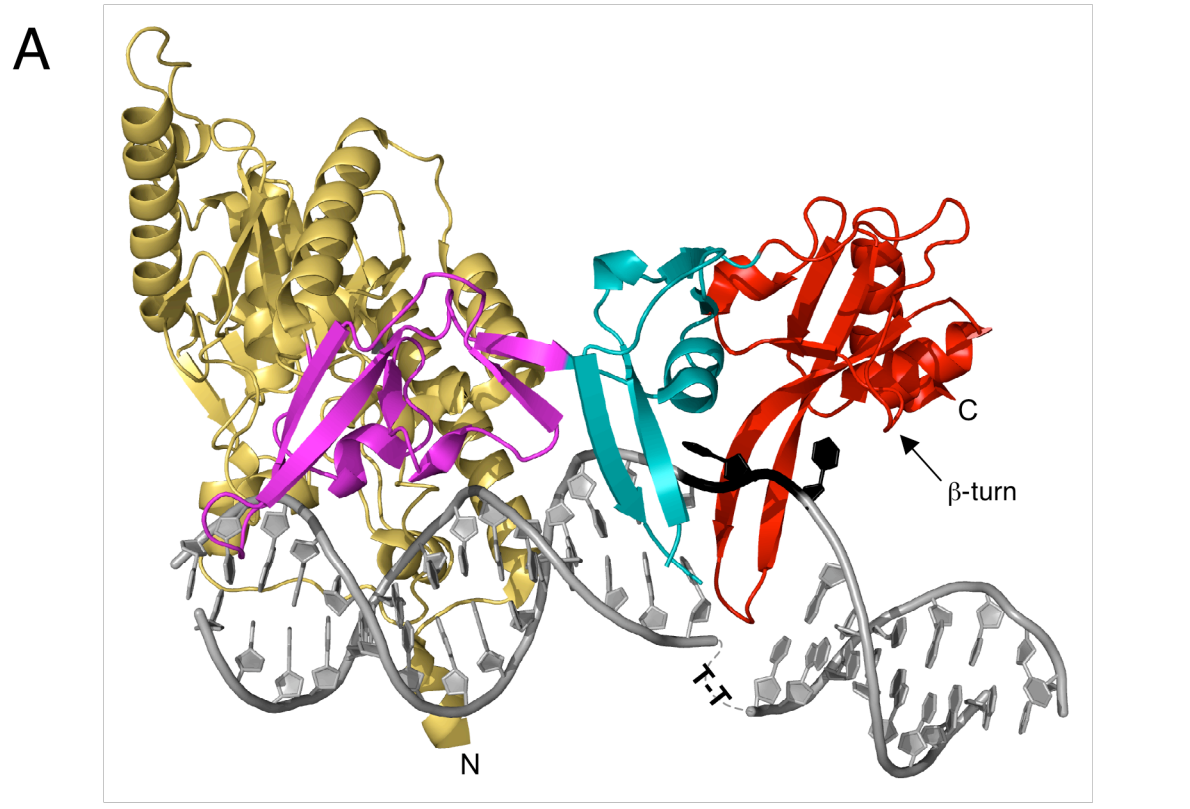

Supplementary Figure 1. Structure of XPC protein inferred from the yeast (*Saccaromyces cerevisiae*) Rad4 homolog. (**A**) Ribbon diagram of the crystal structure of Rad4 protein in complex with DNA containing a cyclobutane pyrimidine dimer (CPD) embedded in 3 base mismatches (Min & Pavletich, 2007). Gold, transglutaminase-homology domain (TGD); magenta, β-hairpin domain 1 (BHD1); cyan, BHD2; red, BHD3. The arrow indicates the location of the β-turn structure where the E755K mutation is introduced. T-T denotes the CPD, which is expelled from the double helix. The figure was made with the PyMol Molecular Viewer using the coordinates PDB 2QSG (**B**). Schematic representation of the aforementioned Rad4 domains and the respective XPC sequences. In human XPC protein, the TGD is divided into two distinct parts by a disordered ~180-residue insertion (Bunick et al, 2006).

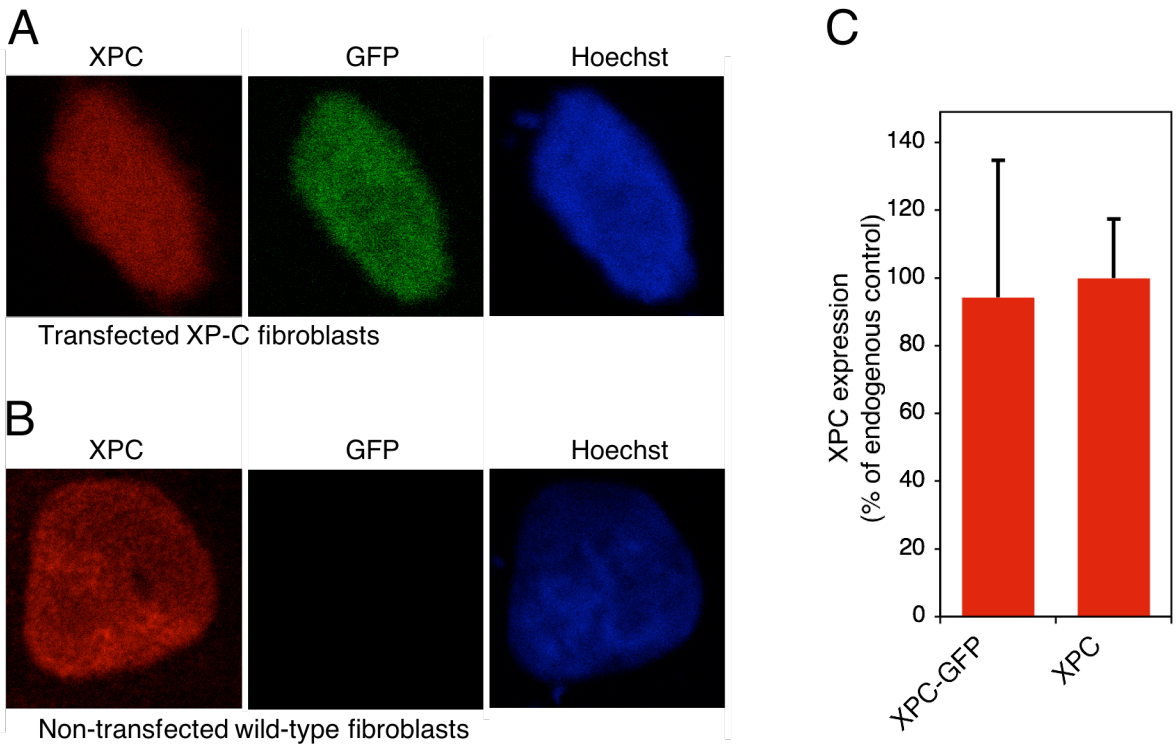

Supplementary Figure 2. Immunocytochemical analysis of XPC protein expression. (**A**) Visualization of XPC-GFP in a typical XP-C fibroblast expressing a low level of fusion protein. The immunological detection was performed with mouse monoclonal antibodies against human XPC (Abcam) followed by secondary antibodies conjugated to the Alexa Fluor 546 red dye (Invitrogen). The nuclear compartment is indicated by the Hoechst reagent. (**B**) Immunochemical detection of endogenous XPC in a representative wild-type fibroblast (GM00637). (**C**) Quantitative assessement of XPC-GFP expression in XP-C cells displaying the low green fluorescence level used as the criterion for imaging studies, in comparison to the endogenous XPC protein in wild-type fibroblasts (n = 10; error bars, standard deviation). Expression levels were compared by immunochemical analysis using antibodies against XPC and represented as the percentage of red fluorescence in normal fibroblasts. These results demonstrate that the XP-C cells targeted for live-cell imaging contain XPC protein in the same expression range as the endogenous protein in wild-type counterparts.

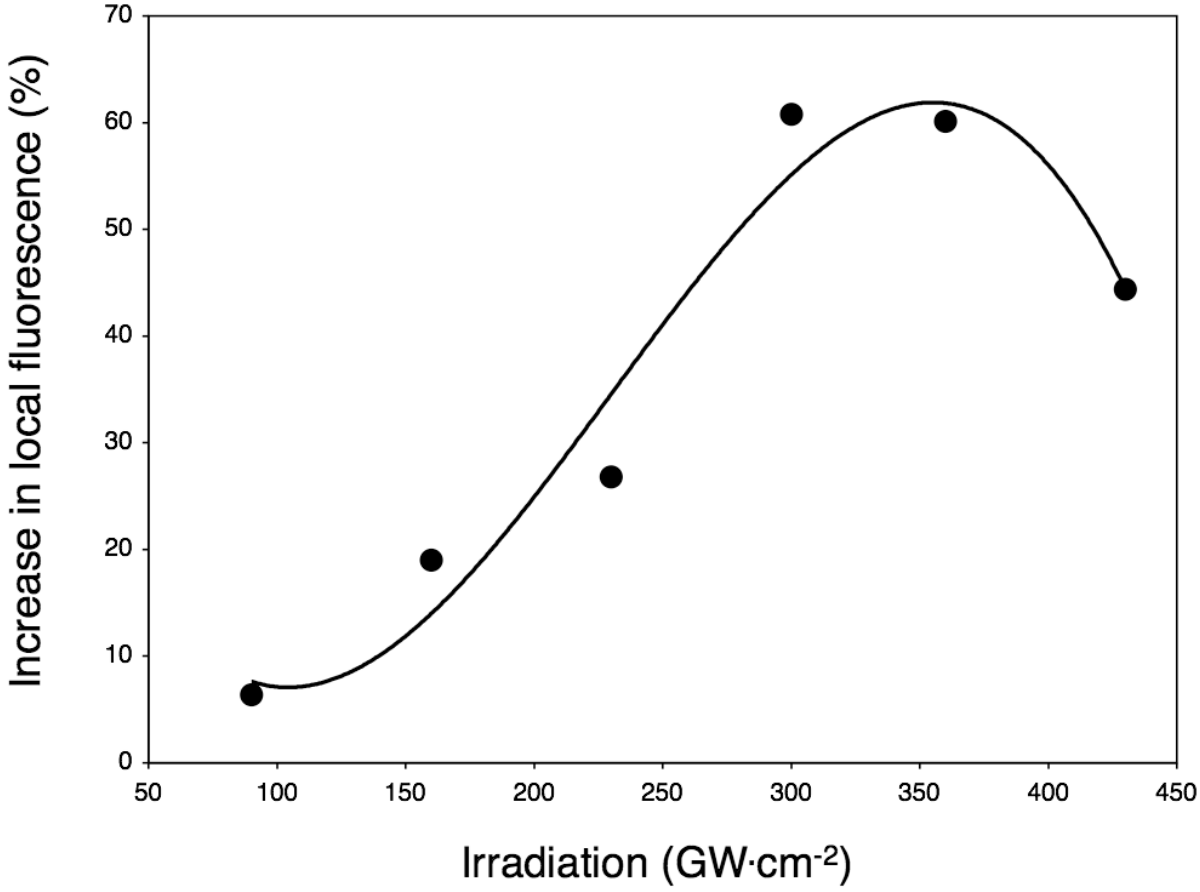

Supplementary Figure 3. Dose-dependent accumulation of XPC-GFP fusion protein in damaged chromatin areas of human XP-C fibroblasts. A single 10-µm line of UV photoproducts was generated at different dose levels of near-infrared irradiation. The local increase in fluorescence, determined 6 min after irradiation, was plotted as a percentage of the average fluorescence measured before irradiation (mean values of 5 experiments).

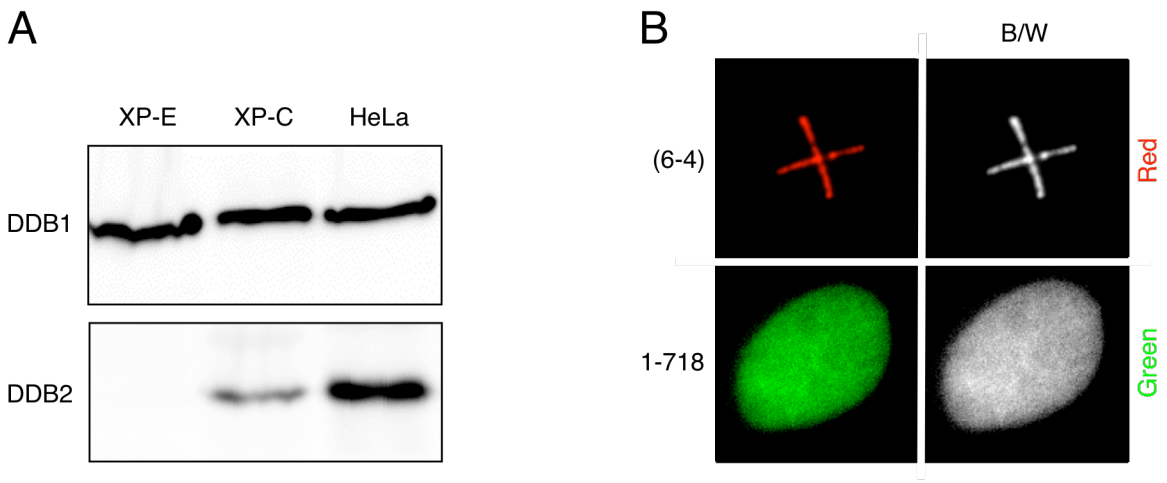

Supplementary Figure 4. Characterization of the XP-C fibroblasts GM16093. (**A**) Immunoblot analysis of endogenous DDB1 and DDB2 expression in the GM16093 cell line compared to HeLa cells and XP-E (GM02415) fibroblasts. Each lane contains 60 µg of cell lysate proteins. The antibodies against DDB1 and DDB2 were from BD Biosciences and Abcam, respectively. (**B**) Defective DNA damage recognition by fragment $XPC_{1\text{-}718}$. The cells GM16093, derived from patient XP14BR, lack functional *XPC* due to a nonsense mutation leading to premature termination at codon 718. The representative images (in color and black-and-white) demonstrate that, if expressed, the truncated XPC protein is unable to relocate to nuclear tracks of UV lesions. The distribution of GFP fusion protein was visualized 6 min after irradiation and DNA lesions were counterstained with antibodies against (6-4) photoproducts.

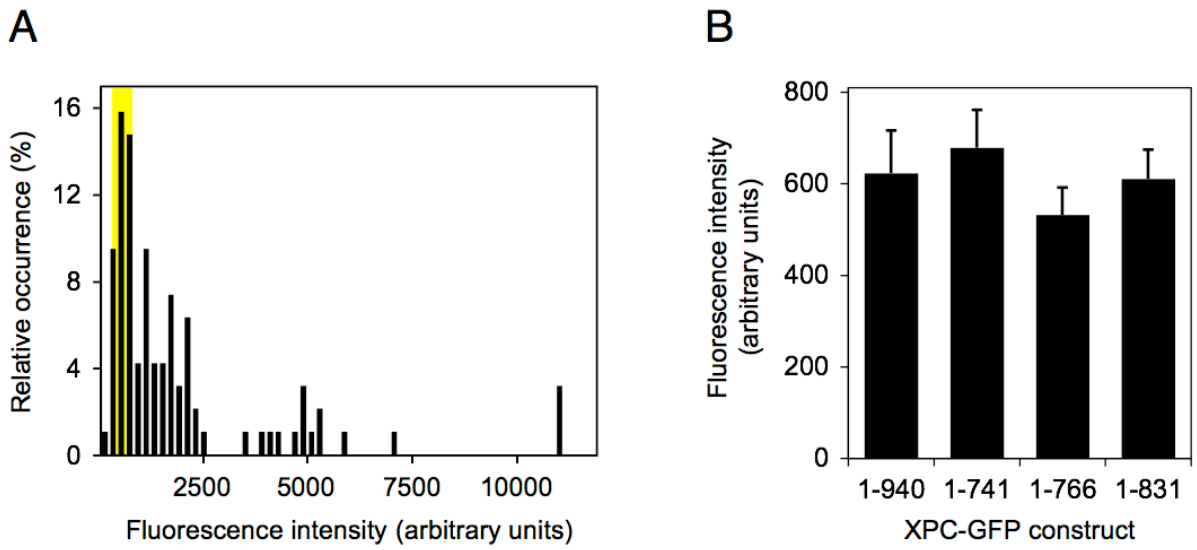

Supplementary Figure 5. Level of XPC-GFP truncates inside individual nuclei. (**A**) Overall fluorescence intensity in 95 representative nuclei of XP-C fibroblasts transfected with the full-length XPC-GFP sequence. The green fluorescence intensity of each nucleus is expressed in arbitrary units and the Y-axis indicates the proportion of cells in each fluorescence category. The yellow box illustrates the narrow range of cells selected for live-cell imaging. A comparison between the level of XPC-GFP in the selected XP-C cells and the normal XPC expression in wild-type fibroblasts is shown in the supplementary Figure 2. (**B**) Expression of wild-type XPC protein and truncated derivatives in nuclei used for live-cell imaging studies (n = 20; error bars, standard errors of the mean). These quantifications of overall fluorescence demonstrate that cells containing comparably low amounts of each construct were used for the experiments.

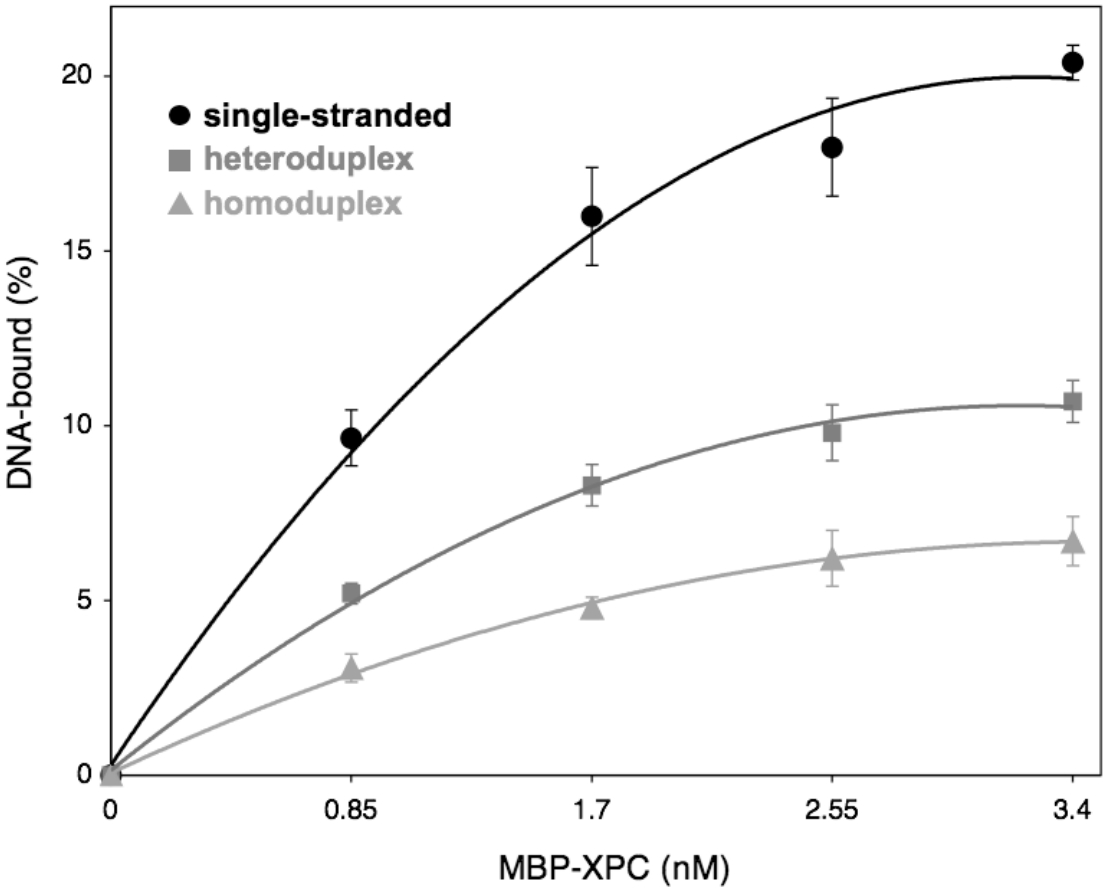

Supplementary Figure 6. DNA-Binding of full-length XPC protein. The indicated amounts of immunoprecipitated MBP-XPC fusion protein linked to magnetic beads (Maillard et al, 2007) were incubated with 2 nM ^{32}P-labeled 135-mer oligonucleotides (single-stranded, 3-mismatch heteroduplexes or homoduplexes). The DNA molecules captured by XPC protein were separated from free oligonucleotides and DNA-binding activity (n = 3) is reported as the percentage of immobilized radioactivity after deduction of the background determined with empty beads. Error bars, standard deviation.

Supplementary Table I. Effective diffusion coefficients (D_{eff}) and equilibrium constants (k^*_{on}/k_{off}) were computed from the FRAP curves of Figure 5 using the effective diffusion model (Sprague et al, 2004). The fit between experimental data and the mathematical model is indicated by the correlation coefficient (R).

XPC construct	***R***	$\boldsymbol{D_{eff}}$ **(μm²/s)**[a]	$\mathbf{k^*_{on}/k_{off}}$[b]
Control (XPC_{1-940})	0.91	0.30	36.3
XPC_{1-831}	0.94	0.49	22.7
XPC_{1-831} + UV[c]	0.91	0.34	33.1
XPC_{1-766}	0.98	0.44	26.1
XPC_{1-766} + UV	0.99	0.37	31.2
XPC_{1-741}	0.99	0.34	34.3
XPC_{1-741} + UV	0.99	0.32	36.5

[a]D_{eff} values were calculated in Matlab (The Math Works, Natick, MA, USA) using the model: $f(t) = e^{-\tau_D/2t} \cdot [I_0(\tau_D/2t) + I_1(\tau_D/2t)]$, where $\tau_D = \omega^2/D_{eff}$ (ω, radius of the bleach spot); I_0 and I_1 are modified Bessel functions.

[b]k^*_{on}/k_{off} (the ratio of bound/free molecules) was calculated from $D_{eff} = D_f/1 + (k^*_{on}/k_{off,})$, where D_f is the expected free diffusion coefficient if the FRAP curve is determined by free movement (11.2 μm²/s for full-length XPC protein, 11.6 μm²/s for XPC_{1-831}, 11.9 μm²/s for XPC_{1-766} and 12.0 μm²/s for XPC_{1-741}) and k^* is the pseudo-on rate. The D_f values were calculated assuming a diffusion coefficient of 20 μm²/s for GFP (Sprague et al, 2004).

[c]The cells were exposed to UV-C light (254 nm) at a dose of 10 J/m².

Supplementary Table II. Forward and reverse oligonucleotide primers used for the construction of truncated XPC derivatives and for site-directed mutagenesis.

$XPC_{118-940}$	Forward: 5'-GGGGTACCGCTACC**ATG**AATGAAGAC-3' Reverse: 5'-ATACCCGGGTT**CAG**CTTCTCAA-3'
XPC_{1-495}	Forward: 5'-ATGGTACCGCCACC**ATG**GCTCGGAAAC-3' Reverse: 5'-ACACCCGGGTC**TGG**GTCCTTACGATG-3'
XPC_{1-718}	Forward: 5'-ATGGTACCGCCACC**ATG**GCTCGGAAAC-3' Reverse: 5'-ACACCCGGGAG**TCG**GGCTTTCCGAGCACG-3'
XPC_{1-741}	Forward: 5'-ATGGTACCGCCACC**ATG**GCTCGGAAAC-3' Reverse: 5'-ATACCCGGGTC**ATA**CTCCTCTGTCTGCC-3'
XPC_{1-766}	Forward: 5'-ATGGTACCGCCACC**ATG**GCTCGGAAAC-3' Reverse: 5'-ATACCCGGGTT**CAT**GCTGGGCAGGAA-3'
XPC_{1-831}	Forward: 5'-ATGGTACCGCCACC**ATG**GCTCGGAAAC-3' Reverse: 5'-ATGGTACC**GAC**TGCCTGCTCATTTTCCCAGG-3'
$XPC_{427-940}$	Forward: 5'-AAGGTACCGCCACC**ATG**GTGTCTTATAAA-3' Reverse: 5-'ATACCCGGGTT**CAG**CTTCTCAA-3'
$XPC_{607-940}$	Forward: 5'-ATGGTACCGCCACC**ATG**TTGAGACCATA-3' Reverse: 5-'ATACCCGGGTT**CAG**CTTCTCAA-3'
$XPC_{607-741}$	Forward: 5'-ATGGTACCGCCACC**ATG**TTGAGACCATA-3' Reverse: 5'-ATACCCGGGTC**ATA**CTCCTCTGTCTGCC-3'
$XPC_{607-766}$	Forward: 5'-ATGGTACCGCCACC**ATG**TTGAGACCATA-3' Reverse: 5'-ATACCCGGGTT**CAT**GCTGGGCAGGAA-3'
W690S	Forward: 5'-GCATTCCAGGGACACGT**C**GCTGAAGAAAGCAAGAG-3' Reverse: 5'-CTCTTGCTTTCTTCAGC**G**ACGTGTCCCTGGAATGC-3'
W690A	Forward: 5'-GCATTCCAGGGACACG**G**CGCTGAAGAAAGCAAGAG-3' Reverse: 5'-CTCTTGCTTTCTTCAGCG**C**CGTGTCCCTGGAATGC-3'
W531A	Forward: 5'-GCTGGTATAGACCAG**GC**GCTAGAGGTGTTC-3' Reverse: 5'-GAACACCTCTAGC**GC**CTGGTCTATACCAGC-3'
W542A	Forward: 5'-GAGCAGGAGGAAAAG**GC**GGTATGTGTAGAC-3' Reverse: 5'-GTCTACACATACC**GC**CTTTTCCTCCTGCTC-3'
F733A	Forward: 5'-GAAAATGACCTGGGCCTG**GC**TGGCTACTGGCAGACAGAG-3' Reverse: 5'-CTCTGTCTGCCAGTAGCCA**GC**CAGGCCCAGGTCATTTTC-3'
E755K	Forward: 5'-GTGCCCCGGAAC**A**AGTTTGGGAATGTGTACC-3' Reverse: 5'-GGTACACATTCCCAAACT**T**GTTCCGGGGCA-3'

Legends to supplementary movies

Movie 1. Accumulation of wild-type XPC in UV-damaged nuclear tracks. XPC-GFP protein was expressed in human XP-C fibroblasts and the near-infrared laser (314 GW·cm^{-2}) was used to generate a single 10-μm track of UV photoproducts across the nucleus. The damaged area is indicated by the white bar shown at the beginning of the movie. Subsequently, the dynamic distribution of XPC-GFP was monitored over a 6-min time period. A clearly distinguishable pattern of XPC-GFP accumulation is already formed 3 seconds after the induction of UV lesions.

Movie 2. Representative video illustrating that the W690S mutant is defective in the accumulation in irradiated areas containing UV lesions. An XP-C fibroblast expressing the W690S mutant was treated with a near-infrared irradiation of 314 GW·cm^{-2} to generate a 10-μm track of UV lesions identical to that of Movie 1. Subsequently, the dynamic distribution of mutant XPC-GFP was monitored over a 6-min time period.

Chapter 3

Discussion and Perspectives

Nucleotide excision repair is of tremendous importance in placental mammals since it is the only mechanism repairing UV light-induced DNA damages. The sequential assembly of the repair machinery is therefore carefully investigated and quite well understood. Nevertheless, there are several gaps of knowledge regarding damage recognition and lesion handover between the NER key players. This discussion aims at putting together the essential findings of the manuscripts in Chapter 2 to describe XPC's mode of action. However, this chapter does not replace the discussions included in each of the presented papers.

Despite its crucial role in DNA damage recognition, there was long only little known about XPC's mode of action. The more intriguing was it as the crystal structure of its yeast homolog Rad4 was solved (*Min* and *Pavletich* 2007) approving the previous findings of XPC binding to the undamaged strand opposite a lesion site (*Buterin et al.* 2005, *Maillard et al.* 2007, *Sugasawa et al.* 2007). Based on the crystal structure, experiments with truncated XPC revealed that a minimal amino acid sequence 607-766 is sufficient to efficiently detect UV-induced damages, but for the formation of a stable nucleoprotein complex the BHD3 segment (residues 767-831) is required (*Camenisch et al.* 2009). To further elucidate the precise mechanism of action, we studied the role of four highly conserved residues (N754, F756, F797, and F799) in lesion recognition and repair located within this sequence. We found that the recruitment of XPC to the DNA damage is dependent on three amino acids N754, F756, and F797, while F799 accounts for single-strand DNA-binding opposite the lesion site. In addition, N754 is important for the mobility of XPC thereby contributing to a fast lesion search mode (*Clement et al.* 2010).

A central question is how XPC actually locates the damaged site within the vast background of native DNA. There are several hypothetical diffusion-based mechanisms by which a DNA-binding protein finds its target sequence. *One-dimensional diffusion* or sliding describes the random walk of a protein along DNA without dissociation. In *one-dimensional hopping*, the protein moves along the same molecule of DNA by short-time dissociation and immediate rebinding in close proximity to the previously sampled site, meaning that a scanned site is only a single step away from the site probed a moment ago. *Jumping* describes the targeting of two sites completely independent of one another via movement over longer distances and rebinding at more distant locations or even on different DNA molecules (*Berg et al.* 1981, *Winter* and *von Hippel* 1981, *Winter et al.* 1981). Based on the results presented in the manuscripts in Chapter 2, we propose a model where XPC seeks for lesions via *facilitated*

diffusion using a combination of three-dimensional diffusion and one-dimensional sliding along DNA molecules. This search mode is enabled by DNA-attractive and DNA-repulsive motifs determined via the amino acid sequence of the protein. Amino acid E755 markedly increased XPC's affinity for DNA when E755 was mutated to K755 (*Camenisch et al.* 2009). Also, the mutation of N754 to alanine results in reduced protein mobility in non-challenged cells (*Clement et al.* 2010). Both E755 and N754 are located in the β-turn motif between BHD2 and BHD3 (*Camenisch et al.* 2009, *Min* and *Pavletich* 2007) suggesting that this motif is a determining factor for facilitated diffusion rapidly investigating base-pair integrity. Upon damage detection, the single-stranded DNA-binding domain BHD3 induces the transition to a stable recognition complex by capturing an extruded nucleotide in the undamaged strand with its aromatic residue F799.

As mentioned in the introduction, CPD recognition requires an additional NER factor, DDB2. Upon damage detection by DDB2, the lesion is handed over to XPC initiating the sequential assembly of the repair machinery. It is known that ubiquitylation of DDB2 leads to degradation of this protein, while ubiquitylation of XPC has a stabilizing function. How DDB2 attracts XPC and passes the damage on still needs to be resolved. According to the crystal structures of DDB2 (*Scrima et al.* 2009) and XPC (*Min* and *Pavletich* 2007), the XPC's BHD2-BHD3 domains would clash with DDB2 attached to double-stranded DNA if they bound to the damaged site at the same time. Hence, there must be a scenario where DDB2 presents the CPD to XPC concurrently dissociating from the DNA. Data from our lab indicate that DDB2 grasps XPC by its β-hairpin of BHD3 and guides it to the appropriate location (*Kaczmarek et al.*, manuscript in preparation).

An issue still to be clarified is where in fact NER takes place in the chromatin context. The results of *Solimando et al.* (2009) assume that DNA damage-detection by XPC happens in condensed chromatin domains followed by a translocation of the damaged sites to the perichromatin region thereby providing more space for the pre-incision complex-assembly. In non-challenged cells, the authors observed that the distribution pattern of XPC resembled the condensed chromatin allocation while XPA distribution was homogeneous. Following UV irradiation, XPA and XPC accumulated in the perichromatin region accompanied by a transient chromatin decompaction enabling damage translocation. However, the exact mechanism of this translocation is not known. The understanding of NER's course of action within the tightly packed DNA would mean a big breakthrough in the field.

I am confident that the present thesis provides a strong model of DNA damage recognition by XPC protein, which contributes to more comprehension in the global genome repair field and particularly opens new perspectives for future investigations.

Appendix

BIBLIOGRAPHY

Aboussekhra A, Biggerstaff M, Shivji MK, Vilpo JA, Moncollin V, Podust VN, Protic M, Hübscher U, Egly JM, and Wood RD (1995) Mammalian DNA nucleotide excision repair reconstituted with purified protein components. *Cell* 80: 859–868.

Alekseev S, Luijsterburg, MS, Pines A, Geyerts B, Mari PO, Giglia-Mari G, Lans H, Houtsmuller AB, Mullenders LH, Hoeijmakers JH, and Vermeulen W (2008) Cellular concentrations of DDB2 regulate dynamic binding of DDB1 at UV-induced DNA damage. *Mol Cell Biol* 28: 7402-7413.

Alexandrov BS, Wille LT, Rasmussen KØ, Bishop AR, Blagoev KB (2006) Bubble statistics and dynamics in double-stranded DNA. *Phys Rev E* 74: 05090.

Andressoo JO and Hoeijmakers JH (2005) Transcription-coupled repair and premature ageing. *Mutat Res* 577: 179-194.

Andressoo JO, Hoeijmakers JH, and Mitchell JR (2006) Nucleotide excision repair disorders and the balance between cancer and aging. *Cell Cycle* 5: 2886-2888.

Anantharaman V, Koonin EV, Aravind L (2001) Peptide-N-glycanases and DNA repair proteins, Xp-C/Rad4, are, respectively, active and inactivated enzymes sharing a common transglutaminase fold. *Hum Mol Genet* 10: 1627-1630.

Araki M, Masutani C, Takemura M, Uchida A, Sugasawa K, Kondoh J, Ohkuma Y, and Hanaoka F (2001) Centrosome protein centrin 2/caltractin 1 is part of the xeroderma pigmentosum group C complex that initiates global genome nucleotide excision repair. *J Biol Chem* 276: 18665-18672.

Araujo SJ, Tirode F, Coin F, Pospiech H, Syväoja JE, Stucki M, Hübscher U, Egly JM, and Wood RD (2000) Nucleotide excision repair of DNA with recombinant human proteins: definition of the minimal set of factors, active forms of TFIIH, and modulation by CAK. *Genes Dev* 14: 349-359.

Balajee AS and Bohr VA (2000) Genomic heterogeneity of nucleotide excision repair. *Gene* 250: 15-30.

Batty D, Rapic'-Otrin V, Levine AS, and Wood RD (2000) Stable binding of human XPC complex to irradiated DNA confers strong discrimination for damaged sites. *J Mol Biol* 300: 275-290.

Berg OG, Winter RB, and van Hippel PH (1981) Diffusion-driven mechanisms of protein translocation on nucleic acids. 1. Models and theory. *Biochemistry* 20: 6929-6948.

Bessho T, Sancar A, Thompson LH, and Thelen MP (1997) Reconstitution of human excision nuclease with recombinant XPF-ERCC1 complex. *J Biol Chem* 272: 3833-3837.

Bertrand-Burggraf E, Kemper B, and Fuchs RP (1994) Endonuclease VII of phage T4 nicks N-2-acetylaminofluorene-induced DNA structures in vitro. *Mutat Res* 314: 287-295.

Blagoev KB, Alexandrov BS, Goodwin EH, and Bishop AR (2006) Ultra-violet light induced changes in DNA dynamics may enhance TT-dimer recognition. *DNA Repair (Amst)* 5: 863-867.

Bochkarev A, Pfuetzner RA, Edwards AM, and Frappier L (1997) Structure of the single-stranded-DNA-binding domain of replication protein A bound to DNA. *Nature* 385: 176-181.

Brooks PJ (2007) The case for 8,5'-cyclopurine-2'-deoxynucleosides as endogenous DNA lesions that cause neurodegeneration in xeroderma pigmentosum. *Neuroscience* 145: 1407-1417.

Bunick CG, Miller MR, Fuller BE, Fanning E, and Chazin WJ (2006) Biochemical and structural domain analysis of xeroderma pigmentosum complementation group C protein. *Biochemistry* 45: 14965-14979.

Buschta-Hedayat N, Buterin T, Hess MT, Missura M, and Naegeli H (1999) Recognition of nonhybridizing base pairs during nucleotide excision repair of DNA. *Proc Natl Acad Sci USA* 96: 6090-6095.

Buterin T, Meyer C, Giese B, and Naegeli H (2005) DNA quality control by conformational readout on the undamaged strand of the double helix. *Chem Biol* 12: 913-922.

Camenisch U, Dip R, Schumacher SB, Schuler B, and Naegeli H (2006) Recognition of helical kinks by xeroderma pigmentosum group A protein triggers DNA excision repair. *Nat Struct Mol Biol* 13: 278-284.

Camenisch U, Dip R, Vitanescu M, and Naegeli H (2007) Xeroderma pigmentosum complementation group A protein is driven to nucleotide excision repair sites by the electrostatic potential of distorted DNA. *DNA Repair* 6: 1819-1828.

Camenisch U, Träutlein D, Clement FC, Fei J, Leitenstorfer A, Ferrando-May E, and Naegeli H (2009) Two-stage dynamic DNA quality check by xeroderma pigmentosum group C protein. *EMBO J* 28: 2387-2399.

Carreau M, Eveno E, Quilliet X, Chevalier-Lagent O, Benoit A, Tanganelli B, Stefanini M, Vermeulen W, Hoeijmakers JH, Sarasin A, and Mezzina M (1995) Development of a new easy complementation assay for DNA repair deficient human syndromes using cloned repair genes. *Carcinogenesis* 16: 1003-1009.

Carreau M, Quilliet X, Eveno E, Salvetti A, Danos O, Heard JM, Mezzina M, and Sarasin A (1995) Functional retroviral vector for gene therapy of xeroderma pigmentosum group D patients. *Hum Gene Ther* 6: 1307-1315.

Chavanne F, Broughton BC, Pietra D, Nardo T, Browitt A, Lehmann AR, and Stefanini M (2000) Mutations in the XPC gene in families with xeroderma pigmentosum and consequenced at the cell, protein and transcription level. *Cancer Res* 60: 1974-1982.

Chen X, Zhang Y, Douglas L, and Zhou P (2001) UV-damaged DNA-binding proteins are targets of CUL-4A-mediated ubiquitination and degradation. *J Biol Chem* 276: 48175-48182.

Clarkson, SG (2003) The XPG story. *Biochimie* 85: 1113-1121.

Cleaver JE (1972) Xeroderma pigmentosum: variants with normal DNA repair and normal sensitivity to ultraviolet light. *J Invest Dermatol* 58: 124-128.

Cleaver JE (2005) Cancer in xeroderma pigmentosum and related disorders of DNA repair. *Nat Rev Cancer* 5: 564-573.

Cleaver JE, Thompson LH, Richardson AS, and States JC (1999) A summary of mutations in the UV-sensitive disorders: xeroderma pigmentosum, Cockayne syndrome, and trichothiodystrophy. *Hum Mutat* 14: 9-22.

Cosman M, Fiala R, Hingerty BE, Laryea A, Lee H, Amin S, Geacintov NE, Broyde S, and Patel D (1993) Solution conformation of the (+)-trans-anti[BPh]dA adduct opposite dT in a DNA duplex: intercalation of the covalently attached benzo[c]phenanthrene to the 5'-side of the adduct site without disruption of the modified base pair. *Biochemistry* 32: 12488-12497.

Cosman M, Hingerty BE, Luneva N, Amin S, Geacintov NE, Broyde S, and Patel DJ (1996) Solution conformation of the (-)-cis-anti-benzo[a]pyrenyl-dG adduct opposite dC in a DNA duplex: intercalation of the covalently attached BP ring into the helix with base displacement of the modified deoxyguanosine into the major groove. *Biochemistry* 35: 9850-9863.

D'Errico M, Parlanti E, Teson M, deJesus BM, Degan P, Calcagnile A, Jaruga P, Bjoras M, Crescenzi M, Pedrini AM, Egly JM, Zambruno G, Stefanini M, Dizdaroglu M, and Dogliotti E (2006) New functions of XPC in the protection of human skin cells from oxidative damage. *EMBO J* 25: 4305-4315.

Despras E, Pfeiffer P, Salles B, Calsou P, Kuhfitting-Kulle S, Angulo JF, and Biard DS (2007) Long-term XPC silencing reduces DNA double-strand break repair. *Cancer Res* 67: 2526-2534.

Dinant C, de Jager M, Essers J, van Cappellen WA, Kanaar R, Houtsmuller AB, and Vermeulen W (2007) Activation of multiple DNA repair pathways by subnuclear damage induction methods. *J Cell Sci* 120: 2731-2740.

Dualan R, Brody T, Keeney S, Nichols AF, Admon A, and Linn S (1995) Chromosomal localization and

cDNA cloning of the genes (DDB1 and DDB2) for the p127 and p48 subunits of a human damage-specific DNA binding protein. *Genomics* 29: 62-69.

Evans E, Fellows J, Coffer A, and Wood RD (1997) Open complex formation around a lesion during nucleotide excision repair provides a structure for cleavage by human XPG protein. *EMBO J* 16: 625-638.

Evans E, Moggs JG, Hwang JR, Egly JM, and Wood RD (1997) Mechanism of open complex and dual incision formation by human nucleotide excision repair factors. *EMBO J* 16: 6559-6573.

Fan L, Arvai AS, Cooper PK, Iwai S, Hanaoka F, and Tainer JA (2006) Conserved XPB core structure and motifs for DNA unwinding: implications for pathway selection of transcription or excision repair. *Mol Cell* 22: 27-37.

Feldberg RS and Grossman L (1976) A DNA binding protein from human placenta specific for ultraviolet damaged DNA. *Biochemistry* 15: 2402-2408.

Fitch ME, Nakajima S, Yasui A, and Ford JM (2003) In vivo recruitment of XPC to UV-induced cyclobutane pyrimidine dimers by the DDB2 gene product. *J Biol Chem* 278: 46906-46910.

Friedberg EC (2001) How nucleotide excision repair protects against cancer. *Nat Rev Cancer* 1: 22-33.

Friedberg EC, Walker GC, Siede W, Wood RD, Schultz RA, and Ellenberger T (2006) *DNA Repair and Mutagenesis*. Washington, DC: ASM Press, p. 698.

Gillet LC and Schärer OD (2006) Molecular mechanisms of mammalian global genome nucleotide excision repair. *Chem Rev* 106: 253-276.

Groisman R, Polanowska J, Kuraoka I, Sawada J, Saijo M, Drapkin R, Kisselev AF, Tanaka K, and Nakatani Y (2003) The ubiquitin ligase activity in the DDB2 and CSA complexes is differentially regulated by the COP9 signalosome in response to DNA damage. *Cell* 113: 357-367.

Gunz D, Hess MT, and Naegeli H (1996) Recognition of DNA adducts by human nucleotide excision repair. Evidence for a thermodynamic probing mechanism. *J Biol Chem* 271: 25089-25098.

Hanawalt PC and Haynes RH (1965) Repair replication of DNA in bacteria: irrelevance of chemical nature of base defect. *Biochem Biophys Res Commun* 19: 462-467.

Hanawalt PC and Spivak G (2008) Transcription-coupled DNA repair: two decades of progress and surprises. *Nat Rev Mol Cell Biol* 9: 958-970.

Hess MT, Gunz D, Luneva N, Geacintov NE, and Naegeli H (1997) Base pair conformation-dependent excision of benzo[a]pyrene diol epoxide-guanine adducts by human nucleotide excision repair enzymes. *Mol Cell Biol* 17: 7069-7076.

Hess MT, Schwitter U, Petretta M, Giese B, and Naegeli H (1997) Bipartite substrate discrimination by human nucleotide excision repair. *Proc Natl Acad Sci USA* 94: 6664-6669.

Hoeijmakers JH (2001) Genome maintenance mechanisms for preventing cancer. *Nature* 411: 366-374.

Hoeijmakers JH (2009) DNA damage, aging, and cancer. *N Engl J Med* 361: 1475-1485.

Hoogstraten D, Bergink S, Verbiest VH, Luijsterburg MS, Geverts B, Raams A, Dinant C, Hoeijmakers JH, Vermeulen W, and Houtsmuller AB (2008) Versatile DNA damage detection by the global genome nucleotide excision repair protein XPC. *J Cell Sci* 121: 2850-2859.

Houtsmuller AB, Rademakers S, Nigg AL, Hoogstraten D, Hoeijmakers JH, and Vermeulen W (1999) Action of DNA repair endonuclease ERCC1/XPF in living cells. *Science* 284: 958-961.

Houtsmuller AB and Vermeulen W (2001) Macromolecular dynamics in living cell nuclei revealed by fluorescence redistribution after photobleaching. *Histochem Cell Biol* 115: 13-21.

Huang JC, Hsu DS, Kazantsev A, and Sancar A (1994) Substrate spectrum of human excinuclease: repair of abasic sites, methylated bases, mismatches and bulky adducts. *Proc Natl Acad Sci USA* 91: 12213-12217.

Huang JC, Svoboda DL, Reardon JT, and Sancar A (1992) Human nucleotide excision nuclease removes thymine dimers from DNA by incising the 22nd phosphodiester bond 5′ and the 6th phosphodiester bond 3′ to the photodimer. *Proc Natl Acad Sci USA* 89: 3664-3668.

Husain I and Sancar A (1987) Binding of E. coli DNA photolyase to a defined substrate containing a single To4T dimer. *Nucleic Acids Res* 15: 1109-1120.

Hwang BJ and Chu G (1993) Purification and characterization of a human protein that binds to damaged DNA. *Biochemistry* 32: 1657-1666.

Hwang BJ, Toering S, Francke U, and Chu G (1998) p48 activates a UV-damaged-DNA binding factor and is defective in xeroderma pigmentosum group E cells that lack binding activity. *Mol Cell Biol* 18: 4391-4399.

Isaacs RJ and Spielmann HP (2004) A model for initial DNA lesion recognition by NER and MMR based on local conformational flexibility. *DNA Rep* 3: 455-464.

Itoh T, Nichols A, and Linn S (2001) Abnormal regulation of DDB2 gene expression in xeroderma pigmentosum group E strains. *Oncogene* 20: 7041-7050.

Janicijevic A, Sugasawa K, Shimizu Y, Hanaoka F, Wijgers N, Djurica M, Hoeijmakers JH, and Wyman C (2003) DNA bending by the human damage recognition complex XPC-HR23B. *DNA Rep* 2: 325-336.

Johnson KA, Fink SP, and Marnett LJ (1997) Repair of propanodeoxyguanosine by nucleotide excision repair in vivo and in vitro. *J Biol Chem* 272: 11434-11438.

Kapetanaki MG, Guerrero-Santoro J, Bisi DC, Hsieh CL, Rapic'-Otrin V, and Levine AS (2006) The DDB1-CUL4ADDB2 ubiquitin ligase is deficient in xeroderma pigmentosum group E and targets histone H2A at UV-damaged DNA sites. *Proc Natl Acad Sci USA* 103: 2588-2593.

Kim JK, Soni SD, Arakali AV, Wallace JC, and Alderfer JL (1995) Solution structure of a nucleic acid photoproduct of deoxyfluorouridylyl-(3'-5')-thymidine monophosphate (d-FpT) determined by NMR and restrained molecular dynamics: structural comparison of two sequence isomer photoadducts (d-U5p5T and d-T5p5U). *Nucleic Acids Res* 23: 1810-1815.

Kim JK and Choi BS (1995) The solution structure of DNA duplex-decamer containing the (6-4) photoproduct of thymidylyl(3'-->5')thymidine by NMR and relaxation matrix refinement. *Eur J Biochem* 228: 849-854.

Kraemer KH, Lee MM, and Scotto J (1984) DNA repair protects against cutaneous and internal neoplasia: evidence from xeroderma pigmentosum. *Carcinogenesis* 5: 511-514.

Kuraoka I, Bender C, Romieu A, Cadet J, Wood RD, and Lindahl T (2000) Removal of oxygen free-radical-induced 50,8-purine cyclodeoxynucleosides from DNA by the nucleotide excision repair pathway in human cells. *Proc Natl Acad Sci USA* 97: 3832-3837.

Kusumoto R, Masutani C, Sugasawa K, Iwai S, Araki M, Uchida A, Mizukoshi T, and Hanaoka F (2001) Diversity of the damage recognition step in the global genomic nucleotide excision repair in vitro. *Mutat Res* 485: 219-227.

Lan L, Nakajima S, Oohata Y, Takao M, Okano S, Masutani M, Wilson SH, and Yasui A (2004) In situ analysis of repair processes for oxidative DNA damage in mammalian cells. *Proc Natl Acad Sci USA* 101: 13738-13743.

Legerski R and Peterson C (1992) Expression cloning of a human DNA repair gene involved in xeroderma pigmentosum group C. *Nature* 359: 70-73.

Lehmann AR (2003) DNA repair-deficient diseases, xeroderma pigmentosum, Cockayne syndrome and

trichothiodystrophy. *Biochimie* 85: 1101-1111.

Li L, Lu X, Peterson CA, and Legerski RJ (1995) An interaction between the DNA repair factor XPA and replication protein A appears essential for nucleotide excision repair. *Mol Cell Biol* 15: 5396-5402.

Li L, Lu X, Peterson CA, and Legerski RJ (1997) XPC interacts with both HHR23B and HHR23A in vivo. *Mutat Res* 383: 197-203.

Lin JJ and Sancar A (1992) (A)BC exinuclease: the Escherichia coli nucleotide excision repair enzyme. *Mol Microbiol* 6, 2219-2224.

Maillard O, Camenisch U, Clement FC, Blagoev KB, and Naegeli H (2007) DNA repair triggered by sensors of helical dynamics. *Trends Biochem Sci* 32: 494-499.

Maillard O, Solyom S, and Naegeli H (2007) An aromatic sensor with aversion to damaged strands confers versatility to DNA repair. *PLoS Biol* 5: e79.

Malta E, Moolenar GF, and Goosen N (2006) Base flipping in nucleotide excision repair. *J Biol Chem* 281: 2184-2194.

Marx A, MacWilliams MP, Bickle TA, Schwitter U, and Giese B (1997) 4'-acylated thymidines: A new class of DNA chain terminators and photocleavable DNA building blocks. *J Am Chem Soc* 119: 1131-1132.

Masutani C, Kusumoto R, Yamada A, Dohmae N, Yokoi M, Yuasa M, Araki M, Iwai S, Takio K, and Hanaoka, F (1999) The XPV (xeroderma pigmentosum variant) gene encodes human DNA polymerase eta. *Nature* 399: 700-704.

Masutani C, Sugasawa K, Yanagisawa J, Sonoyama T, Ui M, Enomoto T, Takio K, Tanaka K, van der Spek PJ, Bootsma D, Hoeijmakers JH, Hanaoka F (1994) Purification and cloning of a nucleotide excision repair complex involving the xeroderma pigmentosum group C protein and a human homologue of yeast RAD23. *EMBO J* 13: 1831-1843.

Meldrum RA, Botchway SW, Wharton CW, and Hirst GJ (2003) Nanoscale spatial induction of ultraviolet photoproducts in cellular DNA by three-photon near-infrared absorption. *EMBO Rep* 4: 1144-1149.

Miao F, Bouziane M, Dammann R, Masutani C, Hanaoka F, Pfeifer G, and O'Connor TR (2000) 3-Methyladenine-DNA glycosylase (MPG protein) interacts with human RAD23 proteins. *J Biol Chem* 275: 28433-28438.

Min JH and Pavletich NP (2007) Recognition of DNA damage by the Rad4 nucleotide excision repair protein. *Nature* 449: 570-575.

Missura M, Buterin T, Hindges R, Hübscher U, Kasparkova J, Brabec V, and Naegeli H (2001) Double-check probing of DNA bending and unwinding by XPA-RPA: an architectural function in DNA repair. *EMBO J* 20: 3554-3564.

Mocquet V, Kropachev K, Kolbanovskiy M, Kolbanovskiy A, Tapias A, Cay Y, Broyde S, Geacintov NE, and Egly JM (2007) The human DNA repair factor XPC-HR23B distinguishes stereoisomeric benzo[a]pyrenyl-DNA lesions. *EMBO J* 26: 2923-2932.

Moggs JG, Yarema KJ, Essigmann JM, and Wood RD (1996) Analysis of incision sites produced by human cell extracts and purified proteins during nucleotide excision repair of a 1,3-intrastrand d(GpTpG)-cisplatin adduct. *J Biol Chem* 271: 7177-7186.

Mone JJ, Bernas T, Dinant C, Goedvree FA, Manders EM, Volker M, Houtsmuller AB, Hoeijmakers JH, Vermeulen W, and van Driel R (2004) In vivo dynamics of chromatin-associated complex formation in mammalian nucleotide excision repair. *Proc Natl Acad Sci USA* 101: 15933-15937.

Moser J, Kool H, Giakzidis I, Caldecott K, Mullenders LH, and Fousteri MI (2007) Sealing of chromosomal DNA nicks during nucleotide excision repair requires XRCC1 and DNA ligase III alpha in a cell-cycle-specific manner. *Mol Cell* 27: 311-323.

Moser J, Volker M, Kool H, Alekseev S, Vrieling H, Yasui A, van Zeeland AA, and Mullenders LH (2005) The UV-damaged DNA binding protein mediates efficient targeting of the nucleotide excision repair complex to UV-induced photo lesions. *DNA Rep* 4: 571-582.

Mouret S, Philippe C Gracia-Chantegrel J, Banyasz A, Karpati S, Markovitsi D, and Douki T (2010) UVA-induced cyclobutane pyrimidine dimers in DNA: a direct photochemical mechanism? *Org Biomol Chem* 8: 1706-1711.

Mu D, Hsu DS, and Sancar A (1996) Reaction mechanism of human DNA repair excision nuclease. *J Biol Chem* 271: 8285-8294.

Mu D, Park CH, Matsunaga T, Hsu DS, Reardon JT, and Sancar A (1995) Reconstitution of human DNA repair excision nuclease in a highly defined system. *J Biol Chem* 270: 2415-2418.

Mu D, Wakasugi M, Hsu DS, and Sancar A (1997) Characterization of reaction intermediates of human excision repair nuclease. *J Biol Chem* 272: 28971-28979.

Nag A, Bondar T, Shiv S, and Raychaudhuri P (2001) The xeroderma pigmentosum group E gene product DDB2 is a specific target of cullin 4A in mammalian cells. *Mol Cell Biol* 21: 6738-6747.

Naegeli H, Bardwell L, and Friedberg EC (1992) The DNA helicase and adenosine triphosphatase activities

of yeast Rad3 protein are inhibited by DNA damage. *J Biol Chem* 267: 392-398.

Ng JM, Vermeulen W, van der Horst GT, Bergink S, Sugasawa K, Vrieling H, and Hoeijmakers JH (2003) A novel regulation mechanism of DNA repair by damage-induced and RAD23-dependent stabilization of xeroderma pigmentosum group C protein. *Genes Dev* 17: 1630-1645.

Nichols AF, Itoh T, Graham JA, Liu W, Yamaizumi M, and Linn S (2000) Human damage-specific DNA-binding protein p48. *J Biol Chem* 275: 21422-21428.

Nichols AF, Ong P, and Linn S (1996) Mutations specific to the xeroderma pigmentosum group E DDB(−) phenotype. *J Biol Chem* 271: 24317-24320.

Niedernhofer LJ (2008) Tissue-specific accelerated aging in nucleotide excision repair deficiency. *Mech Ageing Dev* 129: 408-415.

Nishi R, Okuda Y, Watanabe E, Mori T, Iwai S, Masutani C, Sugasawa K, and Hanaoka F (2005) Centrin 2 stimulates nucleotide excision repair by interacting with xeroderma pigmentosum group C protein. *Mol Cell Biol* 25: 5664-5674.

O'Donovan A, Davies AA, Moggs JC, West SC, and Wood RD (1994) XPG endonuclease makes the 3′ incision in human DNA nucleotide excision repair. *Nature* 371: 432-435.

O'Handley SF, Sanford DG, Xu R, Lester CC, Hingerty BE, Broyde S, and Krugh TR (1993) Structural characterization of an N-acetyl-2-aminofluorene (AAF) modified DNA oligomer by NMR, energy minimization, and molecular dynamics. *Biochemistry* 32: 2481-2497.

Ogi T and Lehmann AR (2006) The Y-family DNA polymerase kappa (pol kappa) functions in mammalian nucleotide-excision repair. *Nat Cell Biol* 8: 640-642.

Plum GE, Grollman AP, Johnson F, and Breslauer KJ (1995) Influence of the oxidatively damaged adduct 8-oxodeoxyguanosine on the conformation, energetics, and thermodynamic stability of a DNA duplex. *Biochemistry* 34: 16148-16160.

Politi A, Moné MJ, Houtsmuller AB, Hoogstraaten D, Vermeulen W, Heinrich R, and van Driel R (2005) Mathematical modeling of nucleo- tide excision repair reveals efficiency of sequential assembly strategies. *Mol Cell* 19: 679-690.

Rapic'-Otrin V, Navazza V, Nardo T, Botta E, McLenigan M, Bisi DC, Levine AS, and Stefanini M (2003) True XP group E patients have a defective UV-damaged DNA binding protein complex and mutations in DDB2 which reveal the functional domains of its p48 product. *Hum Mol Genet* 12: 1507-1522.

Reardon JT, Bessho T, Kung HC, Bolton PH, and Sancar A (1997) In vitro repair of oxidative DNA damage by human nucleotide excision repair system: possible explanation for neurodegeneration in xeroderma pigmentosum patients. *Proc Natl Acad Sci USA* 94: 9463-9468.

Reardon JT, Nichols AF, Keeney S, Smith CA, Taylor JS, Linn S, and Sancar A (1993) Comparative analysis of binding of human damaged DNA-binding protein (XPE) and Escherichia coli damage recognition protein (UvrA) to the major ultraviolet photoproducts: T[c,s]T, T[t,s]T, T[6-4]T, and T[Dewar]T. *J Biol Chem* 268: 21301-21308.

Reardon JT and Sancar A (2003) Recognition and repair of the cyclobutane thymine dimer, a major cause of skin cancers, by the human excision nuclease. *Genes Dev* 17: 2539-2551.

Reardon JT and Sancar A (2006) Repair of DNA-polypeptide crosslinks by human excision nuclease. *Proc Natl Acad Sci USA* 103: 4056-4061.

Riedl T, Hanaoka F, and Egly JM (2003) The comings and goings of nucleotide excision repair factors on damaged DNA. *EMBO J* 22: 5293-5303.

Salisbury JL, Suino KM, Busby R, and Springett M (2002) Centrin-2 is required for centriole duplication in mammalian cells. *Curr Biol* 12: 1287-1292.

Sancar A (1996) DNA excision repair. *Annu Rev Biochem* 65: 43-81.

Schärer OD (2007) Achieving broad substrate specificity in damage recognition by binding accessible nondamaged DNA. *Mol Cell* 28: 184-185.

Scrima A, Konickova R, Czyzewski BK, Kawasaki Y, Jeffrey PD, Groisman R, Nakatani Y, Iwai S, Pavletich NP, and Thomä NH (2008) Structural basis of UV DNA-damage recognition by the DDB1-DDB2 complex. *Cell* 135: 1213-1223.

Shimizu Y, Iwai S, Hanaoka F, and Sugasawa K (2003) Xeroderma pigmentosum group C protein interacts physically and functionally with thymine DNA glycosylase. *EMBO J* 22: 164-173.

Shivji MK, Podust VN, Hübscher U, and Wood RD (1995) Nucleotide excision repair DNA synthesis by DNA polymerase epsilon in the presence of PCNA, RCF, and RPA. *Biochemistry* 34: 5011-5017.

Shiyanov P, Nag A, and Raychaudhuri P (1999) Cullin 4A associates with the UV-damaged DNA-binding protein DDB. *J Biol Chem* 274: 35309-35312.

Sijbers AM, de Laat WL, Ariza RR, Biggerstaff M, Wei YF, Moggs JC, Carter KC, Shell BK, Evans E, de Jong MC, Rademakers S, de Rooij J, Jaspers NG, Hoeijmakers HJ, and Wood RD (1996) Xeroderma

pigmentosum group F caused by a defect in a structure-specific DNA repair endonuclease. *Cell* 86: 811-822.

Solimando L, Luijsterburg MS, Vecchio L, Vermeulen W, van Driel R, and Fakan S (2009) Spatial organization of nucleotide excision repair proteins after UV-induced DNA damage in the human cell nucleus. *J Cell Sci* 122: 83-91.

Sprague BL, Pego RL, Stavreva DA, and McNally JG (2004) Analysis of binding reactions by fluorescence recovery after photobleaching. *Biophys J* 86: 3473-3495.

Staresincic L, Fagbemi AF, Enzlin JH, Gourdin AM, Wijgers N, Dunand-Sauthier I, Giglia-Mari G, Clarkson SG, Vermeulen W, and Schärer OD (2009) Coordination of dual incision and repair synthesis in human nucleotide excision repair. *EMBO J* 28: 1111-1120.

Sugasawa K (2010) Regulation of damage recognition in mammalian global genome nucleotide excision repair. *Mutat Res* 685: 29-37.

Sugasawa K and Hanaoka F (2007) Sensing of DNA damage by XPC/Rad4: one protein for many lesions. *Nat Struct Mol Biol* 14: 887-888.

Sugasawa K, Ng JM, Masutani C, Iwai S, van der Spek PJ, Eker AP, Hanaoka F, Bootsma D, and Hoeijmakers JH (1998) Xeroderma pigmentosum group C protein complex is the initiator of global genome nucleotide excision repair. *Mol Cell* 2: 223-232.

Sugasawa K, Okamoto T, Shimizu Y, Masutani C, Iwai S, and Hanaoka F (2001) A multistep damage recognition mechanism for global genomic nucleotide excision repair. *Genes Dev* 15: 507-521.

Sugasawa K, Okuda Y, Saijo M, Nishi R, Matsuda N, Chu G, Mori T, Iwai S, Tanaka K, and Hanaoka F (2005) UV-induced ubiquitylation of XPC protein mediated by UV-DDB-ubiquitin ligase complex. *Cell* 121: 387-400.

Sugasawa K, Shimizu Y, Iwai S, and Hanaoka F (2002) A molecular mechanism for DNA damage recognition by the xeroderma pigmentosum group C protein complex. *DNA Repair* 1: 95-107.

Tang J and Chu G (2002) Xeroderma pigmentosum group E and UV-damaged DNA-binding protein. *DNA Repair* 1: 601-616.

Tang JY, Hwang BJ, Ford JM, Hanawalt PC, and Chu G (2000) Xeroderma pigmentosum p48 gene enhances global gemomic repair and suppresses UV-induced mutagenesis. *Mol Cell* 5: 737-744.

Tirode F, Busso D, Coin F, and Egly JM (1999) Reconstitution of the transcription factor TFIIH: assignment

of functions for the three enzymatic subunits, XPB, XPD, and cdk7. *Mol Cell* 3: 87-95.

Träutlein D, Adler F, Moutzouris K, Jeromin A, Leitenstorfer A, and Ferrando-May E (2008) Highly versatile confocal microscopy system based on a tunable femtosecond Er:fiber source. *J Biophoton* 1: 53-61.

Trego KS and Turchi JJ (2006) Pre-steady-state binding of damaged DNA by XPC-hHR23B reveals a kinetic mechanism for damage discrimination. *Biochemistry* 45: 1961-1969.

Truglio JJ, Karakas E, Rhau B, Wang H, DellaVecchia MJ, Van Houten B, and Kisker C (2006) Structural basis for DNA recognition and processing by UvrB. *Nat Struct Mol Biol*. 13: 360-364.

Uchida A, Sugasawa K, Masutani C, Dohmae N, Araki M, Yokoi M, Ohkuma Y, and Hanaoka F (2002) The C-terminal domain of the XPC protein plays a crucial role in nucleotide excision repair through interactions with transcription factor IIH. *DNA Rep* 1: 449-461.

Volker M, Mone MJ, Karmakar P, van Hoffen A, Schul W, Vermeulen W, Hoeijmakers JH, van Driel R, van Zeeland AA, and Mullenders LH (2001) Sequential assembly of the nucleotide excision repair factors in vivo. *Mol Cell* 8: 213-224.

Wakasugi M and Sancar A (1998) Assembly, subunit composition, and footprint of human DNA repair excision nuclease. *Proc Natl Acad Sci USA* 95: 6669-6674.

Wang H, Zhai L, Xu J, Joo HY, Jackson S, Erdjument-Bromage H, Tempst O, Xiong Y, and Zhang Y (2006) Histone H3 and H4 ubiquitylation by the CUL4-DDB-ROC1 ubiquitin ligase facilitates cellular response to DNA damage. *Mol Cell* 22: 383-394.

Waters TR, Eryilmaz J, Geddes S, and Barret TE (2006) Damage detection by the UvrABC pathway: crystal structure of UvrB bound to fluorescein-adducted DNA. *FEBS Lett* 580: 6423-6427.

Winter RB and von Hippel PH (1981) Diffusion-driven mechanisms of protein translocation on nucleic acids. 2. The *Escherichia coli* repressor-operator interaction: equilibrium measurements. *Biochemistry* 20: 6948-6960.

Winter RB, Berg OG, and von Hippel PH (1981) Diffusion-driven mechanisms of protein translocation on nucleic acids. 3. The *Escherichia coli lac* repressor-operator interaction: kinetic measurements and conclusions. *Biochemistry* 20: 6961-6977.

Wittschieben BO, Iwai S, and Wood RD (2005) DDB1–DDB2 (xeroderma pigmentosum group E) protein complex recognizes a cyclobutane pyrimidine dimer, mis- matches, apurinic/apyrimidinic sites, and compound lesions in DNA. *J Biol Chem* 280: 39982-39989.

Wood RD (1997) Nucleotide excision repair in mammalian cells. *J Biol Chem* 272: 23465-23468.

Wood RD (1996) DNA repair in eukaryotes. *Annu Rev Biochem* 65: 135-167.

Xie Z, Liu S, Zhang Y, and Wang Z (2004) Roles of Rad23 protein in yeast nucleotide excision repair. *Nucl Acids Res* 15: 5981-5990.

Yasuda G, Nishi R, Watanabe E, Mori T, Iwai S, Orioli D, Stefanini M, Hanaoka F, and Sugasawa K (2007) In vivo destabilization and functional defects of the xeroderma pigmentosum C protein caused by a pathogenic missense mutation. *Mol Cell Biol* 27: 6606-6614.

Yokoi M, Masutani C, Maekawa T, Sugasawa K, Ohkuma Y, and Hanaoka F (2000) The xeroderma pigmentosum group C protein complex XPC-HR23B plays an important role in the recruitment of transcription factor IIH to damaged DNA. *J Biol Chem* 275: 9870-9875.

Zharkov D and Grollmann AP (2005) The DNA trackwalkers: principles of lesion search and recognition by DNA glycosylases. *Mutat Res* 577: 24-54.

ACKNOWLEDGEMENTS

My biggest gratitude goes to Prof. Hanspeter Naegeli for giving me the opportunity to join his group, for supervising my thesis and for the great scientific support and constructive discussions during the last four years.

I am very thankful to Prof. Peter Bütikofer, my mentor within the Graduate School for Cellular and Biomedical Sciences of the University of Bern.

Furthermore, I thank Prof. Ben Schuler, who accepted to be the co-referee of my PhD thesis. He provided valuable input for my work and gave me his opinion and advice on the planning of experiments.

Several people have contributed to some experiments presented in this thesis. For this, I am grateful to Aymone Lenisa, Muriel Träxler, Daniela Hermann, Martin Tomas and Daniel Träutlein.

I warmly thank my fellow PhD and doctoral students Christian Blenn, Jia Fei, Sanjay Gawade, Li Zhang, Malin Olson, Nadine Mathieu, Nina Kaczmarek, Regula Meier and Philippe Wyrsch for their encouraging ideas and their friendship.

During my studies and thesis work, I encountered many amazing people who I hope never to lose contact with: Andrea Pepin, Maria Puorger, Hege Benedikte Asvald Gulsvik, Siri Helland Hansen, Karin Stettler and Kiki Camenisch.

This work would not have been possible without the neverending support and patience of my parents, Arthur and Martina Clement. Thank you very much! I also thank my sister, Renata, and my brothers, Martin and Urs, for always being there.

And last but not least, my cordial thanks go to my loving husband Adrian Frey and our wonderful son Jon Andri for being the family I've always dreamed of.

"Many friends will walk in and out of your life, but only true friends will leave footprints in your heart". Eleanor Roosevelt

DECLARATION OF ORIGINALITY

Last name, first name: **Clement Frey, Flurina Christina**

Matriculation number: **99-723-405**

I hereby declare that this thesis represents my original work and that I have used no other sources except as noted by citations.
All data, tables, figures and text citations which have been reproduced from any other source, including the internet, have been explicitly acknowledged as such.
I am aware that in case of non-compliance, the Senate is entitled to divest me of the doctorate degree awarded to me on the basis of the present thesis, in accordance with the "Statut der Universität Bern (Universitätsstatut; UniSt)", Art. 20, of 17 December 1997.

Place, date Signature

…… ……